

OFFICE OF CIVILIAN RADIOACTIVE WASTE MANAGEMENT

ANALYSIS/MODEL COVER SHEET

Complete Only Applicable Items

1. OA: QA

Page: 1 of 72

2. <input checked="" type="checkbox"/> Analysis Check all that apply		3. <input checked="" type="checkbox"/> Model Check all that apply	
Type of Analysis	<input type="checkbox"/> Engineering <input checked="" type="checkbox"/> Performance Assessment <input type="checkbox"/> Scientific	Type of Model	<input type="checkbox"/> Conceptual Model <input type="checkbox"/> Mathematical Model <input type="checkbox"/> Process Model <input checked="" type="checkbox"/> Abstraction Model <input type="checkbox"/> System Model
Intended Use of Analysis	<input type="checkbox"/> Input to Calculation <input checked="" type="checkbox"/> Input to another Analysis or Model <input type="checkbox"/> Input to Technical Document <input type="checkbox"/> Input to other Technical Products	Intended Use of Model	<input type="checkbox"/> Input to Calculation <input checked="" type="checkbox"/> Input to another Model or Analysis <input type="checkbox"/> Input to Technical Document <input type="checkbox"/> Input to other Technical Products
Describe use: Unit breakthrough curves from the SZ site-scale flow and transport model are used in the TSPA-SR simulations of SZ transport.		Describe use: Provide a simplified one-dimensional radionuclide transport Model for the purpose of simulating radionuclide chains in the TSPA simulator.	

4. Title:
Input and Results of the Base Case Saturated Zone Flow and Transport Model for TSPA

5. Document Identifier (including Rev. No. and Change No., if applicable):
ANL-NBS-HS-000030 Rev. 00

6. Total Attachments:		7. Attachment Numbers - No. of Pages in Each:	
4		I-12, II-27, III-7, IV-6	
	Printed Name	Signature	Date
8. Originator	Bill W. Arnold	SIGNATURE ON FILE	4/24/00
9. Checker	Mike Wallace	SIGNATURE ON FILE	4/24/00
10. Lead/Supervisor	Bill W. Arnold	SIGNATURE ON FILE	4/24/00
11. Responsible Manager	Clifford K. Ho	SIGNATURE ON FILE	4/24/00

12. Remarks:

Per Section 5.5.6 of AP-3.10Q, the responsible manager has determined that the subject AMR is not subject to AP-2.14Q review because the model does not affect a discipline or area other than the originating organization (Performance Assessment). The downstream user of the model resulting from this AMR is Performance Assessment (PA), which is also the originating organization of this work. PA leads, such as Vinod Vallikat and Patrick Mattie, have worked closely with the originator during the development of the model described in this AMR. Nevertheless, this AMR was sent to various Project participants to give representatives of QA, Regulatory and Licensing, and Applied Research and Testing the opportunity to read the AMR and provide informal comments.

The obliterated or illegible information does not impact the technical meaning or content of the record. Figures 6, 7, 8 and
9. *BW/Hs for ck Ho 5/10/00*

OFFICE OF CIVILIAN RADIOACTIVE WASTE MANAGEMENT
ANALYSIS/MODEL REVISION RECORD
Complete Only Applicable Items

1. Page: 2 of 72

2. Analysis or Model Title:

Input and Results of the Base Case Saturated Zone Flow and Transport Model for TSPA

3. Document Identifier (including Rev. No. and Change No., if applicable):

ANL-NBS-HS-000030 REV. 00

4. Revision/Change No.

5. Description of Revision/Change

REV 00

Initial Issue

CONTENTS

	Page
CONTENTS	3
FIGURES	5
TABLES.....	8
1. PURPOSE	9
2. QUALITY ASSURANCE	9
3. COMPUTER SOFTWARE AND MODEL USAGE	10
4. INPUTS.....	11
4.1 DATA AND PARAMETERS	11
4.2 CRITERIA.....	12
4.3 CODES AND STANDARDS.....	12
5. ASSUMPTIONS	13
5.1 TRANSPORT MODEL PARAMETERS	13
5.2 RADIONUCLIDE SOURCE IN THE SATURATED ZONE	14
5.3 RADIONUCLIDE RELEASE TO THE BIOSPHERE.....	14
5.4 ALTERNATIVE GROUNDWATER FLOW FIELDS	15
5.5 CONVOLUTION INTEGRAL METHOD	16
5.6 CLIMATE CHANGE.....	16
5.7 ONE-DIMENSIONAL RADIONUCLIDE TRANSPORT MODELING	17
6. ANALYSIS	18
6.1 OVERVIEW	18
6.2 SATURATED ZONE SITE-SCALE FLOW AND TRANSPORT MODEL.....	19
6.2.1 Transport Model Parameters	19
6.2.2 Radionuclide Source in the Saturated Zone	27
6.2.3 Recharge from the UZ Site-Scale Flow Model.....	28
6.2.4 Radionuclide Release to the Biosphere	30
6.2.5 Alternative Groundwater Flow Fields.....	32
6.2.6 Implementation of Multiple Realizations.....	38
6.2.7 Post-Processor Software Routine	39
6.3 RADIONUCLIDE TRANSPORT RESULTS	40
6.3.1 Expected-Value Case	40
6.3.2 Stochastic Realizations.....	41
6.4 ABSTRACTION FOR TOTAL SYSTEM PERFORMANCE	
ASSESSMENT	51
6.4.1 Convolution Integral Method.....	51
6.4.2 Climate Change	53
6.5 ONE-DIMENSIONAL RADIONUCLIDE TRANSPORT MODEL	55
6.5.1 Model Setup	55

6.5.2 Model Validation and Comparison to SZ Site-Scale Model.....	61
7. CONCLUSIONS.....	65
8. REFERENCES.....	68
8.1 DOCUMENTS CITED.....	68
8.2 PROCEDURES CITED.....	70
8.3 SOURCE DATA, LISTED BY DATA TRACKING NUMBER	70
9. ATTACHMENTS	72
ATTACHMENT I.....	I-1
ATTACHMENT II.....	II-1
ATTACHMENT III	III-1
ATTACHMENT IV	IV-1

FIGURES

	Page
Figure 1. Matrix and Effective Porosity at the Water Table of the SZ Site-Scale Flow and Transport Model. The area in which heterogeneous values of matrix porosity from the ISM rock properties model is outlined by the dashed line, as indicated. (DTN: SNT05070198001.001 and SN0004T0501600.005)	21
Figure 2. Alluvial Uncertainty Zone. The outline of the alluvial uncertainty zone is shown by the solid yellow line. Base map is a shaded relief map of surface elevation. The outline of the repository is shown by the solid blue line. Locations of wells with water-level measurements are indicated by the red crosses.	24
Figure 3. Radionuclide Source Regions for the SZ Site-Scale Flow and Transport Model. Source regions are outlined with the solid black rectangles and numbered from 1 to 4. The coordinates of the vertices of the source region rectangles are given in UTM coordinates (m). The outline of the repository is shown by the blue line (Source: CRWMS M&O 1999b). The dashed red lines indicate the quadrants from which radionuclide arrivals from the unsaturated zone model are applied to the SZ source regions. Coordinates of the dashed red lines are given in Nevada State Plane (NSP) coordinates (m).	28
Figure 4. Nodes from the SZ Site-Scale Model Defining Fences at Which Radionuclide Mass Flux Breakthrough Curves are Output. Fence nodes at 5 km, 20 km, and 30 km distances are shown (DTN: SN0004T0501600.005). Repository outline shown with solid line (Source: CRWMS M&O 1999b).....	31
Figure 5. Simulated Neptunium Mass Breakthrough Curves at Three Distances from the Repository for the Expected-Value Case (DTN: SN0004T0501600.004).	32
Figure 6. Simulated Heads and Residuals at Wells from the Mean Flux Case of the SZ Site-Scale Flow Model (DTN: SN0004T0501600.005). Contours show simulated head at the water table in units of meters above sea level. Head residuals at wells are shown in units of meters with the red labels. The repository outline is shown with the bold purple line in the upper central portion of the plot (Source: CRWMS M&O 1999b).....	34
Figure 7. Simulated Heads and Residuals at Wells from the High Flux Case of the SZ Site-Scale Flow Model (DTN: SN0004T0501600.005). Contours show simulated head at the water table in units of meters above sea level. Head residuals at wells are shown in units of meters with the red labels. The	

repository outline is shown with the bold purple line in the upper central portion of the plot (Source: CRWMS M&O 1999b).....	35
Figure 8. Simulated Heads and Residuals at Wells from the Isotropic Case of the SZ Site-Scale Flow Model (DTN: SN0004T0501600.005). Contours show simulated head at the water table in units of meters above sea level. Head residuals at wells are shown in units of meters with the red labels. The repository outline is shown with the bold purple line in the upper central portion of the plot (Source: CRWMS M&O 1999b).....	37
Figure 9. Simulated Heads and Residuals at Wells from the Anisotropic Case of the SZ Site-Scale Flow Model (DTN: SN0004T0501600.005). Contours show simulated head at the water table in units of meters above sea level. Head residuals at wells are shown in units of meters with the red labels. The repository outline is shown with the bold purple line in the upper central portion of the plot (Source: CRWMS M&O 1999b).....	38
Figure 10. Simulated Particle Paths in the SZ Site-Scale Flow and Transport Model (DTN: SN0004T0501600.005). Simulated particle paths are shown in blue for isotropic conditions. The outline of the repository is shown with the bold red line (Source: CRWMS M&O 1999b). The 20 km fence is shown with the dashed red line. Locations of wells with water-level measurements are shown by the red cross symbols.	42
Figure 11. Simulated Unit Breakthrough Curves of Radionuclide Mass Flux for the Expected-Value Case. Results are shown for 20 km distance from source region 1 (DTN: SN0004T0501600.004).	43
Figure 12. Simulated Unit Breakthrough Curves of Mass Flux for Carbon. Results are shown for 20 km distance from source region 1 (DTN: SN0004T0501600.004).	44
Figure 13. Simulated Unit Breakthrough Curves of Mass Flux for Iodine. Results are shown for 20 km distance from source region 1 (DTN: SN0004T0501600.004).	45
Figure 14. Simulated Unit Breakthrough Curves of Mass Flux for the K_c model for Colloid-Facilitated Transport of Highly Sorbing Radionuclides. Results are shown for 20 km distance from source region 1 (DTN: SN0004T0501600.004).	46
Figure 15. Simulated Unit Breakthrough Curves of Mass Flux for the K_c model for Colloid-Facilitated Transport of Moderately Sorbing Radionuclides. Results are shown for 20 km distance from source region 1 (DTN: SN0004T0501600.004).	47

Figure 16. Simulated Unit Breakthrough Curves of Mass Flux for Neptunium. Results are shown for 20 km distance from source region 1 (DTN: SN0004T0501600.004).....	48
Figure 17. Simulated Unit Breakthrough Curves of Mass Flux for Colloid- Facilitated Transport of Irreversibly Attached Radionuclides. Results are shown for 20 km distance from source region 1 (DTN: SN0004T0501600.004).....	49
Figure 18. Simulated Unit Breakthrough Curves of Mass Flux for Technecium. Results are shown for 20 km distance from source region 1 (DTN: SN0004T0501600.004).....	50
Figure 19. Simulated Unit Breakthrough Curves of Mass Flux for Uranium. Results are shown for 20 km distance from source region 1 (DTN: SN0004T0501600.004).....	51
Figure 20. Scaling of Simulated Breakthrough Curve for Climate Change. The example shown is for ^{237}Np transport in the expected-value case. (DTN: SN0004T0501600.004).....	53
Figure 21. Transport Processes Simulated in One-Dimensional Pipe Pathways in GoldSim.....	57
Figure 22. One-Dimensional Mass Transport Model in the Saturated Zone.....	58
Figure 23. Pipe Connection in the One-Dimensional Radionuclide Transport Model.....	59
Figure 24. Comparison of GoldSim and Sudicky and Frind (1982) Solutions.....	62
Figure 25. Simulated Breakthrough Curves From the One-Dimensional Transport Model and the Three-Dimensional SZ Site-Scale-Model at 5, 20, and 30 km for Carbon.....	63
Figure 26. Simulated Breakthrough Curves From the One-Dimensional Transport Model and the Three-Dimensional SZ Site-Scale-Model at 5, 20, and 30 km for Neptunium.....	64

TABLES

	Page
Table 1. Computer Software Used in this Analysis	10
Table 2. Software Routines Used in this Analysis	10
Table 3. Input Data Used in this Analysis.....	12
Table 4. Stochastic Parameters Used in the Analysis	22
Table 5. Coordinates of the Vertices of the Alluvial Uncertainty Zone	23
Table 6. Realizations Assigned to Alternative Groundwater Flow Fields.....	33
Table 7. Groundwater Flow Scaling Factors for Climate Change	54
Table 8. Average Specific Discharge in Flowpath Segments	61
Table 9. Stochastic Parameter Values	I-1

1. PURPOSE

The purpose of this analysis is to provide radionuclide transport simulation results from the saturated zone (SZ) site-scale model for use in total system performance assessment (TSPA) calculations. The results from this analysis are intended for use in the TSPA for Site Recommendation (SR). The general approach of the analysis is to produce a set of radionuclide breakthrough curves at the accessible environment, 20 km from the repository. These breakthrough curves contain information on the radionuclide travel times through the SZ that is used in the TSPA calculations to determine the arrival times and mass of radionuclides in the biosphere. In addition, this analysis provides a simplified one-dimensional radionuclide transport model for the purpose of simulating radionuclide chains in the TSPA simulator.

Planning of this analysis can be found in the following Work Direction and Planning Document: *Abstraction of SZ Flow and Transport Model, Rev. 01. ID: B2040, Activity: SPP4050* (CRWMS M&O 1999a). Many of the data and component models utilized in this analysis are preliminary. Consequently, the results documented in this Analysis/Modeling Report (AMR) must be considered as unqualified.

2. QUALITY ASSURANCE

This analysis was prepared in accordance with the Civilian Radioactive Waste Management System (CRWMS) Quality Assurance program. The PAO responsible manager has evaluated this activity in accordance with QAP-2-0, *Conduct of Activities*. The QAP-2-0 activity evaluation determined that the development of this analysis is subject to the requirements in the *Quality Assurance Requirements and Description* (DOE 2000). The analysis was conducted and this report developed in accordance with AP-3.10Q, *Analyses and Models*.

3. COMPUTER SOFTWARE AND MODEL USAGE

The software codes listed in Table 1 were used in the analysis documented in this report. Unqualified versions of FEHM and GoldSim software that were used in the analysis have been submitted to the Software Configuration Management System per Section 5.11 of AP-SI.1Q Rev. 2/ICN 4, *Software Management* and are being tracked by that system.

Table 1. Computer Software Used in this Analysis

Computer Software	Computer Platform/ Operating System	Software Tracking Number	Comments
FEHM (Version 2.10)	Sun UltraSPARC SunOS 5.7	10086-2.10-00	FEHM is the computer code used to simulate groundwater flow and radionuclide transport in the SZ site-scale model.
GoldSim (Version 6.03)	Dell OptiPlex GX1 Windows NT 4.00.1381	10296-6.03-00	GoldSim is used to sample values of stochastic input parameters for the SZ site-scale transport model and for radionuclide transport with the one-dimensional radionuclide transport model.

Several software routines were developed to prepare input files and to process the results of the SZ radionuclide transport simulations. These software routines are documented in the Attachments section of this AMR. These routines were checked as part of this analysis to ensure that they provide correct results for the input files used. The use and documentation of the software routines listed in Table 2 complies with Section 5.1.1 of AP-SI.1Q Rev. 2/ICN 4, *Software Management*.

Table 2. Software Routines Used in this Analysis

Software Routine	Computer Platform/ Operating System	Documentation	Comments
SZ_Pre (Version 1.0)	Sun UltraSPARC SunOS 5.7	Attachment II	Reads values for stochastic parameters and writes input files for SZ site-scale flow and transport model.
SZ_Post (Version 1.0)	Sun UltraSPARC SunOS 5.7	Attachment III	Reads output files containing radionuclide transport results from the SZ site-scale flow and transport model and reformats results for input to the SZ_Convolute code.

The commercially available software cited below is appropriate for use in this application. The results were spot-checked by hand to ensure that the results were correct. The computer used was a Dell OptiPlex GX1 with Pentium II processor, running Microsoft Windows NT 4.00.1381. The range of validation for Excel, Surfer, and Grapher is the set of real numbers.

Commercially available software:

- **Excel 97-SR-1:** Used for simple spreadsheet calculations.
- **Surfer 6.03:** Used for plotting and visualization.
- **Grapher 2.00:** Used for plotting graphs.

Input and output files from spreadsheet calculations are included in the data submittal associated with this AMR (DTN: SN0004T0501600.005) and were hand checked for correct implementation. Verification of the spreadsheet calculations is included in Section 6.2.3 of this report. Output from plotting and visualization software was hand- or visually checked for correct plotting of data.

The primary input model used in this analysis is the SZ site-scale flow and transport model (see Item 1, Table 3). This model is used to simulate radionuclide transport in the SZ to obtain results for use in the TSPA-SR. The one-dimensional SZ radionuclide transport model is developed in this report for the purpose of simulating radioactive decay and ingrowth for four decay chains in the TSPA-SR. Validation of the one-dimensional model developed in this report is documented in Section 6.5.2.

4. INPUTS

4.1 DATA AND PARAMETERS

Data used in the analysis are summarized in Table 3. Data that were not obtained from the Technical Data Management System were obtained following QA procedure AP-3.14Q, Rev. 0/ICN, *Transmittal of Input*.

Table 3. Input Data Used in this Analysis

Item	Description	Input Transmittal Number (ITN)	Data Tracking Number (DTN)	Comments
1	Final Calibrated Flow Model	PA-NEP-99327.R	LA9911GZ12213S.001	The final calibrated SZ site-scale flow model provides the input files and groundwater flow field for radionuclide transport simulations.
2	Uncertainty Distributions for Stochastic Parameters AMR	N/A	SN0004T0571599.004	Uncertainty distributions are defined for stochastic SZ transport parameters in this source.
3	ISM Rock Properties Model	N/A	SNT05070198001.001	Matrix porosity and bulk density in the area of the ISM.
4	UZ Site-Scale Model Flow Fields	SNL-LBL-99249.T	LB990801233129.004	Groundwater recharge distribution at the water table under Yucca Mountain. Mean infiltration for present climate.
5	UZ Site-Scale Model Flow Fields	SNL-LBL-99249.T	LB990801233129.009	Mean infiltration for glacial climate.
6	UZ Site-Scale Model Flow Fields	SNL-LBL-99249.T	LB990801233129.015	Mean infiltration for monsoonal climate.

4.2 CRITERIA

Although no specific criteria have been identified in project requirements documents (e.g., System Description Documents) as applicable to this activity, the Input and Results of the Base Case Saturated Zone Flow and Transport Model analysis supports the definition of radionuclide transport for performance assessment as required by the interim guidance from the Department of Energy pending issuance of new regulations by the Nuclear Regulatory Commission (Dyer 1999). Relevant requirements for performance assessment from Section 114 of that document are: “Any performance assessment used to demonstrate compliance with Sec. 113(b) shall: (a) Include data related to the geology, hydrology, and geochemistry ... used to define parameters and conceptual models used in the assessment. (b) Account for uncertainties and variabilities in parameter values and provide the technical basis for parameter ranges, probability distributions, or bounding values used in the performance assessment. ... (g) Provide the technical basis for models used in the performance assessment such as comparisons made with outputs of detailed process-level models”

4.3 CODES AND STANDARDS

No specific, formally established standards have been identified as applying to this analysis activity.

5. ASSUMPTIONS

5.1 TRANSPORT MODEL PARAMETERS

A large number of underlying assumptions is embodied in the transport model parameters used in the SZ site-scale flow and transport model for TSPA simulations and in the one-dimensional radionuclide transport model for decay chains. A complete description of the specific assumptions relevant to these transport parameters is given in CRWMS M&O 2000b. A few of the most important assumptions are enumerated here.

1. Homogeneous material properties are assigned to individual hydrogeologic units, with the exception of matrix porosity and bulk density for those units within the ISM rock properties model domain (Section 6.2.1). The assumption of intra-unit homogeneity is justified primarily on the basis of scale in the SZ site-scale flow and transport model. The horizontal grid resolution of 500 m implies averaging of spatially variable properties over a very large volume. In addition, variations among realizations for stochastic parameters in the analysis encompass probable spatial variations in material properties within the model domain.
2. It is assumed that the equilibrium, linear sorption model applies to sorption of radionuclides in the matrix of the volcanic units and in the alluvium of the valley-fill units (Section 6.2.1). The K_d model of equilibrium, linear sorption is an applicable approximation of sorptive behavior in both laboratory experiments and at the field scale (CRWMS M&O 2000f).
3. The conceptual model of matrix diffusion in the fractured volcanic units of the SZ assumes groundwater flow in evenly spaced, parallel-walled fractures separated by impermeable matrix (Section 6.2.1). Although this conceptual model represents a significant simplification of the complex fracture network observed in fractured volcanic rocks at the site, it is an acceptable approximation at the scale of individual grid blocks in the SZ site-scale flow and transport model. Individual grid blocks in the SZ site-scale model have horizontal dimensions of 500 m by 500 m (CRWMS M&O 2000a), in comparison to a geometric mean flowing interval spacing of approximately 21 m (CRWMS M&O 2000b). This comparison indicates that the grid blocks in the numerical model are more than an order of magnitude larger than the expected spacing between fracture zones that contain flowing groundwater. In addition, the relatively broad range of uncertainty in the flowing interval spacing used in this analysis encompasses the spatial variability of spacing in the actual fracture network. Thus, the variability in flowing interval spacing among stochastic realizations in the TSPA simulations tends to capture the impact of variable spacing between fractures in an ensemble fashion.

5.2 RADIONUCLIDE SOURCE IN THE SATURATED ZONE

4. The interface between radionuclide transport in the UZ and the SZ is assumed to be a point source near the water table (Section 6.2.2). This assumption is physically consistent with a single leaking waste package and highly focused transport of radionuclides in the UZ flow system, as may occur early in the post-closure history of the repository. This assumption is also consistent with the human intrusion scenario, in which a borehole penetrates a waste package and provides a direct pathway for radionuclide migration to the SZ. The assumption of a point source for radionuclides in the SZ transport simulations, while not physically realistic for the situation in which multiple, dispersed leaking waste packages exist, provides a conservative approximation of the source term to the SZ.
5. The location of the point source of radionuclides for transport in the SZ site-scale flow and transport model is assumed to be randomly located within the four source regions defined at the water table (Section 6.2.2). This assumption implies that there are no consistent spatial patterns of waste package failure and delivery of radionuclides at the water table within each of the four source regions. Many of the processes that may lead to waste package failure are spatially random (e.g., manufacturing defects, seepage onto waste packages, etc.). The spatial pattern of preferential groundwater flow pathways in the UZ flow model is represented in a general sense by the locations of the four source regions (e.g., the southeastern source region corresponds to focused vertical groundwater flow along the Ghost Dance fault) (CRWMS M&O 2000c, p 14).

5.3 RADIONUCLIDE RELEASE TO THE BIOSPHERE

6. It is assumed that all radionuclide mass crossing the 20 km fence in the SZ is captured by pumping wells of the hypothetical farming community (Section 6.2.4). This assumption implies that the total volumetric groundwater usage by the hypothetical community is large relative to the volumetric flow in the plume of contaminated groundwater in the SZ. This assumption is justified on the basis of conservatism with respect to the analysis of repository performance. The total mass of radionuclides released to the biosphere for a given time period cannot be larger than the amount of radionuclide mass delivered by groundwater flow (for the nominal case).
7. The assumption is made that the average concentration of radionuclides in the groundwater supply of the hypothetical community is an appropriate estimate of radionuclide concentration for the calculation of radiological dose (Section 6.2.4). Realistically, the concentrations of radionuclides encountered by wells in the hypothetical community could vary from location to location within the contaminant plume in the SZ. However, radionuclide transfer processes within the biosphere (e.g., redistribution of agricultural products, communal water supplies, etc.) would tend to average the overall dose received by the population of the community.
8. Pumping of groundwater by the hypothetical farming community is assumed not to alter significantly the groundwater pathways or radionuclide travel times in the SZ (Section 6.2.4).

Calibration of the SZ site-scale flow model is based on the present-day potentiometric surface observed in the model domain. Whereas the SZ site-scale model does not explicitly include the withdrawal of groundwater by pumping at the location of the hypothetical community, the model does implicitly account for the drawdown of water levels associated with pumping at the specified-head southern boundary of the model domain. Consequently, the model does implicitly include the influence of pumping in terms of increased hydraulic head gradients, especially for the present-day pumping from wells at and to the south of the southern boundary of the SZ site-scale model domain.

5.4 ALTERNATIVE GROUNDWATER FLOW FIELDS

9. It is assumed that the uncertainty in groundwater flux in the volcanic aquifer near Yucca Mountain elicited from the SZ expert elicitation panel is applicable to the entire flowpath from the repository to the accessible environment (Section 6.2.5). The estimates of specific discharge from the SZ expert elicitation were primarily based on data from hydraulic testing in wells in volcanic units and the hydraulic gradient inferred from water level measurements (CRWMS M&O 1998b, p. 3-8). The relative values of groundwater flux in the volcanic aquifer and along the flowpath farther to the south are constrained by the calibration of the SZ site-scale model. It is thus reasonable to extrapolate the degree of uncertainty in the absolute value of groundwater flux from the volcanic aquifer to the flowpath farther to the south.
10. It is assumed that the potential anisotropy of permeability in the horizontal direction is adequately represented by a permeability tensor that is oriented in the north-south and east-west directions (Section 6.2.5). The numerical grid in the SZ site-scale flow and transport model is aligned in the north-south and east-west directions and values of permeability may only be specified in directions parallel to the grid. Analysis of the probable direction of horizontal anisotropy shows that the direction of maximum transmissivity is N 33° E (Winterle and La Femina, 1999, p. iii), indicating that the anisotropy applied on the SZ site-scale model grid is within approximately 30° of the inferred anisotropy.
11. The assumption is made that the horizontal anisotropy in permeability applies to the fractured and faulted volcanic units of the SZ system along the groundwater flowpath from the repository to the south and east of Yucca Mountain (Section 6.2.5). The inferred flowpath from beneath the repository extends to the south and east. This is the area in which potential anisotropy could have significant impact on radionuclide transport in the SZ and is the area in which pumping tests were conducted. Given the conceptual basis for the anisotropy model, it is appropriate to only apply anisotropy to those hydrogeologic units that are dominated by groundwater flow in fractures.
12. It is assumed that potential anisotropy in permeability represents an alternative conceptual model of groundwater flow at the Yucca Mountain site (Section 6.2.5). Sufficient uncertainty in the analysis of horizontal anisotropy exists to warrant consideration of two possible conceptual models; one with anisotropy and one without anisotropy (i.e., isotropic permeability). Given the lack of information on the relative validity of these alternative

conceptual models, they are assigned equal probability for the purposes of TSPA calculations.

5.5 CONVOLUTION INTEGRAL METHOD

13. An assumption inherent to the convolution integral method is that the system being simulated exhibits a linear response to the input function (Section 6.4.1). In the case of solute transport in the SZ system this assumption implies, for example, that a doubling of the input mass flux results in a doubling of the output mass flux. This assumption is valid for the SZ site-scale flow and transport model because the underlying transport processes (e.g., advection and sorption) are all linear with respect to solute mass.
14. It is also assumed that the groundwater flow conditions in the SZ system are in steady state (Section 6.4.1). The SZ site-scale flow model is a steady-state model of the flow conditions (CRWMS M&O, 2000a), reflecting the conclusion that a steady-state representation of the SZ system is accurate. This conclusion is supported by the lack of consistent, large-magnitude variations in water levels observed in wells near Yucca Mountain (Luckey et al. 1996, p. 29-32). The convolution integral method has been extended to incorporate multiple steady-state flow conditions for alternative climate states, as described in Section 6.4.1.

5.6 CLIMATE CHANGE

15. It is assumed that the change in groundwater flow in the SZ from one climatic state to another occurs rapidly and is approximated by an instantaneous shift from one steady-state flow condition to another steady-state flow condition (Section 6.4.2). In reality, even an extremely rapid shift in climatic conditions would result in a transient response of the SZ flow system because of changes in groundwater storage associated with water table rise or fall and because of the response time in the UZ flow system. The assumption of instantaneous shifts to new steady-state conditions would tend to be conservative with regard to radionuclide transport in the TSPA calculations. The progression of climate states in the 10,000 years following repository closure is from drier to wetter climatic conditions and thus from slower to more rapid groundwater flow in the SZ. By assuming an instantaneous shift to higher groundwater flux in the SZ the simulations tend to overestimate the radionuclide transport velocities during the period of transition from drier conditions to wetter conditions.
16. Groundwater flow pathways in the SZ from beneath the repository to the accessible environment are assumed not to be significantly altered for wetter climatic states (Section 6.4.2). Scaling of present-day groundwater flux and radionuclide mass breakthrough curves by a proportionality factor implies that only the groundwater velocities are changed in the SZ system in response to climate change. This assumption is supported by the observation that the shape of the simulated potentiometric surface downgradient from Yucca Mountain remains basically the same under glacial climatic conditions in simulations using the SZ regional-scale flow model (D'Agnese et al., 1999, p. 30). Water table rise directly beneath the repository under wetter climatic conditions would tend to place volcanic units higher in

the stratigraphic sequence at or just below the water table. These higher volcanic units (Prow Pass Tuff and Calico Hills Formation) have lower values of permeability than the underlying Bullfrog Tuff. Disregarding changes in groundwater pathways, which would be redirected into these lower-permeability units with rise in the water table, is generally conservative from the perspective of radionuclide transport.

5.7 ONE-DIMENSIONAL RADIONUCLIDE TRANSPORT MODELING

17. The final radionuclide daughter product in three of the radionuclide decay chains simulated in the one-dimensional radionuclide transport model is assumed to be in secular equilibrium with its parent radionuclide (Section 6.5). This is a reasonable approach because it simplifies the analysis and the final daughter radionuclides have relatively short half lives (less than 25 years). This assumption is also conservative because it implies an instantaneous increase in the mass of the final daughter product to be in equilibrium with the mass of parent radionuclide present.
18. The groundwater flux within each one-dimensional “pipe” segment used in the model is assumed to be constant along the length of the pipe (Section 6.5). This assumption constitutes a reasonable approach because the average groundwater flux along that portion of the radionuclide flowpath is derived from the corresponding area of the three-dimensional SZ site-scale flow and transport model.

6. ANALYSIS

6.1 OVERVIEW

This analysis consists of preparing the input for the SZ site-scale flow and transport model and obtaining the results of radionuclide simulations for use in the TSPA-SR calculations. The starting point of the analysis is the calibrated SZ site-scale groundwater flow model (CRWMS M&O, 2000a). Input files of the SZ site-scale flow model are modified to include relevant radionuclide transport parameters and to perform simulations of radionuclide transport. Preparation of input files for radionuclide transport includes incorporation of values for stochastic parameters that have been generated for 100 random realizations of the SZ system. Uncertainty distributions for stochastic parameters are taken from the analysis documented in CRWMS M&O (2000b). The groundwater flow field for the calibrated SZ site-scale flow model is also modified to incorporate alternative conceptual models of groundwater specific discharge and horizontal anisotropy of permeability to produce a total of six SZ groundwater flow fields.

Automated methods are developed to pre-process the input files for the simulations, conduct the model runs, and post-process the results. A pre-processor software routine is used to read parameter values that have been drawn for stochastic parameters and write the input files for the SZ site-scale flow and transport model in the appropriate format. UNIX script files are prepared to sequentially run the transport simulations and save the output files. A post-processor software routine is used to reformat and combine the simulation results for the breakthrough curves into a format that can be used in the convolution integral method in the TSPA simulator.

A simplified one-dimensional radionuclide transport model is developed for the purpose of simulating radionuclide decay and ingrowth in four decay chains. This additional model is required because the FEHM code used for the three-dimensional SZ site-scale model is currently not capable of simulating radionuclide ingrowth. The one-dimensional radionuclide transport model is also used for the purpose of simulating radionuclide mass breakthrough curves at 80 km distance, as needed for the Environmental Impact Statement (EIS) analyses. The one-dimensional radionuclide transport model is developed for direct implementation with the GoldSim code in the TSPA simulator.

The approach used for radionuclide transport in the SZ for TSPA-SR differs from the approach used in TSPA-VA (DOE 1998) in several ways. For TSPA-SR, the SZ flow and transport model is used to simulate the unit breakthrough curves for radionuclide mass at the interface between the SZ and the biosphere. Radionuclide concentration is calculated as the average concentration in the water supply that is defined for the hypothetical farming community in the biosphere. In contrast, for TSPA-VA, the breakthrough curves of radionuclide concentration in the SZ were simulated directly with the SZ flow and transport model. For TSPA-SR the three-dimensional SZ site-scale flow and transport model is used to simulate radionuclide transport directly for those radionuclides that are not the product of radioactive decay and ingrowth using the FEHM streamline particle tracking algorithm. For TSPA-VA, an abstracted one-dimensional SZ flow and transport model was used to simulate transport of all radionuclides to generate breakthrough

curves at the accessible environment. Use of the convolution integral method to simulate the time-varying radionuclide flux to the biosphere remains the same in the approach for TSPA-SR.

6.2 SATURATED ZONE SITE-SCALE FLOW AND TRANSPORT MODEL

The SZ site-scale flow and transport model is a relatively complex, three-dimensional model of the SZ system developed for the purposes of Yucca Mountain site characterization and performance assessment (CRWMS M&O 2000a). The calibrated SZ site-scale flow model represents a synthesis of site data ranging from geologic information and water level measurements to pump-test results and hydrochemistry.

The nominal case of SZ flow and transport for the TSPA-SR includes the concept of uncertainty in key model parameters and conceptual models. The probabilistic analysis of uncertainty is implemented through Monte Carlo realizations of the SZ flow and transport system, in a manner consistent with the TSPA simulations implemented with the GoldSim software code. Alternative models of groundwater flux and horizontal anisotropy are included as uncertainty among six SZ groundwater flow fields. Uncertainty in the location of the contact between volcanic units and the alluvium is incorporated as geometric variability in the alluvium zone in the SZ site-scale flow and transport model. Alternative models of colloid-facilitated transport of radionuclides are considered in the uncertainty analysis through the use of two coexisting modes of colloid-facilitated transport.

The nominal case of SZ flow and transport for the TSPA-SR explicitly incorporates many features, events, and processes (FEPs) of the SZ system and includes others in an implicit fashion. Those FEPs that are implicitly incorporated are primarily captured in the range of uncertainty assigned to parameters varied in the stochastic analyses. The disposition of these FEPs, that is how they are represented and evaluated in the TSPA models both explicitly and implicitly, is discussed in detail in the SZ FEPs AMR (CRWMS M&O 2000e).

Input files for the SZ site-scale flow and transport model are modified for this analysis to include appropriate values of transport parameters and to produce the output needed for breakthrough curves of radionuclide mass. In addition, the input files are modified for alternative groundwater flow fields that incorporate uncertainty in groundwater flux and horizontal anisotropy in permeability. An archive of results from the multiple realizations of the SZ site-scale flow and transport model for TSPA analyses is contained in the technical data management system (TDMS), DTN: SN0004T0501600.004.

6.2.1 Transport Model Parameters

The parameters controlling groundwater flow in the SZ site-scale model are derived from the calibration process, but the parameters influencing radionuclide transport are independent of the calibration process. The transport parameters are divided into those parameters that are assigned a constant value for all stochastic realizations and those parameters that are varied among the stochastic realizations. The parameters that are assigned constant values are those to which radionuclide transport is relatively insensitive or those for which the uncertainty is relatively small. A few parameters (e.g., thermal conductivity) have no impact on the model simulations

because the heat transport solution is disabled, but are required for the FEHM code to function. The transport parameters and the values used for both constant parameters and the stochastic parameters are discussed in detail in a supporting report (CRWMS M&O 2000b).

6.2.1.1 Constant Parameters

Constant parameters are those parameters that do not change in value from realization to realization in the Monte Carlo TSPA simulations of SZ flow and transport. Constant values of permeability, as determined in the calibration of the SZ site-scale flow model, are assigned to hydrogeologic units and features. Although not utilized in the model simulations, constant values of thermal conductivity and heat capacity are assigned as required “place holders” in the FEHM input files. Constant values of temperature are assigned to all nodes of the SZ site-scale flow and transport model based on the depth below the land surface and a linear geothermal gradient with depth. Solute transport parameters that are given constant values within hydrogeologic units of the model include matrix porosity, bulk density, and effective porosity for those hydrogeologic units that are not present along the flowpath from the repository.

Within most of the domain of the SZ site-scale flow and transport model, matrix porosity and bulk density are assigned uniform values within given hydrogeologic units. However, within the area of the Integrated Site Model (ISM) the heterogeneous rock-properties model values of matrix porosity and bulk density are applied on a node by node basis within the SZ site-scale model. The values for these parameters are assigned within those hydrogeologic units for which the rock-properties model exists (Prow Pass Tuff, Calico Hills Formation, and the Topopah Springs welded unit). These units constitute a relatively thin portion of the upper SZ in the area near the proposed repository. The values of matrix porosity and bulk density within the ISM are taken from the “expected-value” model of rock properties, developed through geostatistical simulation techniques. These values are extracted from the rock properties model files in DTN: SNT05070198001.001. A plot of the matrix porosity at the water table in the SZ site-scale flow and transport model is shown in Figure 1. The values of matrix porosity within the ISM are incorporated into the SZ site-scale model in the FEHM code input files containing the “spr” macro, which controls the streamline particle tracking algorithm. Because of the structure of this input file, the nodes are associated with classes of matrix porosity, with each class spanning a range of 0.02 (e.g., 0.24 to 0.26). The values of bulk density within the ISM are directly assigned to nodes in the file “*props_05_ism3.macro*”.

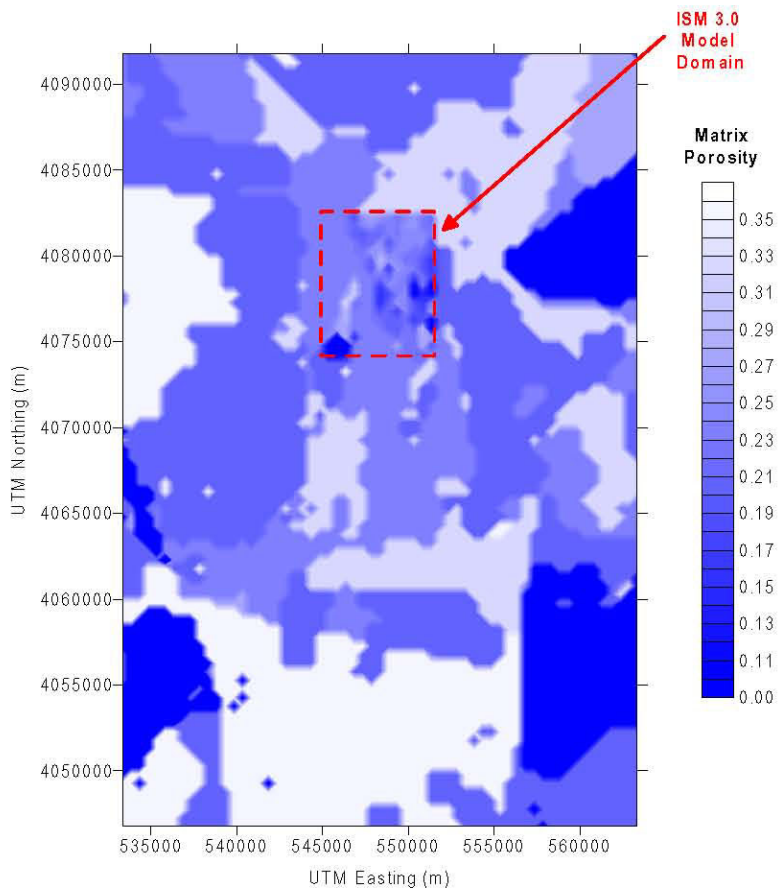


Figure 1. Matrix and Effective Porosity at the Water Table of the SZ Site-Scale Flow and Transport Model. The area in which heterogeneous values of matrix porosity from the ISM rock properties model is outlined by the dashed line, as indicated. (DTN: SNT05070198001.001 and SN0004T0501600.005)

6.2.1.2 Stochastic Parameters

In general, parameters to which the model results are sensitive, due to the combination of the numerical importance of the parameter in the model and the uncertainty in the parameter value, are represented stochastically in the analysis of SZ flow and transport. A summary of the stochastic parameters identified for incorporation in the TSPA analyses is given in Table 4.

Table 4. Stochastic Parameters Used in the Analysis

Parameter Identifier	Description
FPLAW	Parameter to determine the western boundary of the alluvial uncertainty zone
FPLAN	Parameter to determine the northern boundary of the alluvial uncertainty zone
NVF19	Effective porosity of the valley fill hydrogeologic unit and the alluvial uncertainty zone
NVF7	Effective porosity of the undifferentiated valley fill hydrogeologic unit
FISVO	Flowing interval spacing in the fractured volcanic hydrogeologic units (m) (log transformed)
FPVO	Flowing interval porosity in the fractured volcanic hydrogeologic units (log transformed)
DCVO	Effective diffusion coefficient in the fractured volcanic hydrogeologic units (log transformed)
KDNPVO	Sorption coefficient for neptunium in fractured volcanic hydrogeologic units (ml/g)
KDNPAL	Sorption coefficient for neptunium in alluvium units (ml/g)
KDIAL	Sorption coefficient for iodine in alluvium units (ml/g)
KDUVO	Sorption coefficient for uranium in fractured volcanic units (ml/g)
KDUAL	Sorption coefficient for uranium in alluvium units (ml/g)
GWSPD	Parameter determining the groundwater flux case
KDRN10	Sorption coefficient of strongly sorbing radionuclides for the reversible sorption model of colloid-facilitated transport (ml/g)
KDRN9	Sorption coefficient of moderately sorbing radionuclides for the reversible sorption model of colloid-facilitated transport (ml/g)
CORAL	Retardation factor for colloids in the alluvium units for the irreversible sorption model of colloid-facilitated transport (log transformed)
CORVO	Retardation factor for colloids in the fractured volcanic units for the irreversible sorption model of colloid-facilitated transport (log transformed)
SRC4X	Parameter defining the east-west location of the radionuclide source in source region 4
SRC4Y	Parameter defining the north-south location of the radionuclide source in source region 4
SRC3X	Parameter defining the east-west location of the radionuclide source in source region 3
SRC3Y	Parameter defining the north-south location of the radionuclide source in source region 3
SRC2X	Parameter defining the east-west location of the radionuclide source in source region 2
SRC2Y	Parameter defining the north-south location of the radionuclide source in source region 2
SRC1X	Parameter defining the east-west location of the radionuclide source in source region 1
SRC1Y	Parameter defining the north-south location of the radionuclide source in source region 1
HAVO	Parameter determining horizontal anisotropy case
L DISP	Longitudinal dispersivity (m) (log trasformed)
KDTCAL	Sorption coefficient for technetium in alluvium units (ml/g)
Kc_Am_gw_Colloid	Kc parameter for equilibrium colloid-facilitated radionuclide transport (log transformed)

Uncertainty distributions for stochastic parameters, as defined in CRWMS M&O 2000b, are entered in the GoldSim software code input file for the TSPA-SR simulator. Parameter vectors are drawn for 100 realizations of the SZ stochastic parameters using the Latin Hypercube method in the GoldSim software code. The resulting values of the parameters are contained in the file “*RIP.dat*”. A table containing the parameter values for the stochastic parameters in all 100 realizations is presented in Attachment I.

6.2.1.3 Pre-Processor Software Routine

An automated method for preparing the FEHM input files is implemented using a pre-processor software routine, SZ_Pre v. 1.0. This routine reads a file containing a table of the stochastic parameter values that are to be used in the realizations of the SZ site-scale flow and transport model. The routine also reads a file containing tabulated information used to control the FEHM simulation, such as the time step and total simulation time for each realization. Using an existing set of FEHM input files as templates, the SZ_Pre routine writes the appropriate parameter values into the input files for each stochastic realization. A listing of the FORTRAN source code for the SZ_Pre routine is given in Attachment II.

The parameter values for the stochastic parameters are read by the SZ_Pre routine from the file named “*RIP.dat*”. This file contains the stochastic parameter vector for each realization on one line. The SZ_Pre routine then reads values used to control the simulations from the file named “*control_runs.txt*”. The values of the Courant factor, time step, and total simulation time contained in the file “*control_runs.txt*” vary among the radionuclides simulated and among the realizations of the SZ flow and transport system.

Transformations of some parameter values are performed by the SZ_Pre software routine before the parameters are written in the FEHM software code input files of the SZ site-scale flow and transport model. The basis for these transformations is explained fully in the report on parameter uncertainty (CRWMS M&O 2000b).

The parameters FPLAW and FPLAN are used to scale the location of the western and northern boundaries of the alluvial uncertainty zone, respectively. These parameters are used to perform a uniform scaling of the southwest, northwest, and northeast vertices of the alluvial uncertainty zone between the minimum and maximum values shown in Table 5. The coordinates of the alluvial uncertainty zone are written to the file “*final_05_w_fence.macro.00_00.xxxx*”, where xxxx is the realization number.

Table 5. Coordinates of the Vertices of the Alluvial Uncertainty Zone

Vertex	UTM Easting (m)	UTM Northing (m)
Northwest (maximum westerly)	552791.	4066370.
Northwest (minimum westerly)	554152.	4066320.

Vertex	UTM Easting (m)	UTM Northing (m)
Southwest (maximum westerly)	546653.	4057620.
Southwest (minimum westerly)	548588.	4057090.
Northeast	557577.	4066320.
Southeast	555550.	4055400.

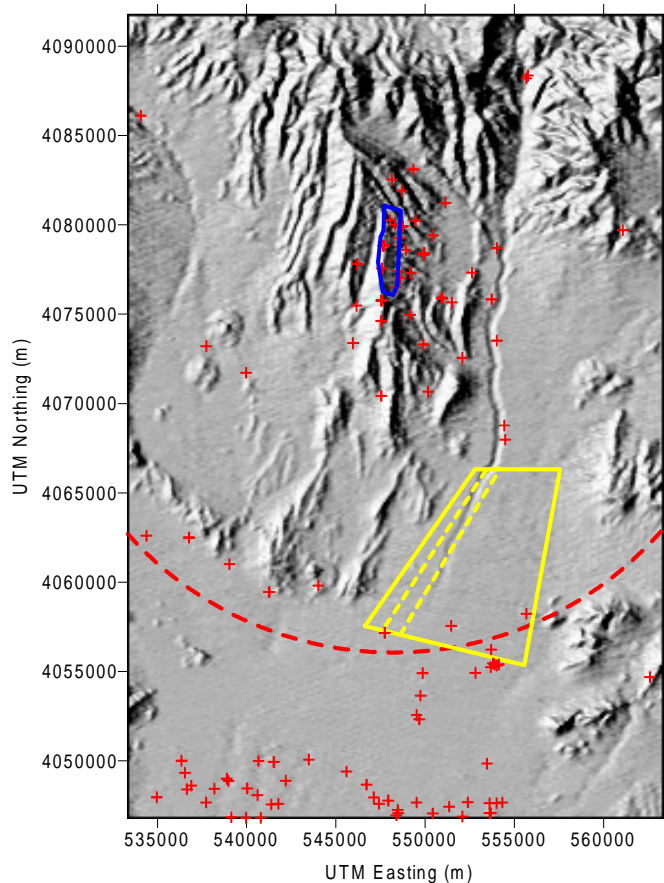


Figure 2. Alluvial Uncertainty Zone. The outline of the alluvial uncertainty zone is shown by the solid yellow line. Base map is a shaded relief map of surface elevation. The outline of the repository is shown by the solid blue line. Locations of wells with water-level measurements are indicated by the red crosses.

The parameters NVF19 and NVF7 are direct samplings of the effective porosity in the valley fill and undifferentiated valley fill hydrogeologic units and are written into the file “01_base_case.dat.yy_00.xxxx”, where yy is the radionuclide indicator and xxxx is the realization number. An explanation of the conceptual basis for the effective porosity approach in the valley-

fill units is given in CRWMS M&O 2000b. In addition, these values of effective porosity in the alluvium are used to calculate the adjusted sorption coefficient for sorbing radionuclides, as explained in the report on parameter uncertainty (CRWMS M&O 2000b), according to the relationship:

$$K_d^{new} = K_d^{orig} \cdot \frac{\phi_e}{\phi_T} \quad (\text{Eq. 1})$$

where: K_d^{new} = adjusted sorption coefficient, K_d^{orig} = original sorption coefficient, and ϕ_T = total porosity (0.35).

The parameter FISVO is transformed to linear space by taking the antilog₁₀ of the sampled value. The flowing interval spacing in the volcanic units is then translated into a value of fracture aperture from the relationship:

$$2b = 2B\phi_f \quad (\text{Eq. 2})$$

where $2b$ is the fracture aperture, $2B$ is the flowing interval spacing, and ϕ_f is the flowing interval porosity (antilog₁₀ of parameter FPVO). The calculated value of fracture aperture is written to the file “*sptr_1000.macro.yy_zz.xxxx*”, where *yy* is the radionuclide indicator, *zz* is the source region, and *xxxx* is the realization number. The parameter FPVO is transformed to linear space by taking the antilog₁₀ of the sampled value. The resulting value of flowing interval porosity is written to the files “*01_base_case.dat.yy_00.xxxx*” and “*props_05_ism3.macro.00_00.xxxx*”, where *yy* is the radionuclide indicator and *xxxx* is the realization number.

The parameter DCVO is transformed to linear space by taking the antilog₁₀ of the sampled value. The resulting value of effective diffusion coefficient is written to the file “*sptr_1000.macro.yy_zz.xxxx*”, where *yy* is the radionuclide indicator, *zz* is the source region, and *xxxx* is the realization number. The values of effective diffusion coefficient for radionuclides subject to the K_c model of colloid-facilitated transport are adjusted according to the relationship:

$$D_e^{adjusted} = \frac{D_e}{(1 + K_c)^2} \quad (\text{Eq. 3})$$

where $D_e^{adjusted}$ is the adjusted effective diffusion coefficient and D_e is the effective diffusion coefficient. The partition coefficient (K_c) conceptual model of colloid-facilitated transport of reversibly sorbed radionuclides is described in CRWMS M&O 2000b and the underlying theoretical derivation of the model is presented in CRWMS M&O 1997, pp. 8-32 to 8-36.

The parameters KDNPVO and KDUVO are written as the sorption coefficients in the matrix of the volcanic units directly into the appropriate files named “*sptr_1000.macro.yy_zz.xxxx*”. The parameters KDNPAL, KDIAL, KDUAL, and KDTCAL are modified by the values of effective porosity in the alluvium to calculate the adjusted sorption coefficient, as described above (see Equation 1). The resulting values of adjusted sorption coefficient are written to the files “*sptr_1000.macro.yy_zz.xxxx*”, where *yy* is the radionuclide indicator, *zz* is the source region, and *xxxx* is the realization number.

The parameters KDRN10 and KDRN9 are used to determine the values of the sorption coefficients in the matrix of the volcanic units and in the alluvium for the K_c model of colloid-facilitated transport for strongly sorbing and moderately sorbing radionuclides, respectively. The parameters KDRN10 and KDRN9 are converted to a value of the sorption coefficient in the SZ_Pre software routine by multiplying by 100 ml/g and 50 ml/g, respectively. This is equivalent to a uniform distribution of 0.0 to 100.0 ml/g for the K_d of strongly sorbing radionuclides and a uniform distribution of 0.0 to 50.0 ml/g for the K_d of moderately sorbing radionuclides. The resulting values of the sorption coefficient for the volcanic matrix are written to the files “*sprt_1000.macro.Kc_zz.xxxx*” and “*sprt_1000.macro.Kf_zz.xxxx*” where *zz* is the source region, and *xxxx* is the realization number. The values of the sorption coefficient in the valley fill and undifferentiated valley fill hydrogeologic units for the colloid-facilitated transport of radionuclides with the K_c model are modified by the value of K_c (parameter *Kc_Am_gw_Colloid*), according to the relationship:

$$K_d^{new} = \frac{K_d^{orig}}{(1 + K_c)} \quad (\text{Eq. 4})$$

as derived from CRWMS M&O 1998a, Equations 8-3 and 8-8, p. 8-54 and 8-56. The adjusted values of the sorption coefficient for the alluvial units are written to the files “*sprt_1000.macro.Kc_zz.xxxx*” and “*sprt_1000.macro.Kf_zz.xxxx*”, where *zz* is the source region, and *xxxx* is the realization number.

The parameters CORAL and CORVO are transformed to linear space by taking the antilog₁₀ of the sampled values. The resulting value of the colloid retardation factor in the alluvium units is converted to a value of effective sorption coefficient according to the relationship:

$$K_d^{eff} = \frac{(R_f - 1)\phi_{eff}}{\rho_b} \quad (\text{Eq. 5})$$

where K_d^{eff} is the effective K_d , R_f is the retardation factor, ϕ_{eff} is the effective porosity, and ρ_b is the bulk density. The resulting value of the effective sorption coefficient is written to the files “*sprt_1000.macro.Pu_zz.xxxx*”, where *zz* is the source region, and *xxxx* is the realization number. The retardation factor in the fractured volcanic units is written directly into the files “*sprt_1000.macro.Pu_zz.xxxx*” as the retardation factor in the fractures.

The parameters SRC4X, SRC4Y, SRC3X, SRC3Y, SRC2X, SRC2Y, SRC1X, and SRC1Y are used to linearly scale the x and y location within the rectangular area of each source region. The coordinates of the vertices of the rectangular areas are given in Figure 3. The resulting x and y coordinates (UTM meters) for each source location are written to the files “*sprt_1000.macro.Pu_zz.xxxx*”, where *zz* is the source region, and *xxxx* is the realization number.

The parameter LDISP is transformed to linear space by taking the antilog₁₀ of the sampled value to obtain the value of longitudinal dispersivity. The values of horizontal transverse dispersivity and vertical transverse dispersivity are calculated based on their statistical correlation with the longitudinal dispersivity, as explained in CRWMS M&O 2000b. The resulting values of longitudinal, horizontal transverse, and vertical transverse dispersivity are written to the files

“*sptr_1000.macro.yy_zz.xxxx*”, where *yy* is the radionuclide indicator, *zz* is the source region, and *xxxx* is the realization number.

6.2.2 Radionuclide Source in the Saturated Zone

The source of radionuclide contamination entering the SZ for simulations of radionuclide transport with the SZ site-scale flow and transport model is specified as a point within each of four source regions beneath the repository (see Figure 3). The point source is located at an elevation of 725 m, which is approximately 5 m below the water table over most of the area beneath the repository. This vertical placement is in the middle of the upper grid blocks in the model and avoids placing the particles too near the upper boundary of the model. The horizontal location of the point source in each of the four source regions varies stochastically from realization to realization, reflecting uncertainty in the location of leaking waste package(s) and transport pathways in the UZ. Radionuclide transport simulations are performed using 1000 particles, which are released at the point source location at the beginning of the simulation.

Radionuclide mass that reaches the water table from the UZ in the TSPA simulator is assigned to one of the four source regions as defined by the quadrants shown in Figure 3. This radionuclide mass represents the source term used in the convolution integral method for that source region for a given time step. A point source of radionuclide mass from an entire quadrant of the UZ transport model is physically realistic for the situation in which contamination is coming from a single leaking waste package or in which a high degree of groundwater flow focusing occurs in the UZ flow system. Combining the radionuclide mass from a quadrant of the UZ transport model at later times, when multiple leaking waste packages contribute contamination, may not be physically realistic, but represents a conservative approximation from the perspective of repository performance.

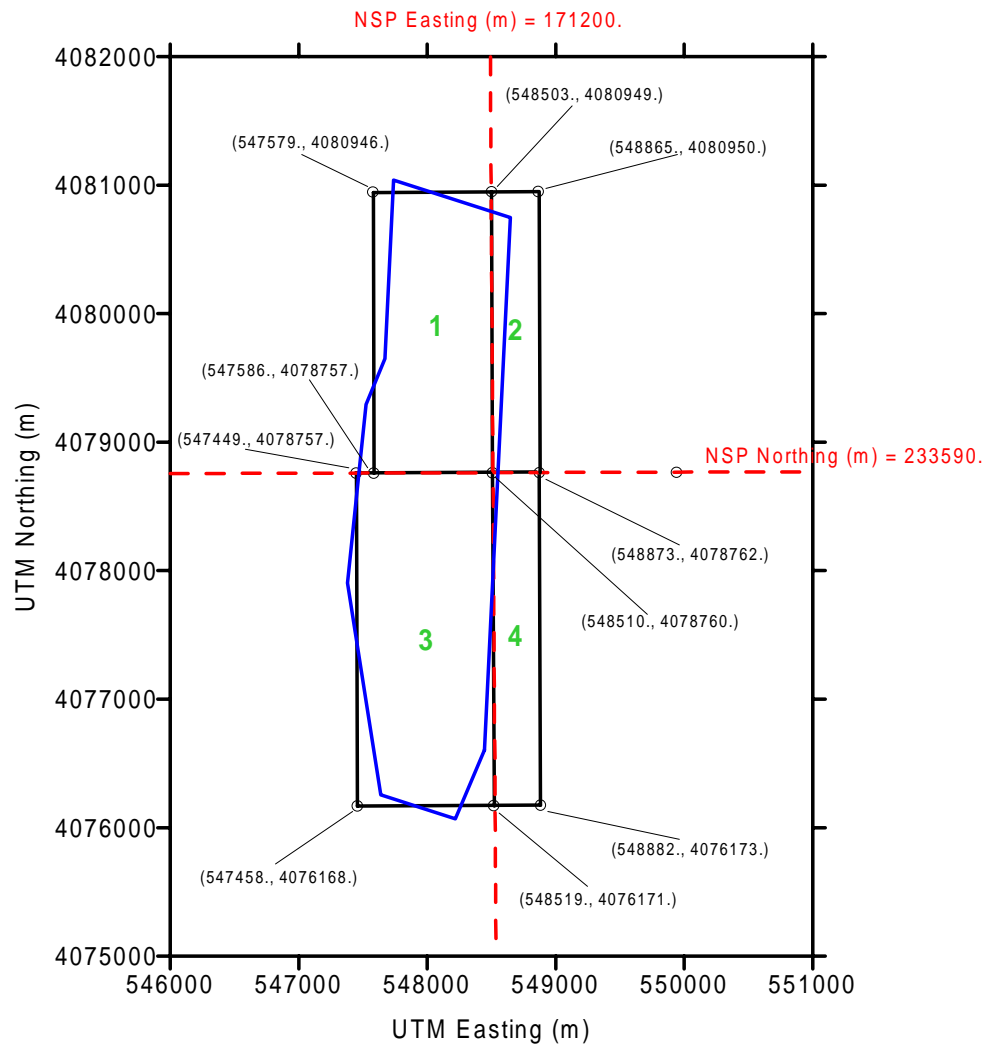


Figure 3. Radionuclide Source Regions for the SZ Site-Scale Flow and Transport Model. Source regions are outlined with the solid black rectangles and numbered from 1 to 4. The coordinates of the vertices of the source region rectangles are given in UTM coordinates (m). The outline of the repository is shown by the blue line (Source: CRWMS M&O 1999b). The dashed red lines indicate the quadrants from which radionuclide arrivals from the unsaturated zone model are applied to the SZ source regions. Coordinates of the dashed red lines are given in Nevada State Plane (NSP) coordinates (m).

6.2.3 Recharge from the UZ Site-Scale Flow Model

Within the area of the UZ site-scale flow model, the simulated groundwater flux at the bottom boundary of the UZ flow model (i.e., the water table) is applied as recharge to the upper boundary of the SZ site-scale flow and transport model. The values of recharge from the UZ site-scale model area used in the SZ site-scale flow model calibration are taken from a previous version of the UZ site-scale flow model (CRWMS M&O 2000a and CRWMS M&O 1999c, p.

6). For the analysis documented in this AMR, the values of recharge within the area of the UZ site-scale flow model are updated to utilize the most current UZ flow modeling results. Updating the recharge from the UZ site-scale flow model for the SZ radionuclide transport simulations for TSPA-SR results in consistency between the UZ flow modeling and the SZ flow and transport modeling, as implemented in the TSPA analyses.

The simulated groundwater flux at the water table from the UZ site-scale model is taken from the model simulation for the present climate state, mean-infiltration case, and perched-water conceptual model #2 (DTN: LB990801233129.004). Elements in the UZ site-scale flow model at the bottom boundary of the model (i.e., the water table) are identified by the prefix “BT” in the input and output files. Elements that are associated with fracture flow use the prefix “F” and elements for matrix flow use the prefix “M” in this dual-permeability model. These prefixes are used to extract the 1324 elements at the water table in the UZ site-scale flow model using the UNIX “grep” command. The following two commands are used to perform the extraction:

```
“grep BT.....F pa_pchm2.out>extract_F2.out”
“grep BT.....M pa_pchm2.out >extract_M2.out”
```

The two output files “*extract_F2.out*” and “*extract_M2.out*” contain the groundwater flux at the water table boundary (in kg/s) in the fourth column of the files for the fracture and matrix components of flow, respectively. These data are combined in an Excel spreadsheet in the file “*wt_flux_uz_present_mean_2.xls*” and the flux is converted to a total recharge rate in mm/year. These values of recharge from the UZ model are combined with the recharge estimates for the rest of the SZ site-scale model area with 500 m resolution. These values of recharge are imposed as values of specified flux in the file “*flow_recharge_combine_newUZ.macro*”, as an input file to the FEHM code for the SZ site-scale flow and transport model.

Verification of the flux computations in the Excel spreadsheet “*wt_flux_uz_present_mean_2.xls*” is provided in this paragraph. The value of fracture flux from cell Bta 1 in file “*extract_F2.out*” (0.30633E-03 kg/s) matches the value of fracture flux from cell Bta 1 (row 6) in the spreadsheet file “*wt_flux_uz_present_mean_2.xls*” in column G (3.06E-04 kg/s). The value of matrix flux from cell Bta 1 in file “*extract_M2.out*” (0.37091E-03 kg/s) matches the value of matrix flux from cell Bta 1 in the spreadsheet file “*wt_flux_uz_present_mean_2.xls*” in column H (3.71E-04 kg/s). The value for the total flux for cell Bta 1 is calculated as the sum of the values in columns G and H as 6.77E-04 kg/s in the spreadsheet file “*wt_flux_uz_present_mean_2.xls*”, which matches the hand-calculated value. The flux per unit area from cell Bta 1 in the spreadsheet file “*wt_flux_uz_present_mean_2.xls*” in column K ($7.65\text{E-}09 \text{ kg/s m}^2$) is calculated by dividing the total flux in column I (6.77E-04 kg/s) by the connection area in column J (8.86E+04 m²), which matches the hand-calculated value. The flux per unit area from cell Bta 1 in the spreadsheet file “*wt_flux_uz_present_mean_2.xls*” in column K ($7.65\text{E-}09 \text{ kg/s m}^2$) is converted to a value of 0.241 mm/year (column L) by multiplying by the conversion factor (31557600 = (1m³/1000 kg)(1000 mm/m)(3155760 s/year)). Hand calculation confirms the value calculated in the spreadsheet.

6.2.4 Radionuclide Release to the Biosphere

The hypothetical release of radionuclides from groundwater in the SZ to the biosphere occurs by pumping of groundwater as the water supply for a future farming community in the nominal case of the TSPA-SR. This hypothetical community is located along the groundwater flowpath from the repository in Amargosa Valley at a distance of 20 km, based on draft regulatory guidance (NRC, 1998, Section 63.115). Radionuclide concentrations in the water supply of the hypothetical farming community are calculated by assuming that all radionuclide mass is captured by pumping wells and that this mass is uniformly distributed in the total volume of groundwater used by the community. Complete capture of the radionuclide plume by groundwater pumping is a reasonable assumption, given the relatively large volumetric groundwater usage of the hypothetical community. The assumption of complete capture is also a bounding, conservative approach. Although it may be reasonably expected that variations in radionuclide concentration would exist among the pumping wells in the community, redistribution of radionuclides by multiple pathways of radionuclide migration in the biosphere would tend to homogenize the dose among the population.

The breakthrough curves of radionuclide mass arrival at the 20 km distance are simulated with the SZ site-scale flow and transport model by obtaining output of particle travel time from the FEHM code when a particle crosses a “fence” of nodes in the model grid. Three fences of nodes corresponding to travel distances of 5 km, 20 km, and 30 km are shown in Figure 4. These fences of grid nodes are located at the prescribed distance from the southern corner of the outline of the repository and extend from the upper surface to the lower surface of the SZ site-scale model domain. The SZ groundwater flow pathway from beneath the repository extends in a generally southerly direction and all particles are “counted” as they cross the intervening fences of grid nodes. An example set of mass breakthrough curves for neptunium at the three fences is shown in Figure 5.

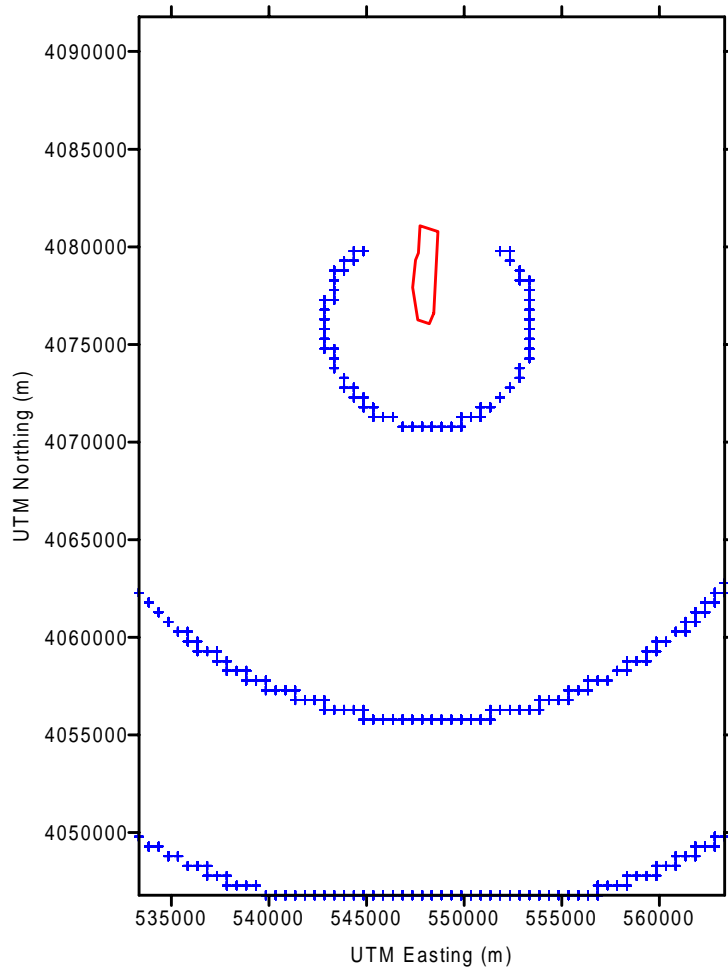


Figure 4. Nodes from the SZ Site-Scale Model Defining Fences at Which Radionuclide Mass Flux Breakthrough Curves are Output. Fence nodes at 5 km, 20 km, and 30 km distances are shown (DTN: SN0004T0501600.005). Repository outline shown with solid line (Source: CRWMS M&O 1999b).

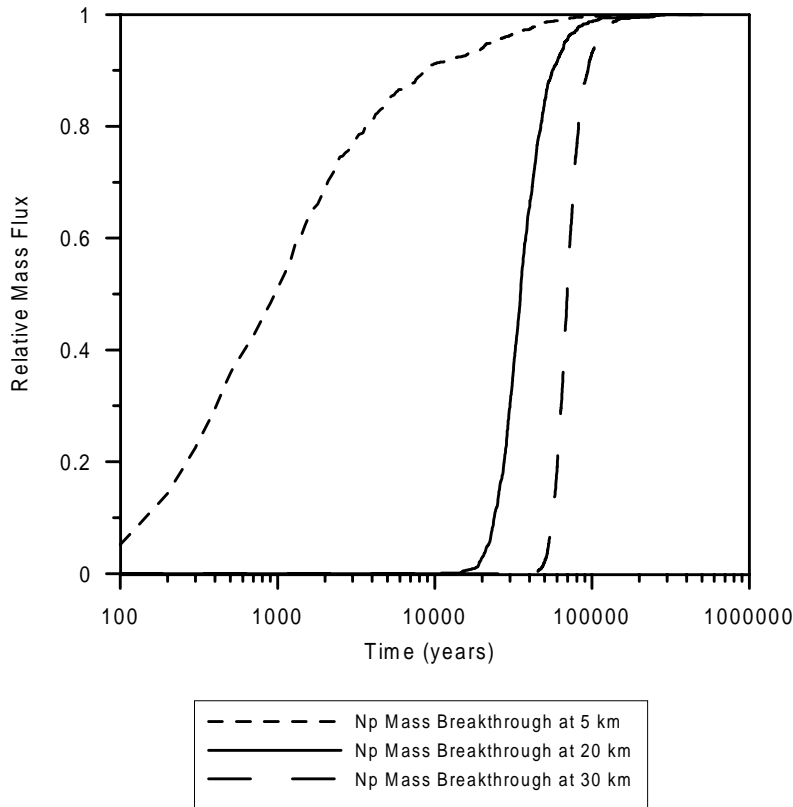


Figure 5. Simulated Neptunium Mass Breakthrough Curves at Three Distances from the Repository for the Expected-Value Case (DTN: SN0004T0501600.004).

6.2.5 Alternative Groundwater Flow Fields

In addition to the relatively high degree of uncertainty in the radionuclide transport characteristics of the SZ system, there is significant uncertainty in the groundwater flow in the system. Uncertainties exist both in the SZ groundwater flux downgradient of the repository and in the direction of groundwater flow. Uncertainty in groundwater flux for three discrete cases is quantified based on the results of the SZ expert elicitation (CRWMS M&O 1998b, p. 3-43, DTN: MO0003SZFWTEEP.000 and CRWMS M&O 2000b). Uncertainty in the direction of groundwater flow along the flowpath from the repository is incorporated as alternative groundwater flow fields, with and without anisotropy in horizontal permeability (CRWMS M&O 2000b). The result of considering both types of uncertainty is six alternative groundwater flow fields (three flux cases times two anisotropy cases).

Implementation of the alternative groundwater flow fields is accomplished by establishing a steady-state solution of groundwater flow in the SZ site-scale model for each of the six cases. The steady-state conditions for each of these cases are imposed as the initial conditions for the

appropriate TSPA realizations of radionuclide transport. In addition, a separate set of input files for the SZ site-scale flow and transport model that incorporate modifications to the boundary conditions and values of permeability for each case are constructed. Each realization is assigned to the appropriate flow field based on the values of the stochastic parameters (GWSPD and HAVO) that represent uncertainty in groundwater flux and horizontal anisotropy, respectively (CRWMS M&O 2000b). The 100 realizations created for the SZ radionuclide transport calculations are divided among the alternative groundwater flow fields as indicated in Table 6.

Table 6. Realizations Assigned to Alternative Groundwater Flow Fields

	Low Flux Isotropic	Low Flux Anisotropic	Mean Flux Isotropic	Mean Flux Anisotropic	High Flux Isotropic	High Flux Anisotropic
Realization Number	13, 17, 24, 33, 37, 38, 47, 54, 61, 75, 83, 96	8, 14, 19, 23, 26, 28, 30, 50, 69, 70, 79, 95	2, 4, 11, 12, 16, 25, 29, 35, 39, 40, 43, 44, 51, 53, 56, 57, 68, 71, 73, 81, 82, 90, 91, 100	3, 7, 10, 18, 20, 22, 27, 32, 36, 41, 42, 46, 52, 55, 60, 62, 66, 77, 80, 84, 85, 86, 88, 89, 92, 93, 97, 99	1, 6, 9, 34, 45, 49, 58, 59, 72, 74, 76, 78, 87, 98	5, 15, 21, 31, 48, 63, 64, 65, 67, 94

6.2.5.1 Uncertainty in Groundwater Flux

Uncertainty in groundwater flux in the SZ system under present-day climatic conditions is incorporated into the analyses of radionuclide transport by defining three discrete cases: low-, mean-, and high-flux cases for groundwater flow. The three cases are implemented by scaling the groundwater flux in the entire domain of the SZ site-scale flow and transport model. The low-flux case is implemented such that groundwater fluxes in the flow field are 1/10 of the mean-flux case and the high-flux case has fluxes of 10 x the mean-flux case. This scaling is accomplished by simultaneously multiplying all values of permeability in the model and all values of groundwater flux at the model boundaries by a scaling factor. Given the linear nature of the SZ site-scale flow model, this method preserves the calibration to water level observations in wells established for the mean-flux case model. Preservation of the flow model calibration is demonstrated by comparing the plots of simulated head and residuals in head at wells for the mean-flux case shown in Figure 6 and the high-flux case (mean-flux case x 10) shown in Figure 7. Thus the flow pathways in the mean-flux case and the high-flux case are the same. The only difference in these alternative flow fields is the velocity of groundwater flow.

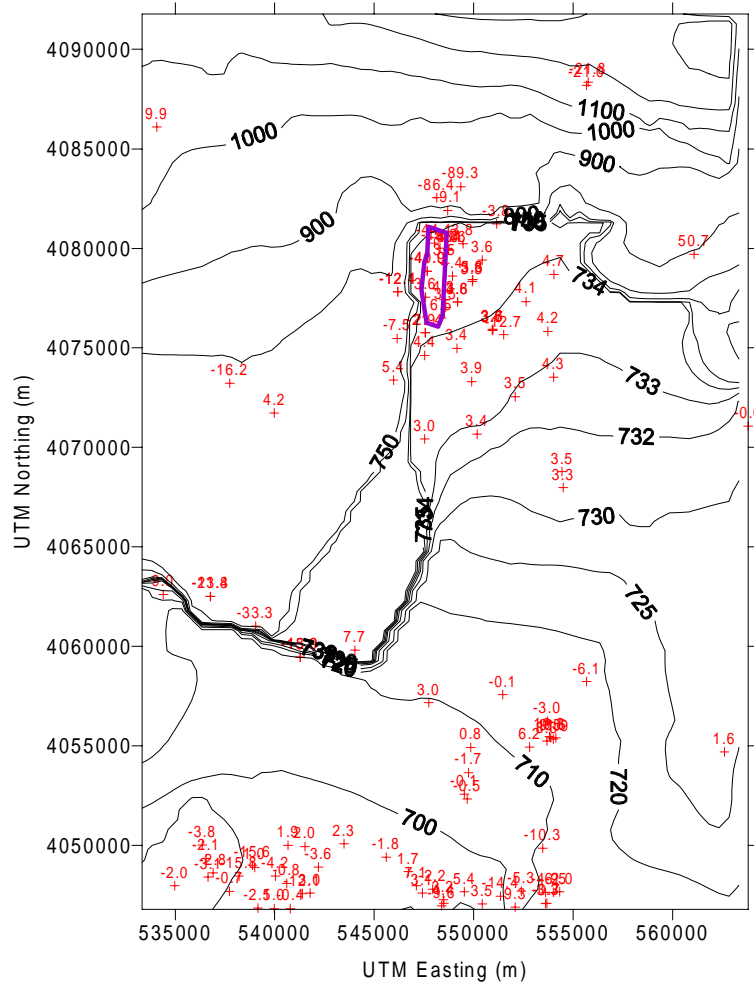


Figure 6. Simulated Heads and Residuals at Wells from the Mean Flux Case of the SZ Site-Scale Flow Model (DTN: SN0004T0501600.005). Contours show simulated head at the water table in units of meters above sea level. Head residuals at wells are shown in units of meters with the red labels. The repository outline is shown with the bold purple line in the upper central portion of the plot (Source: CRWMS M&O 1999b).

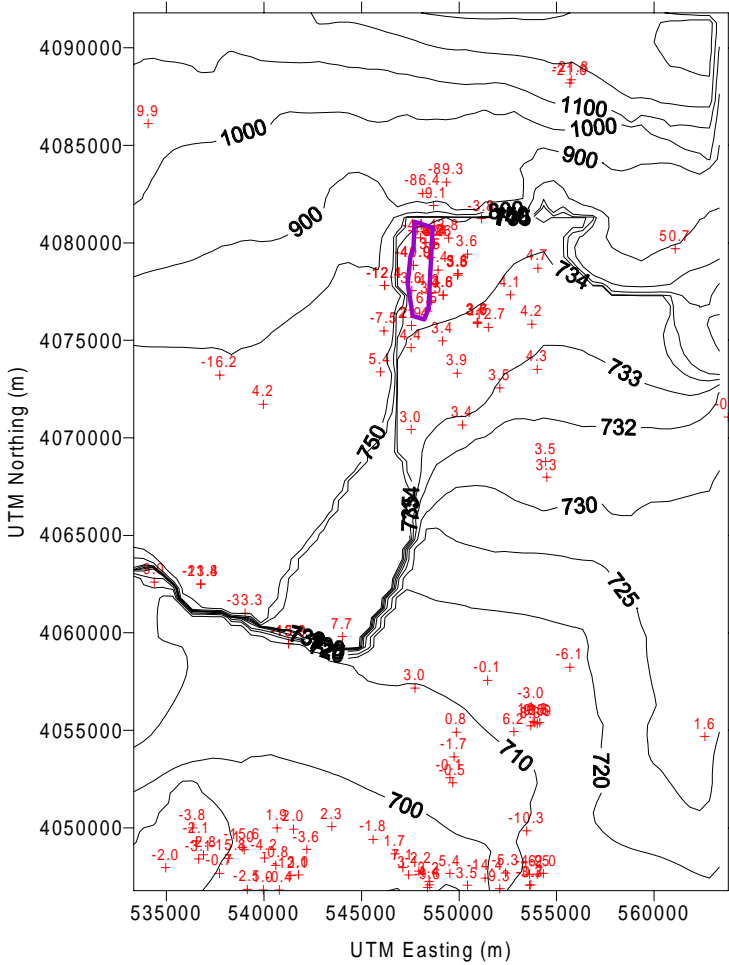


Figure 7. Simulated Heads and Residuals at Wells from the High Flux Case of the SZ Site-Scale Flow Model (DTN: SN0004T0501600.005). Contours show simulated head at the water table in units of meters above sea level. Head residuals at wells are shown in units of meters with the red labels. The repository outline is shown with the bold purple line in the upper central portion of the plot (Source: CRWMS M&O 1999b).

The probability of each of the three cases for a particular scaling factor can be determined from the cumulative distribution function (CDF) of uncertainty from the SZ expert elicitation. For a scaling factor of 10, the probability assigned to the low-flux case and the high-flux case is 0.24 and the probability assigned to the mean-flux case is 0.52 (CRWMS M&O 2000b).

6.2.5.2 Uncertainty in Horizontal Anisotropy

Horizontal anisotropy in permeability of fractured volcanic units near Yucca Mountain may result from the preferred orientation of faults and their interrelationship with the regional stress state (Ferrill et al., 1999, p. 6). The importance of anisotropy to repository performance is that a more southward flowpath would increase travel distances in the tuff and reduce the amount of flow in the alluvium (Ferrill et al., 1999, p. 7). A reduction in the flow path length in the alluvium would decrease the amount of total radionuclide retardation that could occur for those radionuclides with greater sorption coefficients in alluvium than in fractured volcanic rock matrix. In addition, potentially limited matrix diffusion in the fractured volcanic units could lead to shorter travel times in the volcanic units relative to the alluvium.

Uncertainty in the horizontal anisotropy of permeability within the volcanic units near Yucca Mountain is incorporated into the analyses by defining two discrete cases of groundwater flow. The first case is isotropic and consists of the calibrated SZ site-scale flow model as documented in CRWMS M&O 2000a. The second case is anisotropic with an anisotropy ratio of 5:1. Anisotropy in permeability is imposed on the volcanic units in an area to the south and east of Yucca Mountain corresponding approximately to the surface outcrops of faulted volcanic rocks and extending to an elevation of 200 m above sea level (approximately 500 m below the water table in this area). Numerical limitations require that the permeability tensor be aligned with the principal coordinate directions in the FEHM code. To approximate the estimated north-northeast alignment of the direction of maximum permeability based on analysis of pumping test results (Winterle and La Femina, 1999), the values of permeability in the north-south direction are increased and are decreased in the east-west direction within the anisotropic zone. Values of permeability in the north-south direction are multiplied by 2.24 and divided by 2.24 in the east-west direction. This results in an anisotropy ratio of 5:1 and the geometric mean of values of permeability in the north-south and east-west directions for a given hydrogeologic unit is equal to the value of the original permeability in the isotropic case. Given the lack of information on the relative probabilities of these two alternative cases, the probabilities of the isotropic case and the anisotropic case are both set at 0.50.

Modification of the SZ site-scale flow model to incorporate horizontal anisotropy of permeability alters the steady-state solution of groundwater flow in terms of groundwater flowpaths and groundwater flux. No recalibration of the SZ site-scale flow model is performed for the anisotropic case. Comparison of the model calibration to water level observations in wells for the isotropic case (Figure 8) and the anisotropic case (Figure 9) indicates that the residuals of head simulated at wells differ by less than 1 m between the alternative groundwater flow fields. Given the absolute values of the residuals in the original calibration of the SZ site-scale flow model, modification of the model to include horizontal anisotropy does not represent a significant disruption of the calibration. Interestingly, incorporation of horizontal anisotropy of permeability generally decreases the absolute values of the residuals in head along the flowpath to the south and east from the repository. Given the relatively small improvement in flow model calibration associated with the imposition of horizontal anisotropy, it is not appropriate to conclude that the anisotropic case is necessarily the preferred conceptual model.

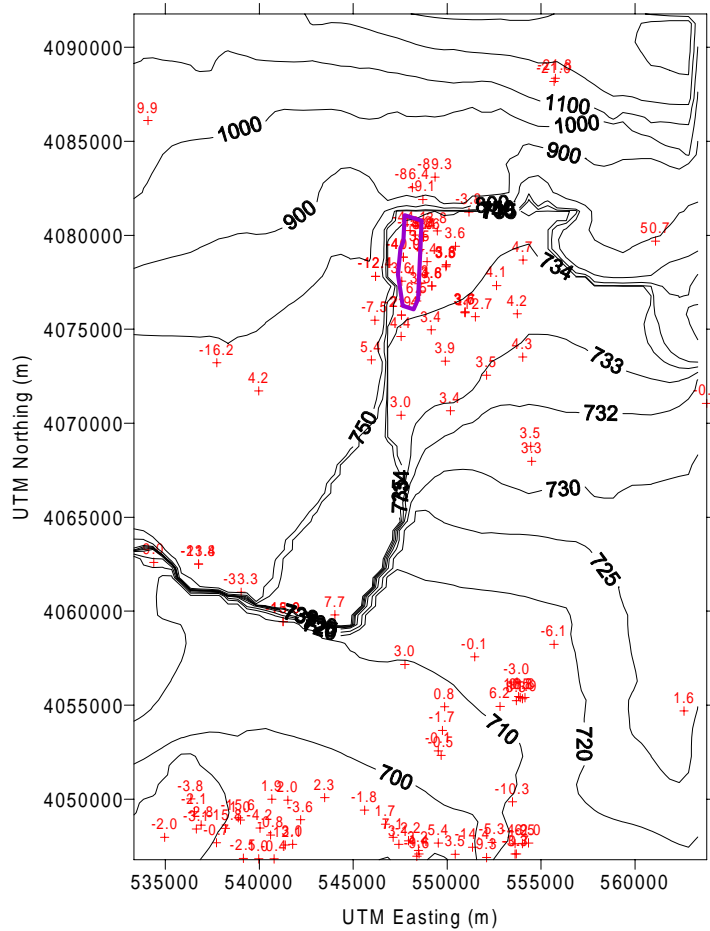


Figure 8. Simulated Heads and Residuals at Wells from the Isotropic Case of the SZ Site-Scale Flow Model (DTN: SN0004T0501600.005). Contours show simulated head at the water table in units of meters above sea level. Head residuals at wells are shown in units of meters with the red labels. The repository outline is shown with the bold purple line in the upper central portion of the plot (Source: CRWMS M&O 1999b).

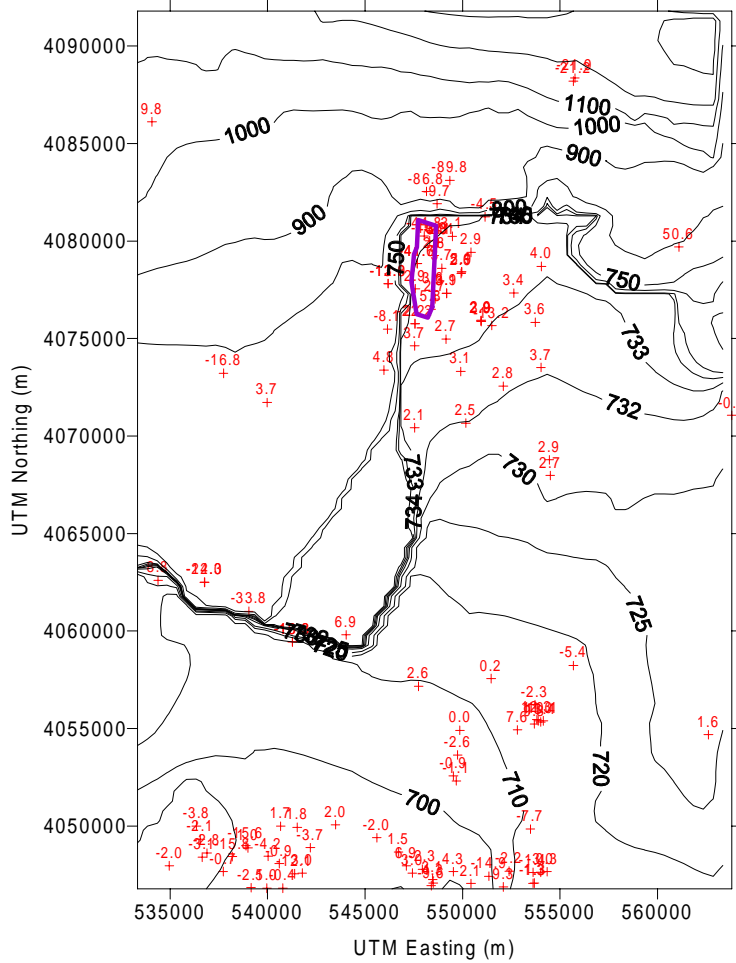


Figure 9. Simulated Heads and Residuals at Wells from the Anisotropic Case of the SZ Site-Scale Flow Model (DTN: SN0004T0501600.005). Contours show simulated head at the water table in units of meters above sea level. Head residuals at wells are shown in units of meters with the red labels. The repository outline is shown with the bold purple line in the upper central portion of the plot (Source: CRWMS M&O 1999b).

6.2.6 Implementation of Multiple Realizations

A series of radionuclide transport simulations are performed with the SZ site-scale flow and transport model for TSPA. A separate model run is conducted for each realization, for each radionuclide (or class of radionuclides), and for each of the four source regions. Parameter vectors for stochastic parameters are generated for all 100 realizations prior to the SZ site-scale model runs, using the parameter-sampling algorithm in the GoldSim software code. Results of the SZ site-scale flow and transport model runs are archived in files for use by the convolution integral subroutine of the TSPA simulator. UNIX script files are prepared to sequentially run the

transport simulations and save the output files. A post-processor software routine is used to reformat and combine the simulation results for the breakthrough curves into a format that can be used in the convolution integral method in the TSPA simulator.

An example UNIX script file for controlling multiple simulations with the FEHM code is given in Attachment IV of this report. This example script file is used to perform all simulations for carbon transport (no sorption) for those realizations with mean groundwater flux and isotropic horizontal permeability. The UNIX script files copy the appropriate FEHM input files that have been generated by the pre-processor for a given realization into the working directory, renaming the files to match the default input file names, and execute the FEHM computer code. The particle tracking output file generated by that model run is then copied to another directory containing simulation results and is given an identifying filename, “02_calib.sptr3.yy_zz.xxxx”, where yy is the radionuclide indicator, zz is the source region, and xxxx is the realization number. This sequence is repeated for each of the four source regions and for each of the realizations for a particular flow field by the script file.

All input files and output files containing the particle tracking results from the FEHM simulations of the SZ site-scale flow and transport model for this analysis are contained in the submittal to the Technical Data Management System under DTN: SN0004T0501600.005. Simulations are conducted in a directory structure that separates individual runs on the basis of radionuclide and SZ flow field, and this directory structure is preserved in the data submittal to the TDMS.

The Monte Carlo realizations of the one-dimensional radionuclide transport model for decay chains are conducted directly in the TSPA simulator with the GoldSim software code. The mass flux for the daughter radionuclides to the biosphere is used to calculate the contribution to total radiological dose from each of these daughter radionuclides, in a manner similar to the radionuclides from the three-dimensional SZ site-scale model.

6.2.7 Post-Processor Software Routine

A post-processing routine is used to convert the particle tracking results from the SZ site-scale flow and transport model to values of relative radionuclide mass flux and to format these results for input to the SZ_Convolute software code. The breakthrough curves from 100 realizations of the SZ system for a particular radionuclide and source region are combined in the output file of the post-processing routine SZ_Post v. 1.0. The FORTRAN source code for the software routine SZ_Post is included in Attachment III of this report.

The breakthrough curves that are output from the SZ_Post software routine consist of relative radionuclide mass flux as a function of time for distances of 5 km, 20 km, and 30 km from the repository. The relative radionuclide mass flux is determined for each time by normalizing the number of particles that have crossed the particular fence by the total number of particles having crossed that fence at the end of the simulation. This normalization of the radionuclide mass flux guarantees that the breakthrough curve attains a value of relative mass flux of 1.0 by the ending time of the simulation. This approach is a conservative approximation that insures that all

radionuclide mass entering the SZ system in the TSPA simulator exits the system to the biosphere (minus mass lost to radioactive decay in transit). In addition, the SZ_Post software routine queries the user for an additional longer time for which the relative mass flux is set to a value of 1.0. This time must be set to a value longer than the longest simulations to be performed with the SZ_Convolute software code.

The SZ_Post software routine combines the results from all 100 realizations by appending the breakthrough curves into a single file. The set of radionuclide mass breakthrough curves for each realization is preceded by the realization number and the number of lines of data for that realization.

6.3 RADIONUCLIDE TRANSPORT RESULTS

The results of radionuclide transport simulations using the SZ site-scale flow and transport model consist of the radionuclide mass breakthrough curves for eight species or classes of species. Results are obtained for 100 stochastic realizations of the SZ system and for one case utilizing the expected value for all stochastic parameters. These results constitute the “library” of SZ flow and transport simulation results that is accessed by the convolution integral software code (SZ_CONVOLUTE) in the TSPA-SR simulations with the GoldSim software code.

Variations in the location of the point source for radionuclide mass within each source region result in differences in the flowpaths taken in the SZ site-scale flow and transport model. Differences in flowpaths also result from variations in transverse dispersivity and horizontal anisotropy of permeability in the volcanic units. The general flowpaths from beneath the repository are shown by the particle tracking results in Figure 10, for a source of 100 particles randomly distributed under the outline of the proposed repository. Flow pathways are to the southeast initially and turn to the south and south-southwest along the flowpath. Narrowing of the plume of particle pathways is the result of convergent groundwater flow and increased specific discharge in the area where flow turns to the south and south-southwest in the SZ site-scale flow and transport model. The flowpaths remain relatively shallow in the SZ domain, staying within several hundred meters of the water table along the flowpath. Flowpaths occur through various volcanic units from beneath the repository to the contact with alluvium. The location of the contact between the volcanic units and the alluvium below the water table is uncertain, as discussed in Section 6.2.1.3 of this report. The flowpaths primarily remain in the alluvial uncertainty zone, the valley-fill unit, and the undifferentiated valley-fill unit from the contact between the tuffs and the alluvium to the southern boundary of the model.

6.3.1 Expected-Value Case

The simulated radionuclide mass breakthrough curves for the expected value case of the SZ site-scale flow and transport model are shown in Figure 11. The distribution of travel times in the SZ from beneath the repository to a distance of 20 km for the non-sorbing species (carbon) is significantly less than 10,000 years and predominantly less than 1000 years. Iodine and technetium are subject to minor sorption in the alluvium and have travel times of predominantly 1000 to 2000 years in the expected value case. For radionuclides that are irreversibly attached to

colloids the travel times in the SZ are somewhat less than 10,000 years for the expected value case. The other species that are subject to moderate to high sorption have simulated travel times in the SZ of greater than 10,000 years for the expected value case. The results presented in Figure 11 are for transport from source region 1 under the northern portion of the repository. Results vary somewhat among the source regions, having generally longer travel times from the northern source regions and generally longer travel times from the eastern source regions. It should be noted that the radionuclide mass breakthrough curves shown in Figure 11 and in subsequent figures do not include radioactive decay, which is implemented in the convolution integral portion of the TSPA analyses.

6.3.2 Stochastic Realizations

The simulated radionuclide mass breakthrough curves from 100 stochastic realizations for carbon, iodine, the K_c model of highly sorbing radionuclides, the K_c model of moderately sorbing radionuclides, neptunium, colloid-facilitated transport of irreversibly attached radionuclides, technetium, and uranium are shown in Figure 12 to Figure 19. These results illustrate the variability in radionuclide transport simulations among individual realizations and among species. Results for carbon indicate relatively short travel times of less than 1000 years for most realizations, but significantly longer distributions of travel times for some realizations. Iodine and technetium experience a small amount of retardation in alluvium and the resulting breakthrough curves in Figure 13 and Figure 19 indicate somewhat longer travel times relative to carbon. The results for neptunium shown in Figure 16 indicate significantly longer travel times than for carbon or technetium. Neptunium is subject to relatively minor sorption in the matrix of volcanic units and to moderate sorption in alluvium. Note that the time axis in Figure 16 extends to 100,000 years. Results for colloid-facilitated transport of strongly sorbing radionuclides with the K_c equilibrium model shown in Figure 14 show a large degree of retardation relative to the other species modeled. The simulated migration of strongly sorbing radionuclides is significantly enhanced relative to purely aqueous transport only for larger values of the K_c parameter (approximately greater than $K_c = 0.1$). Consequently, many of the realizations exhibit long travel times characteristic of retardation of strongly sorbing aqueous-phase radionuclides. Note that the time axis in Figure 14 is expanded to 1,000,000 years.

Radionuclide migration through the SZ affects total system performance in two ways. First, the saturated zone functions as a mechanism to delay the release of radionuclides to the biosphere. This delay potentially allows radioactive decay to attenuate the release of radionuclides to the biosphere. Second, there may be significant dilution of radionuclide concentrations that occur during transport in the SZ. Although the dispersive processes that lead to dilution are incorporated in the SZ site-scale flow and transport modeling, the simplified approach used to calculate concentrations in the water supply of the hypothetical farming community negates the need to analyze *in situ* radionuclide concentrations in the SZ.

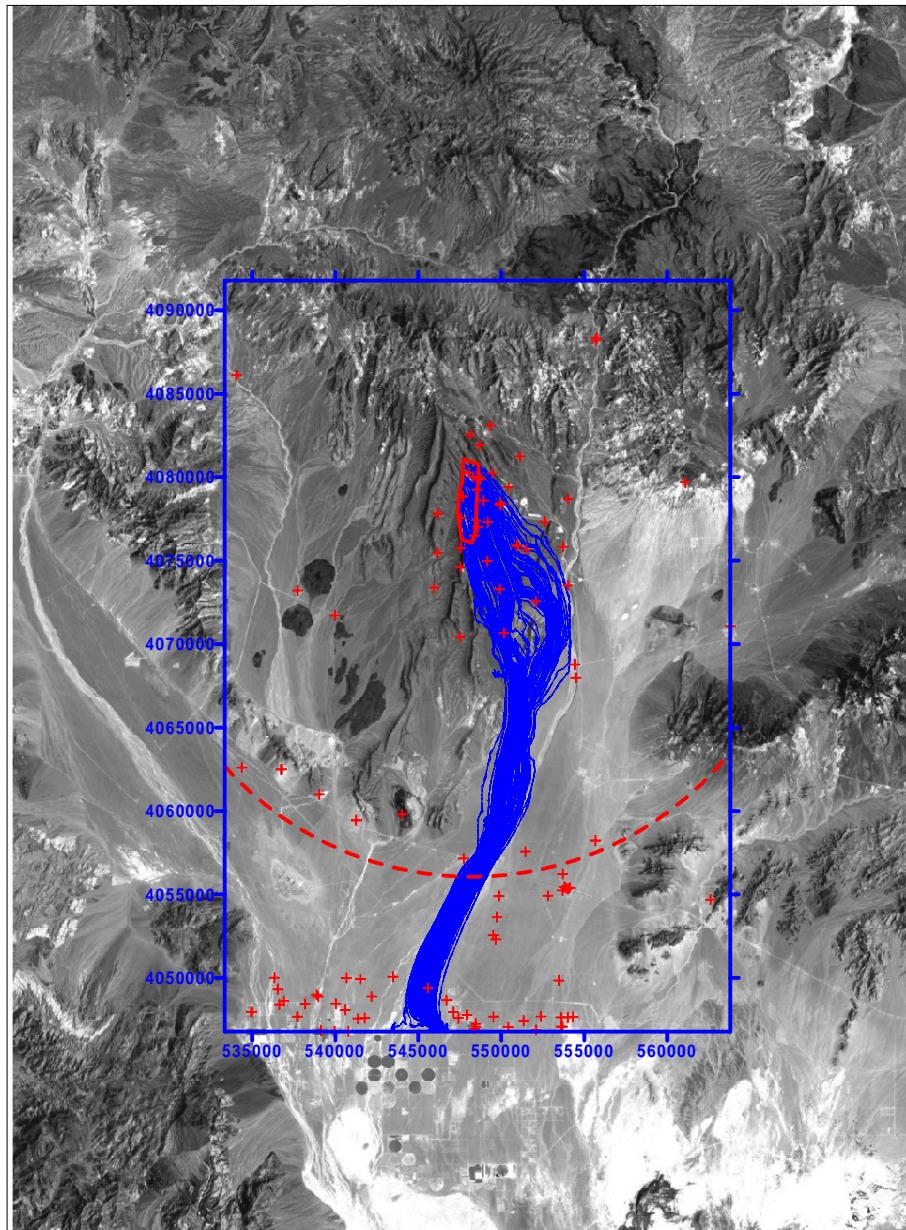


Figure 10. Simulated Particle Paths in the SZ Site-Scale Flow and Transport Model (DTN: SN0004T0501600.005). Simulated particle paths are shown in blue for isotropic conditions. The outline of the repository is shown with the bold red line (Source: CRWMS M&O 1999b). The 20 km fence is shown with the dashed red line. Locations of wells with water-level measurements are shown by the red cross symbols.

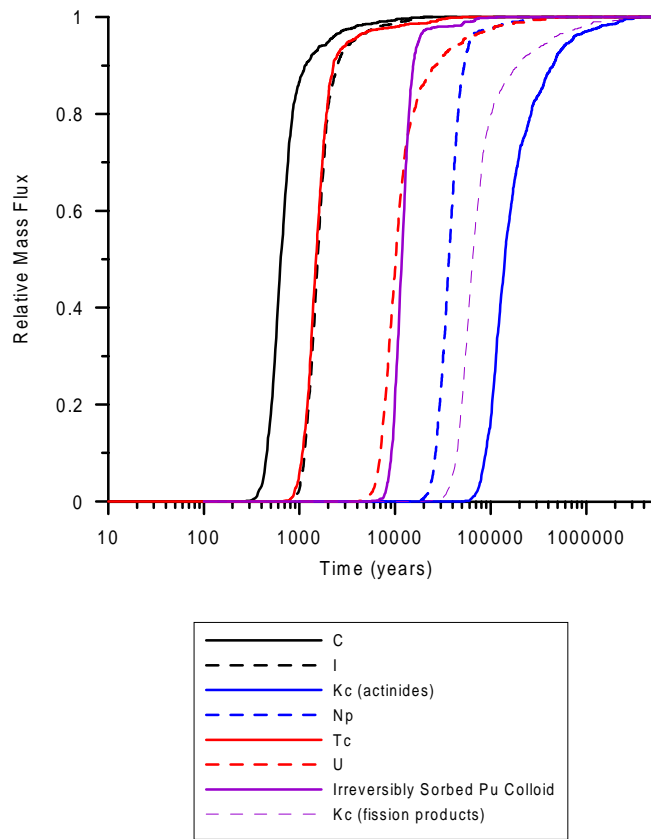


Figure 11. Simulated Unit Breakthrough Curves of Radionuclide Mass Flux for the Expected-Value Case. Results are shown for 20 km distance from source region 1 (DTN: SN0004T0501600.004).

Delay in the release of radionuclides afforded by the SZ is highly variable among the radionuclides that are simulated. Travel times through the SZ for ^{14}C , ^{99}Tc , and ^{129}I are primarily less than 10,000 years, with many realizations having residence times of less than 1000 years. Sorption of ^{99}Tc , and ^{129}I in the alluvial units results in somewhat longer travel times for these radionuclides. ^{14}C , ^{99}Tc , and ^{129}I are thus radionuclides of great concern for early releases from the repository and UZ, in the context of a 10,000 year regulatory standard. Travel times for Pu and Am subject to transport by irreversible attachment to colloids and U are near 10,000 years for the expected-value case as shown in Figure 11. ^{237}Np and radionuclides subject to reversible attachment to colloids have travel times in the range of about 20,000 years to 100,000 years in the SZ for the expected-value case, indicating that they are of lesser importance in the context of a 10,000 year regulatory standard.

Variability in the travel times through the SZ for a particular radionuclide among the realizations indicates a high degree of compound uncertainty in the transport processes in the SZ. Variations in the mean arrival times for different realizations apparently reflect the influences of sorption in the volcanic and alluvium units, the groundwater flux case, matrix diffusion in fractured units,

effective porosity in the alluvium units, and fraction of the flowpath in alluvium. Formal sensitivity analyses using the TSPA simulator will provide a quantitative assessment of the impact of individual parameters. The impacts of uncertainty in these processes, other than sorption, are visible in the breakthrough curves shown in Figure 12 for ^{14}C transport in the SZ. Variations among realizations for sorbing radionuclides are even greater (e.g., see Figure 16).

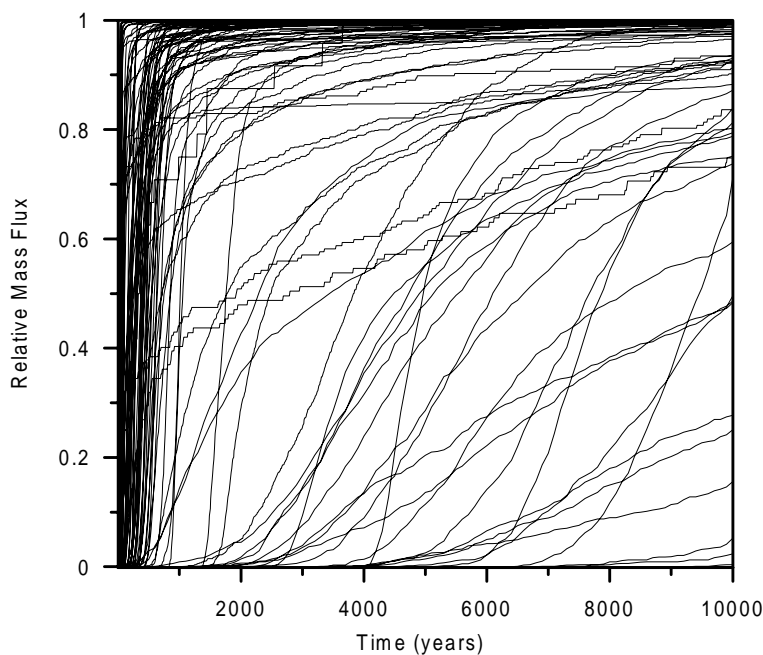


Figure 12. Simulated Unit Breakthrough Curves of Mass Flux for Carbon. Results are shown for 20 km distance from source region 1 (DTN: SN0004T0501600.004).

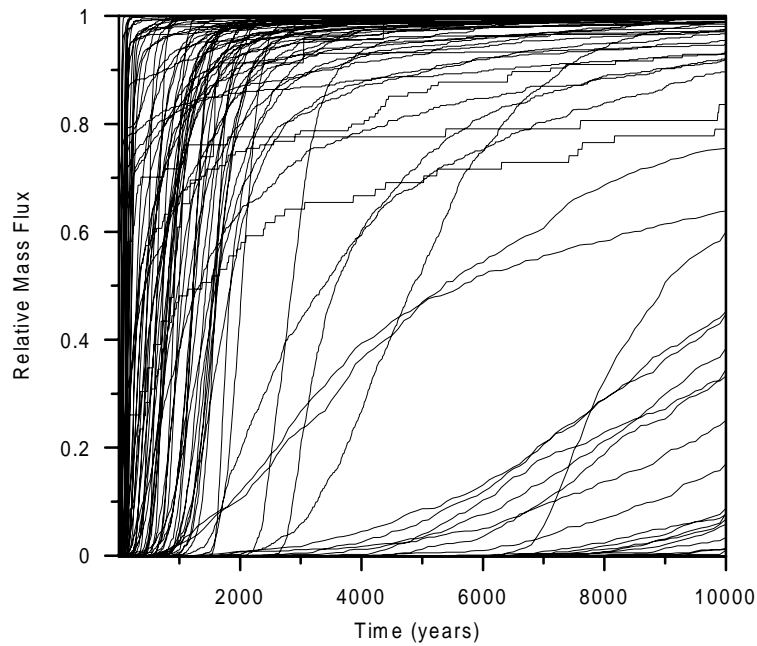


Figure 13. Simulated Unit Breakthrough Curves of Mass Flux for Iodine. Results are shown for 20 km distance from source region 1 (DTN: SN0004T0501600.004).

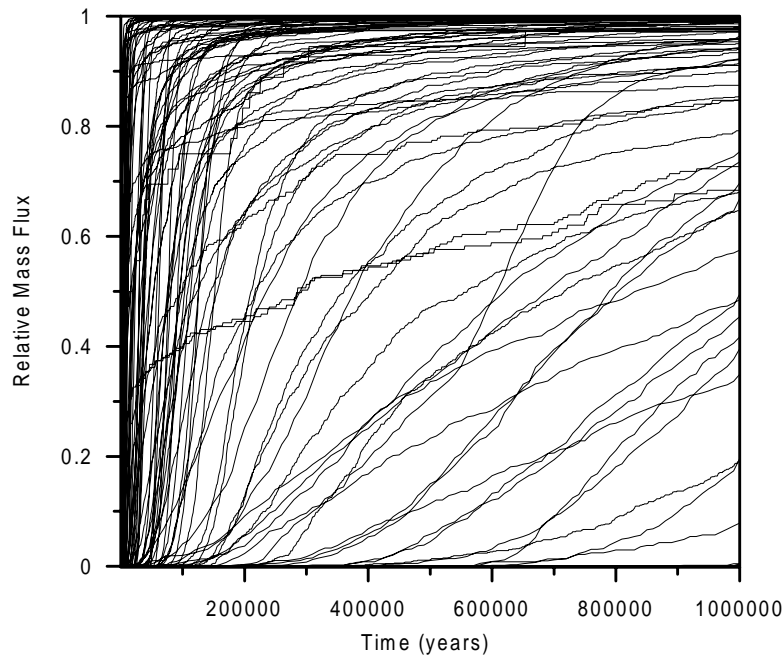


Figure 14. Simulated Unit Breakthrough Curves of Mass Flux for the K_c model for Colloid-Facilitated Transport of Highly Sorbing Radionuclides. Results are shown for 20 km distance from source region 1 (DTN: SN0004T0501600.004).

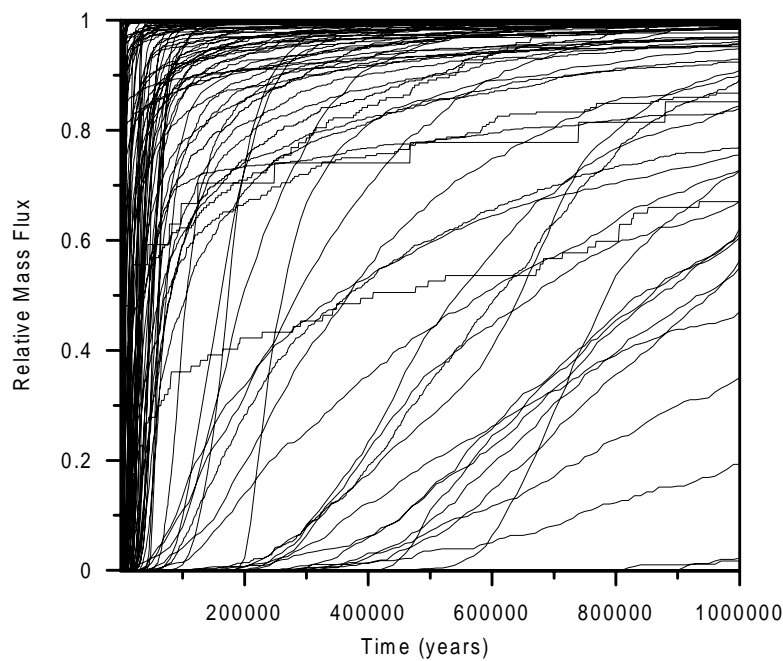


Figure 15. Simulated Unit Breakthrough Curves of Mass Flux for the K_c model for Colloid-Facilitated Transport of Moderately Sorbing Radionuclides. Results are shown for 20 km distance from source region 1 (DTN: SN0004T0501600.004).

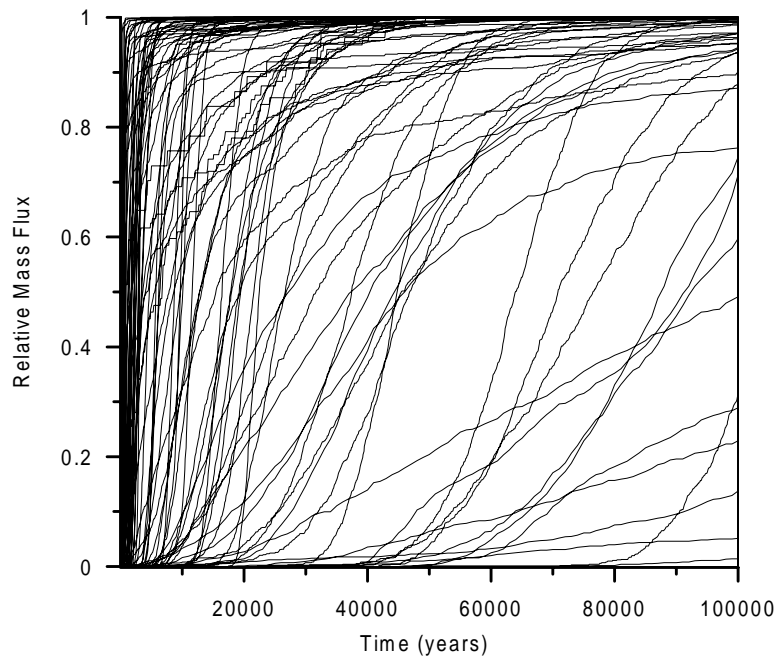


Figure 16. Simulated Unit Breakthrough Curves of Mass Flux for Neptunium. Results are shown for 20 km distance from source region 1 (DTN: SN0004T0501600.004).

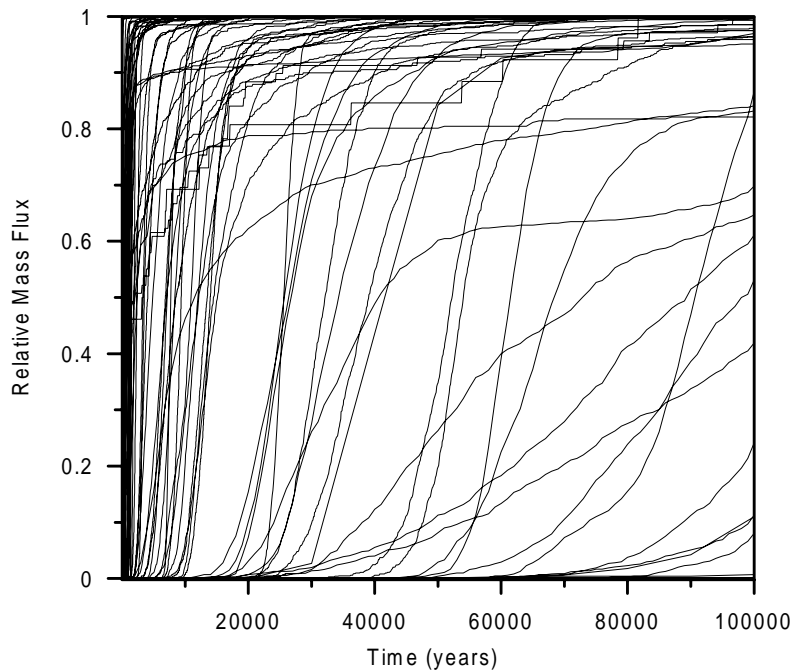


Figure 17. Simulated Unit Breakthrough Curves of Mass Flux for Colloid-Facilitated Transport of Irreversibly Attached Radionuclides. Results are shown for 20 km distance from source region 1 (DTN: SN0004T0501600.004).

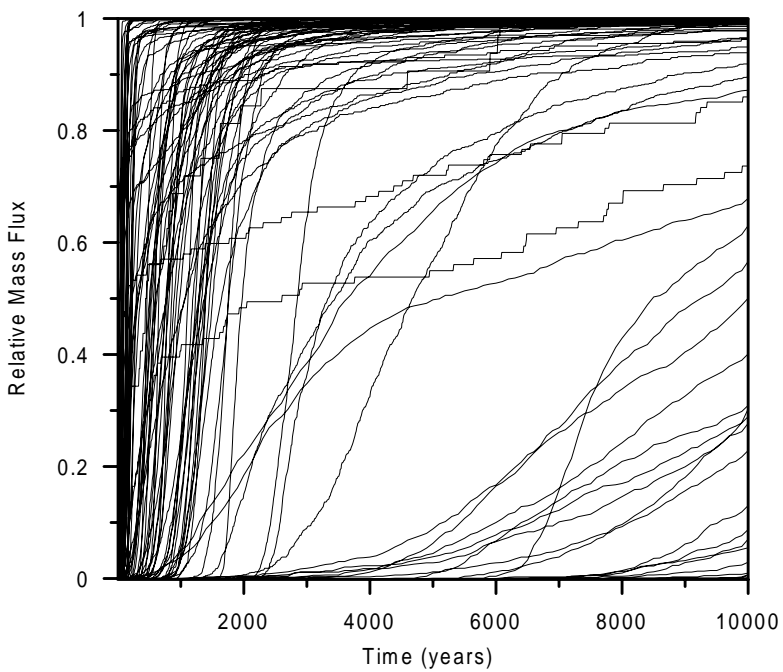


Figure 18. Simulated Unit Breakthrough Curves of Mass Flux for Technecium. Results are shown for 20 km distance from source region 1 (DTN: SN0004T0501600.004).

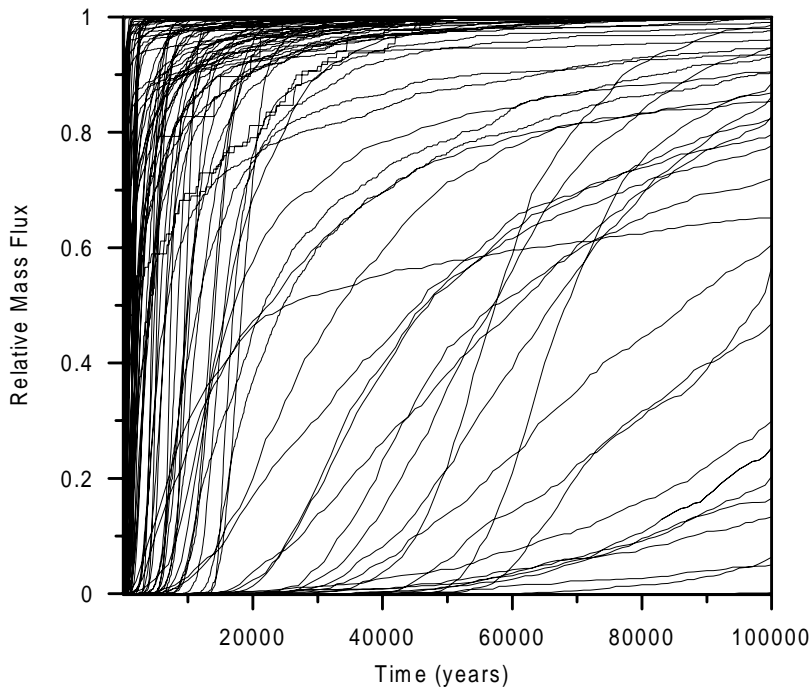


Figure 19. Simulated Unit Breakthrough Curves of Mass Flux for Uranium. Results are shown for 20 km distance from source region 1 (DTN: SN0004T0501600.004).

6.4 ABSTRACTION FOR TOTAL SYSTEM PERFORMANCE ASSESSMENT

Two types of abstraction for TSPA analyses are discussed in this section. The convolution integral method is described with regard to incorporating results of the SZ site-scale flow and transport model in TSPA calculations. An abstracted method for including the effects of climate change is also described.

6.4.1 Convolution Integral Method

The convolution integral method is used in the TSPA-SR calculations to determine the radionuclide mass flux at the SZ / biosphere interface, 20 km downgradient of the repository as a function of the transient radionuclide mass flux at the water table beneath the repository. This computationally efficient method combines information about the unit response of the system, as simulated by the SZ site-scale flow and transport modeling, with the radionuclide source history

from the UZ to calculate transient system behavior. The most important assumptions of the convolution method are linear system behavior and steady-state flow conditions in the saturated zone.

The convolution integral method provides an approximation of the transient radionuclide mass flux at a specific point downgradient in the SZ in response to the transient radionuclide mass flux from transport in the UZ. This coupling method makes full use of detailed SZ flow and transport simulations for a given realization of the system, without requiring complete numerical simulation of the SZ for the duration of each TSPA realization. The two input functions to the convolution integral method are: 1) a unit radionuclide mass breakthrough curve in response to a step-function mass flux source as simulated by the SZ flow and transport model, and 2) the radionuclide mass flux history as simulated by the UZ transport model. The output function is the radionuclide mass flux history downgradient in the SZ.

The mathematical expression for the convolution integral method is written as:

$$M_{sz}(t) = \int_0^t \dot{m}_{uz}(t-t') \frac{\bar{M}_{sz}(t')}{m_p} dt' \quad (\text{Eq. 6})$$

where $M_{sz}(t)$ is the radionuclide mass flux downstream in the SZ, t is time, $\dot{m}_{uz}(t)$ is the time dependent radionuclide mass flux entering the SZ from the UZ, and $\bar{M}(t')$ is the derivative of the downstream radionuclide mass flux-time response curve to a step input of mass m_p . This expression is taken from the convolution integral for concentration (CRWMS M&O 1998a, p. 8-39) and rewritten in terms of radionuclide mass.

The effects of climate change on radionuclide transport in the saturated zone are incorporated into the convolution integral analysis by assuming instantaneous change from one steady-state flow condition to another steady-state condition in the saturated zone. Changes in climate state are assumed to affect the magnitude of groundwater flux through the saturated zone system but have a negligible impact on flowpaths. The effect of changes in groundwater flux is incorporated into the convolution method by scaling the timing of radionuclide mass breakthrough curves proportionally to the change in saturated zone specific discharge.

Radioactive decay is also applied to radionuclide mass flux calculated with the convolution integral computer code (SZ_CONVOLUTE). The convolution integral method consists of numerical integration that accounts for the contributions to the outlet radionuclide mass flux from a series of time intervals. Because the travel time for each contribution to radionuclide mass flux is known, the loss of radionuclide mass (and consequent decrease in mass flux) during transport is calculated by first-order decay for that time interval.

There are several important assumptions in the use of the convolution integral method. Groundwater flow in the SZ is assumed to be in steady state. The transport processes in the SZ are assumed to be linear with respect to the solute source term (i.e., a doubling of the solute mass source results in a doubling of mass flux). In addition, the flow and transport processes in the UZ and the SZ are assumed to be independent of one another.

6.4.2 Climate Change

The effects of climate change on the transport of radionuclides in the SZ is incorporated in TSPA calculations by scaling the radionuclide mass breakthrough curves simulated for present climatic conditions. An example of the scaling method is shown in Figure 20. The scaling procedure is performed as part of the convolution integral method and assumes a proportional scaling of groundwater flux in the entire SZ system in response to wetter climatic conditions. This method treats the shift in climatic conditions as an instantaneous change from one steady-state groundwater flow condition in the SZ to another steady state, in a manner consistent with other components of the TSPA simulations.

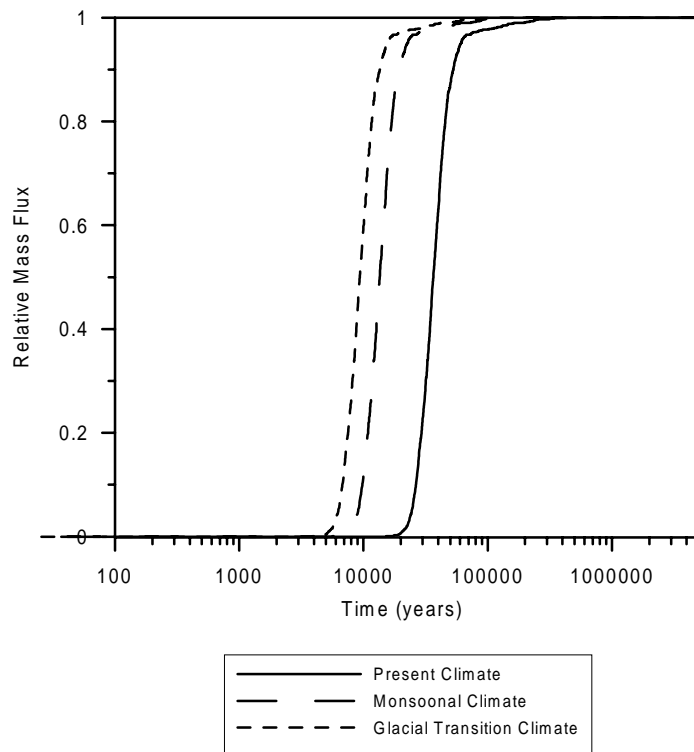


Figure 20. Scaling of Simulated Breakthrough Curve for Climate Change. The example shown is for ^{237}Np transport in the expected-value case. (DTN: SN0004T0501600.004).

Three climate states are defined for the period from repository closure to 10,000 years in the future in the TSPA-SR calculations. For the base-case TSPA analyses, present-day climatic conditions are assumed to occur from the present to 600 years in the future, monsoonal conditions are imposed from 600 years to 2000 years in the future, and glacial-transition climatic conditions occur from 2000 years to 10,000 years. The monsoonal climatic state is wetter than

present-day conditions and the glacial-transition state is conceptualized to be wetter and cooler than present-day conditions.

Estimates of the scaling factors for groundwater flux in the SZ under alternative climatic conditions are based on simulations using the SZ regional-scale flow model (D'Agnese et al., 1999 and CRWMS M&O 1998a) and on models of infiltration for the UZ site-scale flow model. Simulations using the SZ regional-scale flow model were conducted for the past-climate state that likely existed about 21,000 years ago. This climatic state approximately corresponds to the glacial-transition state, as defined for TSPA-SR calculations. An evaluation of the change in groundwater flux in the SZ near Yucca Mountain under past-climate conditions using the SZ regional-scale model indicates an increase in flux of approximately 3.9 relative to present-day simulations, as shown in Table 7.

Simulations of SZ flow under monsoonal climatic conditions have not been performed using the SZ regional-scale flow model. Information on the increased infiltration through the UZ site-scale flow model is used as the basis for estimating flux increases in the SZ for monsoonal conditions. Values of total infiltration in the area of the UZ site-scale flow model (second column of Table 7) are taken from the total of specified mass flow in the "GENER" card of the TOUGH2 input files "*pa_chm1.dat*", "*pa_glam1.dat*", and "*pa_monm1.dat*". Note in Table 7 that the ratio of glacial-transition infiltration in the UZ model to the present-day infiltration is the same value as the estimate of increased SZ groundwater flux from the SZ regional-scale flow model (i.e., 3.9). This correspondence suggests that the UZ infiltration ratio provides a reasonable estimate of the flux ratio for the SZ. For monsoonal climatic conditions, the ratio of UZ infiltration to the infiltration for present-day conditions is 2.7 and this value is applied to the SZ flux as well. The values of flux ratio used as scaling factors of SZ flow and transport for alternative climate states are given in the last column of Table 7.

Table 7. Groundwater Flow Scaling Factors for Climate Change

Climate State	Infiltration, UZ Model (Mean Case) (kg/s)	Ratio to Present Climate, UZ Model	SZ Groundwater Flux Ratio from SZ Regional-Scale Model	SZ Groundwater Flux Ratio for TSPA Simulations
Present-Day	5.64 ^a	1.0	1.0	1.0
Glacial-Transition	22.0 ^b	3.9	3.9 ^d	3.9
Monsoonal	15.2 ^c	2.7	N/A	2.7

^a DTN: LB990801233129.004

^b DTN: LB990801233129.009

^c DTN: LB990801233129.015

^d CRWMS M&O (1998a), Table 8-16, p. T8-20.

6.5 ONE-DIMENSIONAL RADIONUCLIDE TRANSPORT MODEL

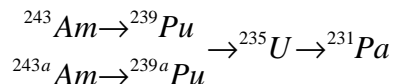
The one-dimensional radionuclide transport model for TSPA-SR is used for the purpose of simulating radioactive decay and ingrowth for four decay chains. This simplified model is required because the radionuclide transport methodology used in the three-dimensional SZ site-scale flow and transport model is not capable of simulating ingrowth by radioactive decay. Although it is not anticipated that the decay products from these radioactive decay chains are significant contributors to the total radiological dose, regulations concerning groundwater protection may require explicit analysis of their concentrations in the water supply of the critical group. The results of the one-dimensional transport modeling are only used for the daughter radionuclides. Although transport of the parent radionuclides is also included in the one-dimensional transport model, the results from the three-dimensional SZ site-scale flow and transport model are used for the parent radionuclides in the TSPA-SR simulations. The one-dimensional radionuclide transport model for TSPA differs from the SZ site-scale flow and transport model in that it is implemented directly with the GoldSim software code in the TSPA model.

The one-dimensional radionuclide transport model is implemented with the GoldSim software code in the TSPA simulator as a series of “pipes”. The same radionuclide transport processes that are simulated in the three-dimensional SZ site-scale flow and transport model (e.g., sorption, matrix diffusion in fractured units, and colloid-facilitated transport) are analyzed in the “pipe” segments, with the exception of transverse dispersion. Although strict consistency between the one-dimensional transport model and the three-dimensional SZ site-scale model is not possible, average groundwater flow and transport characteristics of the SZ site-scale model are used to define flow and transport properties within the “pipe” segments of the one-dimensional model. Average specific discharge along different segments of the flowpath is estimated using the 3-D SZ site-scale flow model. The resulting values of average specific discharge are applied to the individual “pipe” segments in the one-dimensional transport model.

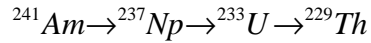
6.5.1 Model Setup

The one-dimensional model is intended to provide simulation results for several radionuclide chains that are not simulated in the three-dimensional site scale FEHM model. The simplified decay chains considered consist of the following.

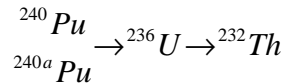
- 1) Actinium series:



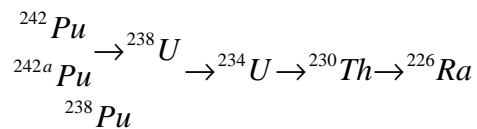
2) Neptunium Series:



3) Thorium Series:



4) Uranium Series:



The radionuclide decay chain analysis is simplified in a conservative manner by assuming secular equilibrium between the final daughter products and their parents in three of these chains. ^{227}Ac is in secular equilibrium with ^{231}Pa in the actinium chain at the downstream end of the SZ analysis. ^{228}Ra is in secular equilibrium with ^{232}Th in the thorium series. ^{210}Pb is in secular equilibrium with ^{226}Ra in the uranium series.

In the model setup, radionuclides ^{241}Am , ^{243}Am , ^{239}Pu , ^{240}Pu , and ^{242}Pu are subject to transport as irreversibly attached to colloids; and ^{243a}Am , ^{238}Pu , ^{239a}Pu , ^{240a}Pu , ^{242a}Pu , ^{231}Pa , ^{229}Th , ^{230}Th , ^{232}Th , and ^{226}Ra are subject to the equilibrium colloid-facilitated transport mode. The one-dimensional model is set up using the Pathway Component of the Contaminant Transport Module in the GoldSim Graphical Simulation Environment (Golder Associates, 2000). The pipe component is able to simulate advection, longitudinal dispersion, retardation, decay and ingrowth, and matrix diffusion (Figure 21) (Golder Associates, 1998).

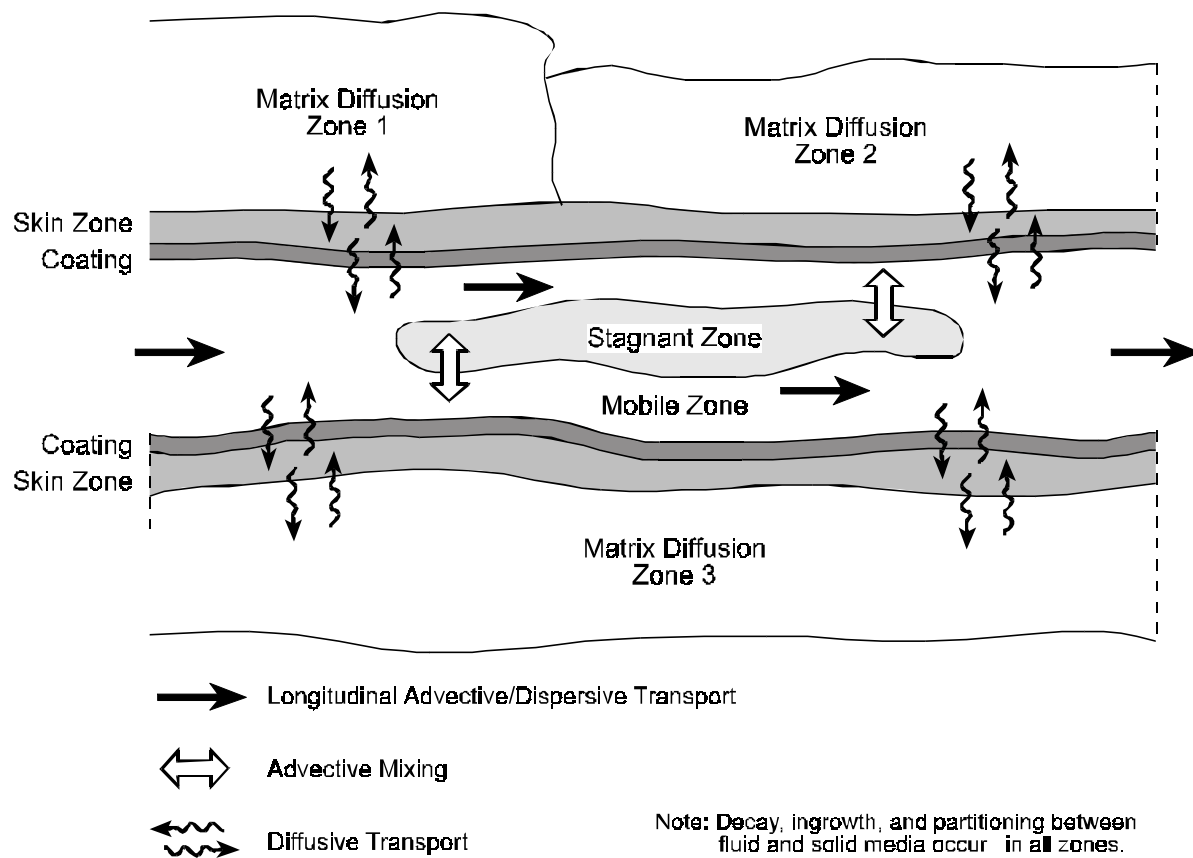


Figure 21. Transport Processes Simulated in One-Dimensional Pipe Pathways in GoldSim.

Each pipe in the GoldSim model represents a one-dimensional mass transport model with uniform properties. The ratio of the volumetric outflow rate to the cross-sectional area of each pipe pathway represents the specific discharge in the pipe. A mass flux loading at the beginning of the first pipe is the source of the radionuclides that were transported along the connected pipes. The GoldSim model also provides a container that isolates all of the model components in one compartment to better organize the model components graphically on screen. For example, components of the one-dimensional mass transport in the saturated zone are contained in the container "SZ1D_model" except for input, output, Species, Water, and MasterClock components (Figure 22). The "Species" component defines the radionuclides and their decay and ingrowth properties in the mass transport model. The "MasterClock" component controls the time and the simulation. Within the "SZ1D_model" container, five pipes are used to represent the mass transport paths in the saturated zone (Figure 23). The "Pipe_5km" pipe is the transport pathway from the repository to a distance 5-km away from the repository boundary. The "Pipe_12km" pipe is the transport pathway from the 5-km distance to the boundary between the fractured volcanic hydrogeologic units and the alluvium unit. The "Pipe_20km" pipe is the transport pathway from the boundary between the volcanic units and the alluvium unit to the 20-km distance. The "Pipe_30km" pipe is the transport pathway from the 20-km distance to the 30-km distance. The "Pipe_80km" pipe is the transport pathway from the 30 km distance to the 80-km

distance. Hydraulic properties are generally grouped into two categories: fractured volcanic unit for the pipe pathways "Pipe_5km" and "Pipe_12km", and porous medium alluvium unit for the pipe pathways "Pipe_20km", "Pipe_30km", and "Pipe_80km". The input parameters correspond to those in the three-dimensional model and are generated by the parameter sampling module in the GoldSim software code. The sorption coefficients of ^{237}Np , ^{233}U , ^{234}U , ^{235}U , ^{236}U , and ^{238}U are used directly (KDPVO and KDUVO) in the matrix of the fractured volcanic units. There is no sorption within the fracture for the species. The sorption coefficients (KDNPAL and KDUAL) in the alluvium for the species are modified according to

$$K_d^{NP} = KDNPAL * NVF19 / 0.35 \text{ or } K_d^U = KDUAL * NVF19 / 0.35$$

where NVF19 is the effective porosity of the alluvium. This modification of the value of sorption coefficients is required in the effective porosity approach to maintain the appropriate retardation factor, as explained in the AMR on uncertainty distributions for stochastic parameters (CRWMS M&O 2000b).

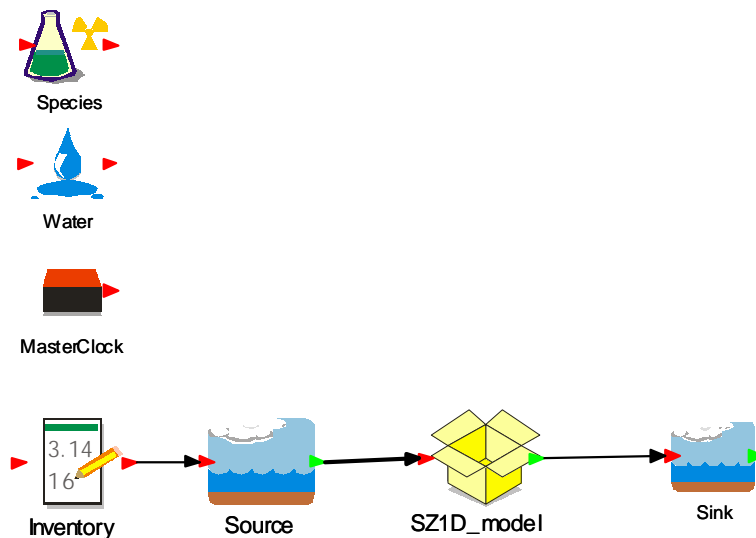


Figure 22. One-Dimensional Mass Transport Model in the Saturated Zone.

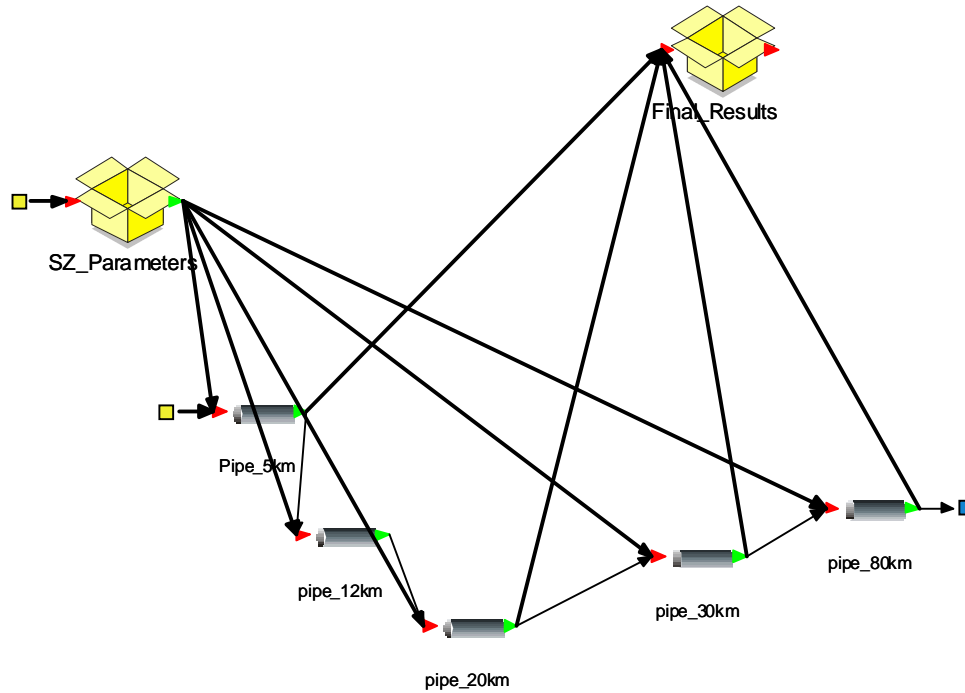


Figure 23. Pipe Connection in the One-Dimensional Radionuclide Transport Model.

There is no matrix diffusion in fractured media for colloids with irreversibly attached radionuclides. Consequently, there is no sorption in the matrix for irreversible colloids. This is simulated by specifying an arbitrarily small value of available matrix porosity ($\sim 10^{-10}$) and zero sorption coefficients for these species in the volcanic matrix.

The retardation in fractures for colloids with irreversibly attached radionuclides is calculated according to the retardation factor (CORVO) of the colloids using the fracture coating option in the GoldSim software code. The equation for calculating the retardation factor in the fracture with the coating on fracture surface is:

$$R_{m,s} = 1 + \frac{PT}{A_m n_p} (\rho_c K_{c,s} + n_c) \quad (\text{Eq. 7})$$

where $R_{m,s}$ is the retardation factor due to the coating, P is the perimeter of the pathway, T is the thickness of the coating, A_m is the cross-sectional area of the mobile zone, ρ_c is the dry bulk density of the coating material, and n_c is the porosity of the coating material. For a given value of $R_{m,s}$, the sorption coefficient is specified as:

$$K_{c,s} = \frac{1}{\rho_c} \left[\frac{A_m n_p}{PT} (R_{m,s} - 1) - n_c \right] \quad (\text{Eq. 8})$$

The sorption coefficient in the alluvium for the species is calculated as

$$Kd = NVF19(R_{m,s} - 1) / \text{alluvium_density} \quad (\text{Eq. 9})$$

where the *alluvium_density* is the bulk density of the alluvium.

In the fracture matrix, the value of sorption coefficients for actinides subject to reversible attachment to colloids (the K_c model of colloid facilitated transport) is a uniform distribution with a minimum of 0.0 and a maximum of 100.0 ml/g. However, radionuclide sorption is also affected by the reduced availability of the radionuclide in the aqueous phase of the fractures. This process is simulated by reducing the porosity in the matrix by the following relationship:

$$\text{Porosity in matrix} = \frac{\text{Original porosity}}{1 + Kc} \quad (\text{Eq. 10})$$

There is no sorption in the volcanic fractures for the species subject to reversible attachment to colloids. In the alluvium, the sorption coefficient for the species is modified by:

$$Kd = \frac{\text{Original } Kd}{1 + Kc} \frac{NVF19}{0.35} \quad (\text{Eq. 11})$$

The diffusion coefficient in the 1-D model is defined by the tortuosity since the reference diffusivity may be used by other processes in the TSPA model. It is assumed that reference diffusivity is an arbitrary value of $1 \text{ m}^2/\text{s}$.

Values of specific discharge for segments represented by pipe pathways in the one-dimensional radionuclide transport model vary along the flowpath from the repository. A plot of the particle paths in the 3-D SZ site-scale flow and transprt model indicates that the flowpath length

through the alluvium varies with an uncertainty from approximately 1 km to 8 km. This uncertainty is represented by variation in the geometry of the "alluvial uncertainty zone" (FPLAN stochastic parameter) in the SZ site-scale flow and transport model. Secondarily, this variability is the result of different flowpaths (i.e., width of the plume). In the one-dimensional radionuclide transport model, the length of the alluvium (out to 20-km distance) is varied from 1 km to 8 km in proportion to the FPLAN parameter value.

Average specific discharge along different segments of the flowpath is estimated using the 3-D SZ site-scale flow model. A total of 1000 particles is released beneath the repository, matrix diffusion is not used, and all porosities are assigned a value of 1.0 for the assessment of average specific discharge. The "average specific discharge" is calculated from the 50th percentile of travel times among the particles. The values of specific discharge scale linearly for the low-, mean-, and high-flux cases (by factors of 10, up and down from the mean). The average specific discharge also varies somewhat between the groundwater flow cases in the SZ site-scale model with and without horizontal anisotropy. The resulting values of average specific discharge, as used in the one-dimensional radionuclide transport model, are shown in Table 8. Note in Table 8 that the groundwater flux case is determined by the value of the GWSPD parameter and the anisotropy case is determined by the HAV0 parameter. The volumetric flow rate is the same for all five pipe segments in the 1-D model.

Table 8. Average Specific Discharge in Flowpath Segments

HAV0	GWSPD	Average Specific Discharge (m/yr.)			
		0-5 km	5-20 km	20-30 km	30-80 km
<0.5	<0.24	0.066	0.23	0.25	0.25
<0.5	>=0.24 and <=0.76	0.66	2.3	2.5	2.5
<0.5	>0.76	6.6	23	25	25
>0.5	<0.24	0.075	0.29	0.24	0.24
>0.5	>=0.24 and <=0.76	0.75	2.9	2.4	2.4
>0.5	>0.76	7.5	29	24	24

6.5.2 Model Validation and Comparison to SZ Site-Scale Model

To verify the solution for matrix diffusion in fractured media obtained with the GoldSim software code, an analytical solution developed by Sudicky and Frind (1982) is used for comparison. The analytical solution by Sudicky and Frind (1982) solves for solute mass transport along uniformly spaced parallel fractures in a porous matrix. The analytical solution has been programmed as a calculation routine, FRACT_P, and is used to calculate the type curves of mass transport in parallel fractures in FEHM (CRWMS M&O, 2000d). In the verification exercise, the following parameter values are used: fracture half aperture = 0.001 m, fracture half spacing = 10 m, fracture groundwater velocity = 600 m/yr., matrix porosity = 0.1, fracture retardation factor = 1.0, matrix retardation factor = 1.0, and matrix diffusion coefficient

$= 1.0 \times 10^{-13}$ m²/sec. No dispersion is simulated in the verification. The breakthrough curves for time $t = 0$ to 5.0×10^9 days at distance = 20000 m calculated by the GoldSim and the analytical solution are shown in Figure 24. The two solutions match very well.

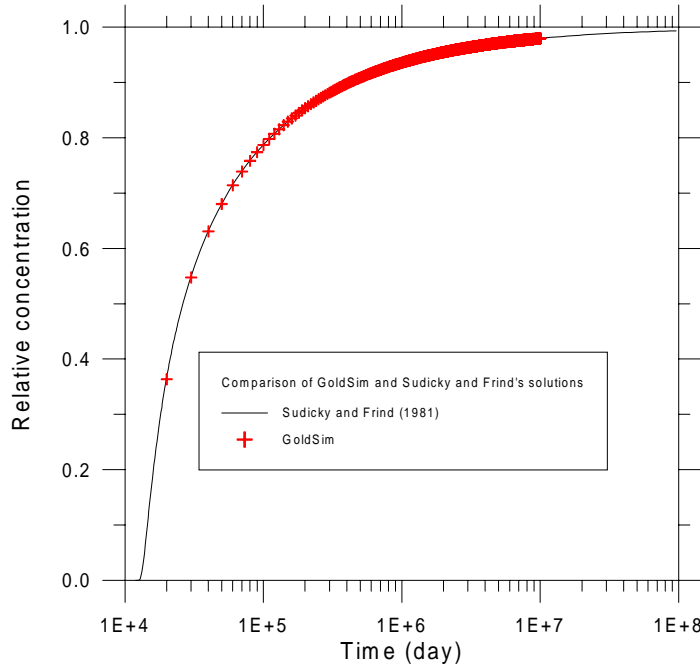


Figure 24. Comparison of GoldSim and Sudicky and Frind (1982) Solutions.

Simulation results with the SZ site-scale flow and transport model and the one-dimensional transport model are compared to check that implementation of the one-dimensional transport model is correct and consistent with the 3-D model. Results from the two simulation approaches are not expected to be identical because of dimensionality differences in the geometry of the models and variability in groundwater flux along the flowpaths in the three-dimensional SZ site-scale flow and transport model.

Figure 25 and Figure 26 show the breakthrough curves of carbon and neptunium at 5, 20, and 30 km for the expected value case of SZ flow and transport. The breakthrough curves are generally comparable, but not the same. For example, at 5 km, the breakthrough curves calculated from the one-dimensional radionuclide transport model show early breakthrough. One hundred realizations of the breakthrough curves for all of these seven radionuclides are also simulated. The results indicate that the breakthrough curves calculated by the one-dimensional radionuclide transport model show earlier breakthrough in some realizations and later breakthrough in other realizations. The difference may be caused by the uniform values of specific discharge and material properties assigned from 0 to 5km, from 5 to 20km, and from 20 to 30km in the one-

dimensional radionuclide transport model. However, the average breakthrough times are generally comparable for the one-dimensional radionuclide transport model and the three-dimensional SZ site-scale model.

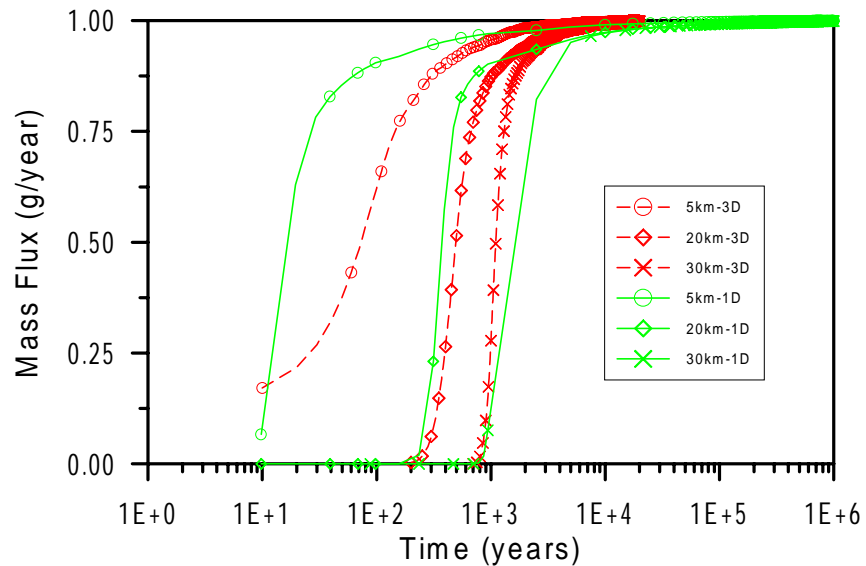


Figure 25. Simulated Breakthrough Curves From the One-Dimensional Transport Model and the Three-Dimensional SZ Site-Scale-Model at 5, 20, and 30 km for Carbon.

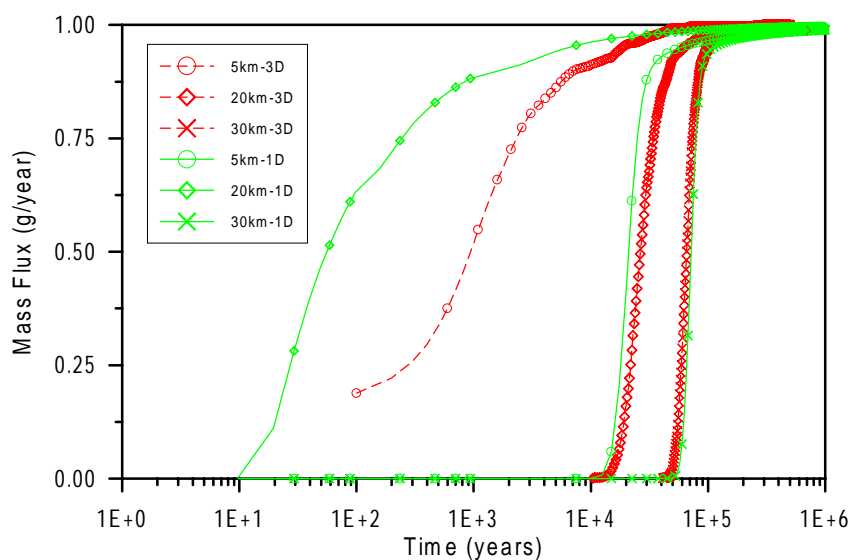


Figure 26. Simulated Breakthrough Curves From the One-Dimensional Transport Model and the Three-Dimensional SZ Site-Scale-Model at 5, 20, and 30 km for Neptunium.

7. CONCLUSIONS

This analysis consists of preparing the input for the SZ site-scale flow and transport model and obtaining the results of radionuclide simulations for use in the TSPA-SR calculations. The TSPA SZ site-scale flow and transport model is used to simulate the unit breakthrough curves for radionuclide *mass* at the interface between the SZ and the biosphere. The starting point of the analysis is the calibrated SZ site-scale groundwater flow model (CRWMS M&O 2000a). Input files of the SZ site-scale flow model are modified to include relevant radionuclide transport parameters and to perform simulations of radionuclide transport. Preparation of input files for radionuclide transport includes incorporation of values for stochastic parameters that have been generated for 100 random realizations of the SZ system. Uncertainty distributions for stochastic parameters are taken from the analysis documented in CRWMS M&O (2000b). The groundwater flow field for the calibrated SZ site-scale flow model is also modified to incorporate alternative conceptual models of groundwater specific discharge and horizontal anisotropy of permeability to produce a total of six SZ groundwater flow fields.

Automated methods are developed to pre-process the input files for the simulations, conduct the model runs, and post-process the results. A pre-processor software routine is used to read parameter values that have been drawn for stochastic parameters and write the input files for the SZ site-scale flow and transport model in the appropriate format. UNIX script files are prepared to sequentially run the transport simulations and save the output files. A post-processor software routine is used to reformat and combine the simulation results for the breakthrough curves into a format that can be used in the convolution integral method in the TSPA simulator. These results are contained in the TDMS in DTN: SN0004T0501600.004. The results of this analysis are “to be verified” because of the use of unqualified software that is being controlled under procedure AP-SI.1Q Rev. 2/ICN 4, *Software Management*. The input files used in this analysis are archived in the TDMS in DTN: SN0004T0501600.005.

A simplified one-dimensional radionuclide transport model is developed for the purpose of simulating radionuclide decay and ingrowth in four decay chains. This additional model is required because the FEHM code used for the three-dimensional SZ site-scale model is currently not capable of simulating radionuclide ingrowth. The one-dimensional radionuclide transport model is developed for direct implementation with the GoldSim code in the TSPA simulator. Because the one-dimensional radionuclide transport model is an integral component of the TSPA simulator, it will be submitted to the TDMS with the GoldSim input file for the TSPA-SR model.

The results of this analysis are appropriate for their intended use in the TSPA-SR simulations of radionuclide transport in the SZ. The analysis explicitly incorporates uncertainties in key parameters and in conceptual models and thus, the outputs from the analysis include the consequences of these uncertainties. This AMR relies on several other AMRs that are still in preparation and must be considered preliminary until the appropriate “upstream” AMRs are approved.

Sensitivity of the analysis to the number and distribution of source regions is not quantitatively assessed in this report. However, the potential spatial distribution of radionuclide mass from the UZ is examined and the location of the source regions for SZ transport calculations is specified based on that distribution. Variability in the radionuclide breakthrough curves is not great among the four source regions. This implies that four source regions are sufficient to capture the variability in radionuclide travel times in the SZ.

The results of this analysis are appropriate for use in TSPA-SR calculations for the evaluation of the Yucca Mountain site relative to proposed and anticipated regulations, with some exceptions. The nominal case scenario assumes transport of radionuclides in the SZ to a distance of 20 km where the contaminated groundwater is intercepted by pumping wells of the hypothetical farming community. For the human intrusion scenario, in which a borehole penetrates a waste package and provides direct access to the SZ, the radionuclide mass breakthrough curve results of a single point source may be used in TSPA analyses. The point source in the human intrusion scenario should be chosen from either source region 1 or source region 3, which directly underlie the repository. Potential regulations governing groundwater protection may be appropriately evaluated using the results of this analysis, providing that the representative volume of groundwater considered in the analysis is not small. The assumption of complete capture of the radionuclide mass in the volume of groundwater may render the approach used in this analysis overly conservative for small volumetric rates (approximately less than a few hundred acre-ft/year).

The accuracy and representativeness of this analysis and the underlying model are difficult to assess in absolute terms. Both accuracy and representativeness must be considered within the context of the uncertainty analysis implemented in this report. Given the large number of stochastic parameters and the relatively wide range of uncertainty in some key parameters, the results of the analysis almost certainly encompass the actual behavior of the SZ flow and transport system. The SZ site-scale flow and transport model obeys basic laws of mass conservation for groundwater flow. The outputs are reasonable compared to the inputs and the processes being analyzed.

Limitations exist in the applicability of the results of this analysis. The continuum representation of flow and transport through fractured media in the SZ site-scale model implies that a minimum travel distance in fractured media is required for the influence of individual fractures to be “averaged”. Short travel distances (less than a few thousand meters) do not meet this requirement. Thus, the model would be inappropriate for the simulation of radionuclide migration over distances of less than approximately a few kilometers. The radionuclide transport results using the SZ site-scale flow and transport model would be inappropriate for use in an analysis in which the volume of groundwater assumed to be used by the critical group is very small. The implicit assumption that all radionuclide mass crossing the 20 km boundary is captured by the pumping wells of the critical group would be unreasonably conservative for small total volumes of groundwater usage. The one-dimensional radionuclide transport model does not simulate the effects of transverse dispersion and is thus incapable of modeling the dilution associated with this process. Consequently, the one-dimensional radionuclide transport model should not be used for the purpose of simulating *in situ* concentrations at the compliance boundary.

This document may be affected by technical product input information that requires confirmation. Any changes to the document that may occur as a result of completing the confirmation activities will be reflected in subsequent revisions. The status of the input information quality may be confirmed by review of the Document Input Reference System database.

8. REFERENCES

8.1 DOCUMENTS CITED

CRWMS M&O 1997. *The Site-Scale Unsaturated Zone Transport Model of Yucca Mountain*. Milestone SP25BM3, Rev. 1. Las Vegas, Nevada: CRWMS M&O. ACC: MOL.19980224.0314.

CRWMS M&O 1998a. "Saturated Zone Flow and Transport." Chapter 8 of *Total System Performance Assessment-Viability Assessment (TSPA-VA) Analyses Technical Basis Document*. B00000000-01717-4301-00008 REV 01. Las Vegas, Nevada: CRWMS M&O. ACC: MOL.19981008.0008.

CRWMS M&O 1998b. *Saturated Zone Flow and Transport Expert Elicitation Project*. Deliverable Number SL5X4AM3. Las Vegas, Nevada: CRWMS M&O. ACC: MOL.19980825.0008.

CRWMS M&O 1999a. *Abstraction of SZ Flow and Transport Model, Rev 01. ID: B2040*, Activity: SPP4050. Work Direction and Planning Document. Las Vegas, Nevada: CRWMS M&O. ACC: MOL.19990707.0104.

CRWMS M&O 1999b. *Subsurface Design for Enhanced Design Alternative (EDA) II*. Design Input Transmittal SEI-SSR-99172.T. Las Vegas, Nevada: CRWMS M&O. ACC: MOL.19990409.0100.

CRWMS M&O 1999c. *Recharge and Lateral Groundwater Flow Boundary Conditions for the Saturated Zone Site-Scale Flow and Transport Model*. ANL-NBS-MD-000010 REV 00. Las Vegas, Nevada: CRWMS M&O. ACC: MOL.19991118.0188.

CRWMS M&O 2000a. *Calibration of the Site-Scale Saturated Zone Flow Model*. MDL-NBS-HS-000011 REV 00. Las Vegas, Nevada: CRWMS M&O. Submit to RPC URN-0191

CRWMS M&O 2000b. *Uncertainty Distribution for Stochastic Parameters*. ANL-NBS-MD-000011 REV 00. Las Vegas, Nevada: CRWMS M&O. Submit to RPC URN-0189

CRWMS M&O 2000c. *Analysis of Base-Case Particle Tracking Results of the Base-Case Flow Fields*. ANL-NBS-HS-000024 REV 00. Las Vegas, Nevada: CRWMS M&O. ACC: MOL.20000207.0690.

CRWMS M&O 2000d. *Type Curve Calculations Mass Transport in Parallel Fractures Used in Particle-Tracking Scheme in the Saturated Zone*. B00000000-01717-0210-00089 Rev 00A. Las Vegas, Nevada: CRWMS M&O. Submit to RPC URN-0190

CRWMS M&O 2000e. *Features, Events, and Processes in SZ Flow and Transport*. ANL-NBS-MD-000002 REV 00. Las Vegas, Nevada: CRWMS M&O. Submit to RPC URN-0034

CRWMS M&O 2000f. *Unsaturated Zone and Saturated Zone Transport Properties*. ANL-NBS-HS-000019 REV 00. Las Vegas, Nevada: CRWMS M&O. Submit to RPC URN-0038

D'Agnese, F.A.; O'Brien, G.M.; Faunt, C.C.; and San Juan, C.A. 1999. *Simulated Effects of Climate Change on the Death Valley Regional Ground-Water Flow System, Nevada and California*. Water-Resources Investigations Report 98-4041. Denver, Colorado: U.S. Geological Survey. TIC: 243555.

DOE (U.S. Department of Energy) 1998. *Total System Performance Assessment*. Volume 3 of *Viability Assessment of a Repository at Yucca Mountain*. DOE/RW-0508. Washington, D.C.: U.S. Department of Energy, Office of Civilian Radioactive Waste Management. ACC: MOL.19981007.0030.

DOE (U.S. Department of Energy) 2000. *Quality Assurance Requirements and Description*. DOE/RW-0333P, Rev. 9. Washington, D.C.: U.S. Department of Energy, Office of Civilian Radioactive Waste Management. ACC: MOL.19991028.0012.

Dyer, J.R. 1999. "Revised Interim Guidance Pending Issuance of New U.S. Nuclear Regulatory Commission (NRC) Regulations (Revision 01, July 22, 1999), for Yucca Mountain, Nevada." Letter from Dr. J.R. Dyer (DOE/YMSCO) to Dr. D.R. Wilkins (CRWMS M&O), September 3, 1999, OL&RC:SB-1714, with enclosure, "Interim Guidance Pending Issuance of New NRC Regulations for Yucca Mountain (Revision 01)." ACC: MOL.19990910.0079.

Ferrill, D.A.; Winterle, J.; Wittmeyer, G.; Sims, D.; Colton, S.; Armstrong, A.; and Morris, A.P. 1999. "Stressed Rock Strains Groundwater at Yucca Mountain, Nevada." *GSA Today*, 9, (5), 1-8. Boulder, Colorado: Geological Society of America. TIC: 246229.

Golder Associates 1998. *Repository Integration Program RIP Integrated Probabilistic Simulator for Environmental Systems Theory Manual and User's Guide*. Redmond, Washington: Golder Associates. TIC: 238560.

Golder Associates 2000. *User's Guide, GoldSim, Graphical Simulation Environment*. Version 6.02. Manual Draft #4 (March 17, 2000). Redmond, Washington: Systems Simulation Group Golder Associates Inc. TIC: 247347.

Luckey, R.R.; Tucci, P.; Faunt, C.C.; Ervin, E.M.; Steinkampf, W.C.; D'Agnese, F.A.; and Patterson, G.L. 1996. *Status of Understanding of the Saturated-Zone Ground-Water Flow System at Yucca Mountain, Nevada, as of 1995*. Water-Resources Investigations Report 96-4077. Denver, Colorado: U.S. Geological Survey. ACC: MOL.19970513.0209.

NRC (U.S. Nuclear Regulatory Commission) 1998. "Proposed Rule 10 CFR Part 63, Disposal of High-Level Radioactive Wastes in a Proposed Geologic Repository at Yucca Mountain, Nevada. SECY-98-225." Washington, D.C.: U.S. Nuclear Regulatory Commission. Accessed 10/20/98. TIC: 240520. <http://www.nrc.gov/NRC/COMMISSION/SECYS/1998-225scy.html>

Sudicky, E.A. and Frind, E.O. 1982. "Contaminant Transport in Fractured Porous Media: Analytical Solutions for a System of Parallel Fractures." *Water Resources Research*, 18, (6), 1634-1642. Washington, D.C.: American Geophysical Union. TIC: 217475.

Winterle, J.R. and La Femina, P.C. 1999. *Review and Analysis of Hydraulic and Tracer Testing at the C-Holes Complex Near Yucca Mountain, Nevada.* San Antonio, Texas: Center for Nuclear Waste Regulatory Analyses. TIC: 246623.

Software Codes Cited:

Los Alamos National Laboratory. 1999. *Software Code: FEHM V2.10.* V2.10. SUN Ultra Sparc, PC. 10086-2.10-00.

Sandia National Laboratory. 2000. *Software Code: GoldSim V6.03.* V6.03. 10296-6.03-00.

8.2 PROCEDURES CITED

AP-3.10Q, Rev. 2, ICN 0. *Analyses and Models.* Washington, D.C.: U.S. Department of Energy, Office of Civilian Radioactive Waste Management. ACC: MOL.20000217.0246.

AP-3.14Q, Rev. 0, ICN 0. *Transmittal of Input.* Washington, D.C.: U.S. Department of Energy, Office of Civilian Radioactive Waste Management. ACC: MOL.19990701.0621.

AP-SI.1Q, Rev. 2, ICN 4. *Software Management.* Washington, D.C.: U.S. Department of Energy, Office of Civilian Radioactive Waste Management. ACC: MOL.20000223.0508.

QAP-2-0, Rev. 5, ICN 1. *Conduct of Activities.* Las Vegas, Nevada: CRWMS M&O. ACC: MOL.19991109.0221.

8.3 SOURCE DATA, LISTED BY DATA TRACKING NUMBER

LA9911GZ12213S.001. SZ Flow and Transport Model. Submittal date: 12/23/1999.

SN0004T0571599.004. Uncertainty Distributions for Stochastic Parameters Revision to Include New U Sorption Coefficients in the Alluvium and Supporting Electronic Files. Submittal date: 04/10/2000. Submit to RPC URN-0273

SNT05070198001.001. Three-Dimensional Rock Property Models for FY98. Submittal date: 07/30/1998.

LB990801233129.004. TSPA Grid Flow Simulations for AMR U0050, "UZ Flow Models and Submodels" (Flow Field #4). Submittal date: 11/29/1999.

LB990801233129.009. TSPA Grid Flow Simulations for AMR U0050, "UZ Flow Models and Submodels" (Flow Field #9). Submittal date: 11/29/1999.

LB990801233129.015. TSPA Grid Flow Simulations for AMR U0050, "UZ Flow Models and Submodels" (Flow Field #15). Submittal date: 11/29/1999.

MO0003SZFWTEEP.000. Data Resulting from the Saturated Zone Flow and Transport Expert Elicitation Project. Submittal date: 03/06/2000.

9. ATTACHMENTS

Attachment	Title
I	Stochastic Parameter Values
II	FORTRAN Source Code for Software Routine SZ_Pre
III	FORTRAN Source Code for Software Routine SZ_Post
IV	UNIX Script file <i>xrun_C_mean_iso_all</i>

ATTACHMENT I

Table 9. Stochastic Parameter Values

real. #	FPLAW	FPLAN	NVF19	NVF7	FISVO	FPVO	DCVO	KDNPVO	KDNPAL	KDIAL	KDUVO
1	0.36069	0.98069	0.20253	0.13542	0.59155	-2.1972	-10.388	0.78027	28.627	0.35742	3.1628
2	0.98312	0.67312	0.13587	0.097752	1.5198	-1.5075	-10.771	0.83848	0.94526	0.56587	1.0125
3	0.67125	0.19125	0.096864	0.20692	1.7773	-2.035	-10.716	0.018233	31.656	0.39789	3.725
4	0.19113	0.0513	0.20693	0.23777	1.5688	-1.9548	-12.636	0.91696	3.2667	0.6087	0.8852
5	0.051887	0.70189	0.23792	0.21311	1.5967	-4.5125	-10.624	0.078308	53.16	0.38878	1.9275
6	0.70805	0.87805	0.21408	0.21735	0.80445	-1.8078	-12.226	1.4761	2.7529	0.4713	1.0722
7	0.87245	0.74245	0.21642	0.12077	1.6408	-3.9902	-10.203	0.060918	10.819	0.40136	2.7298
8	0.74465	0.76465	0.12132	0.22196	1.0079	-1.2614	-12.326	0.30383	3.5825	0.53224	0.37862
9	0.7657	0.1257	0.22215	0.14657	1.9439	-4.0972	-11.543	0.087559	22.394	0.34967	3.0228
10	0.12125	0.79125	0.14586	0.25577	0.96165	-3.075	-12.216	0.64148	0.56635	0.55289	1.965
11	0.79331	0.25331	0.25657	0.14124	1.2729	-3.9468	-10.95	0.010797	27.945	0.47293	2.9332
12	0.25894	0.93894	0.1422	0.17861	1.0268	-2.2443	-12.703	0.82736	11.556	0.54907	3.7957
13	0.93325	0.22325	0.17789	0.14776	1.4955	-4.627	-10.74	0.31534	26.172	0.61241	1.373
14	0.22411	0.48411	0.14789	0.20443	0.72774	-1.9836	-11.518	0.76381	56.307	0.42667	2.1764
15	0.4818	0.2618	0.2041	0.11227	1.5829	-3.0328	-10.805	1.4962	5.6716	0.48796	1.3272
16	0.26006	0.68006	0.11173	0.21441	1.2802	-2.0797	-10.18	0.14499	13.518	0.42232	1.6803
17	0.68314	0.093137	0.2149	0.17915	1.558	-1.2275	-11.971	0.38781	5.4152	0.45117	1.2525
18	0.096651	0.75665	0.1796	0.21228	1.9842	-3.6134	-11.36	0.14196	8.5571	0.41816	2.9066
19	0.75269	0.49269	0.21167	0.26049	1.1172	-2.8292	-12.002	0.22771	4.8208	0.54404	3.4508
20	0.49047	0.73047	0.25952	0.15908	1.3344	-3.6781	-11.739	0.12014	25.102	0.58675	0.56187
21	0.73655	0.94655	0.15993	0.18597	1.11	-3.2938	-12.05	0.74525	40.994	0.36543	0.54619
22	0.94328	0.34328	0.18555	0.15808	1.2079	-3.7469	-10.83	1.151	1.2519	0.36132	2.4531
23	0.34516	0.54516	0.15834	0.17042	1.0845	-2.0994	-10.405	0.026739	1.1244	0.5107	3.3806
24	0.54108	0.33108	0.16989	0.15492	1.5424	-1.5557	-12.577	0.021518	17.423	0.58074	2.4843
25	0.33946	0.42946	0.15612	0.21117	1.7737	-4.4022	-12.582	0.51741	38.574	0.51513	2.0378
26	0.42629	0.31629	0.21068	0.23657	0.83995	-4.4548	-11.151	1.0906	18.356	0.47695	3.6652
27	0.31891	0.72891	0.2372	0.12697	0.82596	-2.5244	-10.453	0.53518	12.013	0.60486	2.8756

real. #	FPLAW	FPLAN	NVF19	NVF7	FISVO	FPVO	DCVO	KDNPVO	KDNPAL	KDIAL	KDUVO
28	0.72148	0.86148	0.12531	0.12298	1.4123	-1.6341	-11.136	0.32672	48.694	0.54056	1.7659
29	0.86459	0.14459	0.12372	0.19485	1.7262	-2.5016	-11.486	1.3608	24.622	0.45782	1.0984
30	0.14688	0.13688	0.19516	0.23219	1.4296	-2.9725	-10.249	0.7221	9.3439	0.40583	3.8275
31	0.13528	0.61528	0.23185	0.19628	1.2965	-1.3389	-10.854	0.25392	3.834	0.61614	3.7011
32	0.61118	0.84118	0.19573	0.18017	1.8701	-2.1553	-11.676	0.091262	58.35	0.60557	2.6447
33	0.84978	0.62978	0.18127	0.25161	1.5408	-3.2009	-12.161	1.6012	52.66	0.52763	0.47913
34	0.62343	0.50343	0.24949	0.20873	1.2299	-3.9063	-10.14	1.4024	20.802	0.35516	3.3337
35	0.50546	0.91546	0.20904	0.17305	1.0352	-1.1782	-10.224	0.60791	0.84698	0.57899	2.1018
36	0.9152	0.7152	0.17301	0.1496	2.0204	-1.2992	-11.004	0.016459	36.71	0.48281	2.6208
37	0.71289	0.44289	0.14925	0.26538	1.9031	-2.3484	-12.661	1.0454	12.672	0.5224	1.7316
38	0.44989	0.27989	0.26925	0.25525	1.4795	-4.5205	-10.48	0.36768	20.555	0.45636	0.43954
39	0.27852	0.95852	0.25473	0.20222	0.78453	-1.6459	-11.414	0.59363	9.0113	0.35364	0.87409
40	0.95659	0.92659	0.20195	0.11927	1.7121	-2.8936	-11.03	0.24369	0.73874	0.38714	3.2664
41	0.92546	0.66546	0.11898	0.22978	1.3182	-2.3782	-11.694	0.013793	2.4994	0.57279	1.5418
42	0.66618	0.11618	0.22993	0.18336	1.4633	-3.2553	-12.681	0.057542	34.404	0.43972	0.18474
43	0.11433	0.83433	0.18312	0.20024	1.22	-4.5827	-12.357	0.98604	7.035	0.33374	1.8973
44	0.8354	0.5254	0.20039	0.17175	0.75516	-4.1384	-10.554	0.18783	0.17158	0.46737	0.7416
45	0.52747	0.65747	0.17201	0.11683	0.95616	-1.7301	-11.838	0.002794	10.608	0.37811	2.1499
46	0.65801	0.43801	0.11698	0.14033	1.6808	-3.448	-12.856	0.29497	1.9542	0.48678	3.312
47	0.4395	0.1095	0.14059	0.22659	1.1706	-4.802	-11.562	0.044369	13.49	0.57714	0.99799
48	0.10843	0.21843	0.22639	0.1656	0.58226	-3.0863	-12.435	0.38059	35.867	0.39701	0.1137
49	0.21819	0.81819	0.16556	0.095352	1.2674	-4.2472	-11.385	1.0301	3.1931	0.32874	0.67276
50	0.81792	0.38792	0.095217	0.17721	0.9113	-2.8483	-10.516	0.075967	0.074713	0.37206	2.0717
51	0.3882	0.048204	0.17724	0.13495	1.3319	-1.6872	-12.255	0.000987	1.6432	0.48064	0.072816
52	0.042678	0.47268	0.13389	0.18419	1.6884	-4.0293	-12.932	0.033236	12.191	0.32393	2.5707
53	0.47776	0.18776	0.18484	0.22822	0.99868	-4.8889	-12.497	0.34982	0.034467	0.52081	0.27106
54	0.18398	0.53398	0.22747	0.14469	0.45085	-4.3441	-11.458	0.000242	19.489	0.33983	2.2959
55	0.53628	0.82628	0.14506	0.081392	0.87563	-2.9349	-12.951	0.56891	0.32774	0.49865	0.82512
56	0.82583	0.24583	0.081017	0.13055	1.3078	-4.9367	-11.063	0.005375	15.397	0.38381	3.8633
57	0.24544	0.025439	0.13047	0.18199	0.37811	-2.4182	-12.804	0.43975	2.2977	0.61929	1.6218
58	0.021747	0.16175	0.18152	0.065005	1.4466	-4.753	-11.285	0.050415	61.812	0.44454	0.28699
59	0.16398	0.51398	0.068362	0.19882	0.64034	-2.7041	-12.388	1.6282	7.7199	0.34293	3.8959

Input and Results of the Base Case Saturated Zone Flow and Transport Model for TSPA

real. #	FPLAW	FPLAN	NVF19	NVF7	FISVO	FPVO	DCVO	KDNPVO	KDNPAL	KDIAL	KDUVO
60	0.51597	0.015972	0.19909	0.10328	1.373	-4.1761	-10.102	0.20929	0.41393	0.62255	1.2239
61	0.018071	0.64807	0.1041	0.19005	0.94231	-1.1277	-11.776	0.007559	68.757	0.4155	1.1923
62	0.65	0.069998	0.1903	0.13893	2.0992	-3.36	-12.76	1.7454	4.7487	0.413	0.35999
63	0.064468	0.57447	0.13794	0.27209	1.1872	-4.7021	-10.077	0.11545	4.3333	0.34619	0.93787
64	0.57716	0.20716	0.2739	0.16807	0.68167	-1.0914	-12.079	0.10996	0.52353	0.39352	2.3886
65	0.20932	0.96932	0.16835	0.1082	2.1676	-3.7627	-12.102	0.009894	2.9832	0.50579	1.3173
66	0.96853	0.40853	0.10793	0.28327	1.0765	-3.8059	-12.734	0.070419	16.676	0.42185	2.3541
67	0.40115	0.071151	0.27683	0.15348	1.0551	-4.6754	-12.307	0.4665	5.0605	0.50016	2.5246
68	0.076752	0.97675	0.1543	0.15283	0.70856	-4.053	-11.21	0.13351	16.005	0.51739	2.427
69	0.97757	0.30757	0.15295	0.11094	0.98471	-2.6097	-12.017	0.46032	19.074	0.50835	2.7903
70	0.30481	0.29481	0.11005	0.14318	1.3937	-3.7008	-11.246	0.54647	17.049	0.53539	3.0992
71	0.29577	0.085773	0.14334	0.19236	1.0973	-2.6569	-11.093	0.49233	23.151	0.56049	2.2231
72	0.080968	0.23097	0.19173	0.15634	1.3784	-2.4761	-11.197	0.66274	29.608	0.4908	0.12387
73	0.23193	0.59193	0.15648	0.19055	1.4354	-2.5923	-10.924	0.86232	14.124	0.3299	3.5677
74	0.59245	0.32245	0.19062	0.19725	1.4022	-2.2302	-10.683	0.40238	0.096601	0.59666	3.5298
75	0.32036	0.58036	0.19697	0.19297	1.5041	-1.9186	-11.349	0.001143	44.789	0.59291	0.60144
76	0.58055	0.63055	0.19299	0.20536	1.6089	-2.7978	-12.908	1.2566	43.156	0.36667	1.4822
77	0.63604	0.60604	0.20616	0.2187	1.3512	-4.8558	-10.312	1.2383	1.4523	0.43657	1.4242
78	0.60032	0.69032	0.21774	0.18646	0.49251	-1.4387	-10.359	0.028654	6.5715	0.4286	1.1213
79	0.69543	0.77543	0.18711	0.088069	1.8305	-1.4583	-12.534	0.17776	6.0907	0.40848	0.70171
80	0.77617	0.55617	0.088545	0.24428	1.8092	-4.3753	-11.871	0.15942	4.1113	0.37461	1.8647
81	0.55568	0.035678	0.24414	0.24141	0.85708	-3.4973	-11.933	0.10134	1.7605	0.46436	2.2627
82	0.034941	0.89494	0.24122	0.12827	1.1542	-3.5802	-12.145	0.037784	10.078	0.49513	1.6598
83	0.89833	0.88833	0.12899	0.16425	1.1353	-3.8467	-12.465	0.28253	14.989	0.44968	3.2333
84	0.88339	0.15339	0.16358	0.16087	1.0453	-4.3065	-11.61	0.41989	8.0615	0.56905	3.4135
85	0.15276	0.37276	0.16078	0.15075	0.88661	-3.1489	-11.312	0.21656	32.892	0.58436	1.8111
86	0.37438	0.35438	0.15099	0.13227	1.2526	-2.7425	-11.757	0.95561	39.246	0.46086	0.017511
87	0.35291	0.28291	0.13198	0.17529	1.3587	-3.3484	-10.591	1.1137	9.5842	0.3209	1.5716
88	0.28753	0.17753	0.17588	0.18868	1.2016	-1.7699	-10.427	0.26894	0.0079475	0.44324	3.1501
89	0.17253	0.46253	0.18803	0.16877	1.6562	-1.5899	-11.642	7.95E-06	7.321	0.56259	3.6101
90	0.46469	0.56469	0.16906	0.22379	1.7449	-3.1812	-12.986	0.19725	30.978	0.60046	3.9788
91	0.56321	0.41321	0.22351	0.23358	1.2405	-4.9872	-11.82	0.8938	47.088	0.62789	1.4528

Input and Results of the Base Case Saturated Zone Flow and Transport Model for TSPA

real. #	FPLAW	FPLAN	NVF19	NVF7	FISVO	FPVO	DCVO	KDNPVO	KDNPAL	KDIAL	KDUVO
92	0.41461	0.80461	0.23389	0.17422	0.21402	-3.4216	-10.646	1.316	81.345	0.43303	3.9384
93	0.80038	0.85038	0.17368	0.017518	1.1716	-1.8785	-10.299	1.842	6.2505	0.62392	2.6815
94	0.85476	0.45476	0.048979	0.16644	1.6294	-1.3809	-10.016	0.16758	72.641	0.52918	0.77905
95	0.45429	0.0042893	0.16637	0.22013	1.8522	-1.0228	-11.907	1.7823	21.563	0.38023	0.21716
96	0.0034309	0.39343	0.21998	0.24639	2.3568	-3.5463	-10.05	0.62469	2.056	0.33656	2.8137
97	0.39625	0.78625	0.24724	0.31639	1.1444	-1.055	-10.971	0.047702	0.24754	0.53894	3.505
98	0.78395	0.90395	0.30801	0.16231	2.2121	-2.3042	-12.418	0.00361	23.78	0.59093	2.9758
99	0.90658	0.99658	0.16267	0.29294	1.4874	-4.2137	-12.83	0.69807	42.528	0.55144	3.0663
100	0.99861	0.36861	0.29616	0.20365	0.92798	-4.7656	-10.874	1.2089	27.515	0.55827	0.51443
Expected Value	0.5	0.5	0.18	0.18	1.32	-3.0	-10.49	0.5	18.2	0.47	2.0

real. #	KDUAL	KCPU	GWSPD	KDRN10	KDRN9	CORAL	CORVO	SRC4Y	SRC4X	SRC3X	SRC2Y
1	2.0056	-0.72999	0.91425	0.50425	0.62425	0.49705	2.066	0.34425	0.94425	0.73425	0.49425
2	7.4649	-2.3516	0.71046	0.91046	0.50046	0.89067	2.1431	0.54046	0.34046	0.94046	0.73046
3	1.77	-3.3701	0.44643	0.71643	0.91643	0.41569	2.05	0.33643	0.54643	0.34643	0.94643
4	3.8504	0.74359	0.2755	0.4455	0.7155	2.4592	2.4159	0.4255	0.3355	0.5455	0.3455
5	2.0951	0.57933	0.95395	0.27395	0.44395	3.2581	2.6441	0.31395	0.42395	0.33395	0.54395
6	5.5044	-1.0184	0.92214	0.95214	0.27214	0.096253	1.1932	0.72214	0.31214	0.42214	0.33214
7	0.73961	-4.3312	0.66006	0.92006	0.95006	0.088924	1.1109	0.86006	0.72006	0.31006	0.42006
8	6.0372	0.020328	0.11565	0.66565	0.92565	1.8583	2.3176	0.14565	0.86565	0.72565	0.31565
9	3.9656	-1.8756	0.83954	0.11954	0.66954	3.1688	2.6167	0.13954	0.14954	0.86954	0.72954
10	5.85	-1.0887	0.52976	0.83976	0.11976	1.9355	2.3303	0.61976	0.13976	0.14976	0.86976
11	7.5465	-2.4072	0.65082	0.52082	0.83082	1.2575	2.2149	0.84082	0.61082	0.13082	0.14082
12	2.7915	-4.3591	0.43597	0.65597	0.52597	3.601	2.7431	0.62597	0.84597	0.61597	0.13597
13	4.346	-3.6837	0.10441	0.43441	0.65441	2.3985	2.406	0.50441	0.62441	0.84441	0.61441
14	2.6729	-0.10655	0.21303	0.10303	0.43303	0.99372	2.1633	0.91303	0.50303	0.62303	0.84303
15	3.3744	-2.6714	0.81687	0.21687	0.10687	0.31076	2.0146	0.71687	0.91687	0.50687	0.62687
16	2.4805	-4.7307	0.38929	0.81929	0.21929	3.949	2.8256	0.44929	0.71929	0.91929	0.50929
17	5.7851	-2.1729	0.045317	0.38532	0.81532	3.6761	2.7609	0.27532	0.44532	0.71532	0.91532
18	6.9332	-3.8963	0.47838	0.048382	0.38838	2.1467	2.3648	0.95838	0.27838	0.44838	0.71838
19	1.1416	-1.7888	0.18406	0.47406	0.04406	0.079215	1.0018	0.92406	0.95406	0.27406	0.44406
20	1.0437	-0.063532	0.53465	0.18465	0.47465	3.0765	2.5884	0.66465	0.92465	0.95465	0.27465
21	4.9324	-3.5113	0.82233	0.53233	0.18233	1.3558	2.2342	0.11233	0.66233	0.92233	0.95233
22	6.7463	-4.8593	0.2402	0.8202	0.5302	2.0473	2.3485	0.8302	0.1102	0.6602	0.9202
23	5.0013	-4.0201	0.022989	0.24299	0.82299	0.94786	2.1543	0.52299	0.83299	0.11299	0.66299
24	4.0087	-1.909	0.16501	0.025006	0.24501	0.07372	0.94008	0.65501	0.52501	0.83501	0.11501
25	7.3556	-4.9349	0.51203	0.16203	0.022034	0.16843	1.6696	0.43203	0.65203	0.52203	0.83203
26	5.7303	-1.1427	0.013264	0.51326	0.16326	2.9503	2.5476	0.10326	0.43326	0.65326	0.52326
27	3.5912	-4.6058	0.64229	0.01229	0.51229	0.71639	2.1089	0.21229	0.10229	0.43229	0.65229
28	2.1718	-1.5682	0.063041	0.64304	0.013041	0.036119	0.11186	0.81304	0.21304	0.10304	0.43304
29	7.6367	-3.741	0.57903	0.069028	0.64903	1.1581	2.1955	0.38903	0.81903	0.21903	0.10903
30	7.415	0.78266	0.20534	0.57534	0.065341	0.12247	1.4877	0.045341	0.38534	0.81534	0.21534

Input and Results of the Base Case Saturated Zone Flow and Transport Model for TSPA

real. #	KDUAL	KCPU	GWSPD	KDRN10	KDRN9	CORAL	CORVO	SRC4Y	SRC4X	SRC3X	SRC2Y
31	5.3223	-2.5498	0.96371	0.20371	0.57371	1.4101	2.2444	0.47371	0.043714	0.38371	0.81371
32	0.88947	-4.5235	0.40039	0.96039	0.20039	2.9904	2.5612	0.18039	0.47039	0.040388	0.38039
33	6.7183	0.86554	0.070612	0.40061	0.96061	0.23116	1.8644	0.53061	0.18061	0.47061	0.040612
34	4.1875	-3.1498	0.97584	0.075844	0.40584	0.025683	0.035965	0.82584	0.53584	0.18584	0.47584
35	5.2437	-3.2229	0.30585	0.97585	0.075848	0.11064	1.3548	0.24585	0.82585	0.53585	0.18585
36	3.4816	-4.4825	0.29947	0.30947	0.97947	1.3427	2.2316	0.029473	0.24947	0.82947	0.53947
37	0.82314	-3.5648	0.082942	0.29294	0.30294	0.017853	0.030645	0.16294	0.022942	0.24294	0.82294
38	1.7591	-1.4036	0.23158	0.081577	0.29158	2.0001	2.3408	0.51158	0.16158	0.021577	0.24158
39	6.5482	-3.0502	0.5904	0.2304	0.080405	0.046655	0.41465	0.010405	0.5104	0.1604	0.020405
40	3.0927	-1.4606	0.32321	0.59321	0.23321	1.6261	2.2797	0.64321	0.01321	0.51321	0.16321
41	0.36366	-1.1815	0.58725	0.32725	0.59725	0.15792	1.637	0.067247	0.64725	0.017247	0.51725
42	3.8095	-1.3763	0.63815	0.58815	0.32815	4.0711	2.8425	0.57815	0.068149	0.64815	0.018149
43	1.4746	-0.81168	0.60432	0.63432	0.58432	0.81695	2.1286	0.20432	0.57432	0.064316	0.64432
44	4.2832	-0.34133	0.69396	0.60396	0.63396	0.054881	0.65101	0.96396	0.20396	0.57396	0.063959
45	6.6197	-1.642	0.77241	0.69241	0.60241	4.1872	2.8506	0.40241	0.96241	0.20241	0.57241
46	1.9841	-4.7915	0.55816	0.77816	0.69816	0.37946	2.0426	0.078163	0.40816	0.96816	0.20816
47	0.23599	0.34631	0.038456	0.55846	0.77846	0.35815	2.0339	0.97846	0.078456	0.40846	0.96846
48	1.3474	0.32275	0.89655	0.036549	0.55655	0.06252	0.81427	0.30655	0.97655	0.076549	0.40655
49	4.1455	-4.0798	0.88266	0.89266	0.03266	0.21371	1.8102	0.29266	0.30266	0.97266	0.07266
50	0.14339	-2.7207	0.15078	0.88078	0.89078	1.7223	2.2954	0.080784	0.29078	0.30078	0.97078
51	5.1856	-2.8655	0.37826	0.15826	0.88826	0.4697	2.0606	0.23826	0.088258	0.29826	0.30826
52	0.50142	-3.3079	0.35425	0.37425	0.15425	1.6866	2.2896	0.59425	0.23425	0.084255	0.29425
53	4.6221	-3.924	0.28045	0.35045	0.37045	1.9393	2.3309	0.32045	0.59045	0.23045	0.080451
54	1.6319	-2.1832	0.17858	0.28858	0.35858	1.8196	2.3113	0.58858	0.32858	0.59858	0.23858
55	7.7302	-1.5936	0.46514	0.17514	0.28514	2.2931	2.3887	0.63514	0.58514	0.32514	0.59514
56	3.2466	-2.5122	0.56341	0.46341	0.17341	2.726	2.4718	0.60341	0.63341	0.58341	0.32341
57	0.60351	-0.16668	0.41354	0.56354	0.46354	1.5185	2.2621	0.69354	0.60354	0.63354	0.58354
58	7.774	0.12337	0.80099	0.41099	0.56099	0.028808	0.038089	0.77099	0.69099	0.60099	0.63099
59	2.4318	-2.2535	0.85278	0.80278	0.41278	3.4367	2.699	0.55278	0.77278	0.69278	0.60278
60	2.3678	-4.9507	0.45399	0.85399	0.80399	3.3822	2.6823	0.033988	0.55399	0.77399	0.69399
61	0.70457	-2.6541	0.0064028	0.4564	0.8564	0.10491	1.2904	0.8964	0.036403	0.5564	0.7764
62	1.92	-0.28089	0.39701	0.0070099	0.45701	0.69228	2.1042	0.88701	0.89701	0.03701	0.55701

Input and Results of the Base Case Saturated Zone Flow and Transport Model for TSPA

real. #	KDUAL	KCPU	GWSPD	KDRN10	KDRN9	CORAL	CORVO	SRC4Y	SRC4X	SRC3X	SRC2Y
63	4.7557	0.4137	0.78646	0.39646	0.0064595	0.59846	2.0858	0.15646	0.88646	0.89646	0.03646
64	2.6172	0.9455	0.90213	0.78213	0.39213	0.32231	2.0193	0.37213	0.15213	0.88213	0.89213
65	4.7145	-2.7838	0.99568	0.90568	0.78568	0.11661	1.4218	0.35568	0.37568	0.15568	0.88568
66	5.1083	0.90691	0.36649	0.99649	0.90649	1.1008	2.1842	0.28649	0.35649	0.37649	0.15649
67	4.8092	-0.94458	0.98675	0.36675	0.99675	1.5908	2.2739	0.17675	0.28675	0.35675	0.37675
68	5.574	-3.8486	0.67803	0.98803	0.36803	0.87957	2.1409	0.46803	0.17803	0.28803	0.35803
69	6.2205	-4.6978	0.19896	0.67896	0.98896	2.9261	2.5394	0.56896	0.46896	0.17896	0.28896
70	4.4385	-0.75896	0.053983	0.19398	0.67398	3.1963	2.6252	0.41398	0.56398	0.46398	0.17398
71	0.28619	0.25899	0.70239	0.052391	0.19239	1.0364	2.1716	0.80239	0.41239	0.56239	0.46239
72	7.1277	-0.5325	0.8791	0.7091	0.059102	0.015524	0.029061	0.8591	0.8091	0.4191	0.5691
73	7.0554	-0.41966	0.74881	0.87881	0.70881	0.7918	2.1237	0.45881	0.85881	0.80881	0.41881
74	1.2196	-4.2789	0.76634	0.74634	0.87634	2.7988	2.4964	0.0063435	0.45634	0.85634	0.80634
75	2.9629	-0.23391	0.12616	0.76616	0.74616	3.5222	2.7245	0.39616	0.0061569	0.45616	0.85616
76	2.8044	-3.483	0.7967	0.1267	0.7667	4.8496	2.8968	0.7867	0.3967	0.0067048	0.4567
77	2.2883	0.58823	0.25503	0.79503	0.12503	0.63757	2.0935	0.90503	0.78503	0.39503	0.0050257
78	1.3626	-3.6347	0.93575	0.25575	0.79575	4.5511	2.876	0.99575	0.90575	0.78575	0.39575
79	3.7234	-2.1105	0.2267	0.9367	0.2567	2.1923	2.3723	0.3667	0.9967	0.9067	0.7867
80	4.5293	-3.3996	0.48264	0.22264	0.93264	0.1269	1.5374	0.98264	0.36264	0.99264	0.90264
81	3.3254	-0.89339	0.262	0.482	0.222	0.041558	0.26816	0.672	0.982	0.362	0.992
82	6.4395	-4.4544	0.68599	0.26599	0.48599	2.3525	2.3984	0.19599	0.67599	0.98599	0.36599
83	6.8666	-0.46463	0.09409	0.68409	0.26409	3.3209	2.6634	0.05409	0.19409	0.67409	0.98409
84	3.6271	-2.0197	0.75687	0.096867	0.68687	2.5766	2.435	0.70687	0.056867	0.19687	0.67687
85	0.022107	-0.6101	0.49905	0.75905	0.099055	2.7015	2.4635	0.87905	0.70905	0.059055	0.19905
86	3.155	0.6439	0.73071	0.49071	0.75071	0.083251	1.0471	0.74071	0.87071	0.70071	0.050712
87	6.2633	-2.9133	0.94842	0.73842	0.49842	2.8668	2.5194	0.76842	0.74842	0.87842	0.70842
88	7.2603	-1.7293	0.34449	0.94449	0.73449	0.26163	1.959	0.12449	0.76449	0.74449	0.87449
89	7.9403	-2.9812	0.54262	0.34262	0.94262	3.7347	2.7748	0.79262	0.12262	0.76262	0.74262
90	2.9176	-2.4215	0.33216	0.54216	0.34216	0.19066	1.7387	0.25216	0.79216	0.12216	0.76216
91	7.8657	-3.1398	0.42481	0.33481	0.54481	1.1845	2.2006	0.93481	0.25481	0.79481	0.12481
92	5.3968	-0.6782	0.31937	0.42937	0.33937	0.2943	2.0079	0.22937	0.93937	0.25937	0.79937
93	1.523	0.1818	0.72509	0.31509	0.42509	2.2381	2.3798	0.48509	0.22509	0.93509	0.25509
94	0.4381	-4.1416	0.86201	0.72201	0.31201	0.065836	0.85152	0.26201	0.48201	0.22201	0.93201

Input and Results of the Base Case Saturated Zone Flow and Transport Model for TSPA

real. #	KDUAL	KCPU	GWSPD	KDRN10	KDRN9	CORAL	CORVO	SRC4Y	SRC4X	SRC3X	SRC2Y
95	5.6343	-4.1988	0.1408	0.8608	0.7208	2.5988	2.4385	0.6808	0.2608	0.4808	0.2208
96	6.9874	-1.3203	0.1384	0.1484	0.8684	1.2465	2.2128	0.0984	0.6884	0.2684	0.4884
97	5.97	0.060254	0.61672	0.13672	0.14672	2.5205	2.4259	0.75672	0.096716	0.68672	0.26672
98	6.1116	-1.2531	0.84295	0.61295	0.13295	3.8178	2.7945	0.49295	0.75295	0.092951	0.68295
99	1.0127	-1.9761	0.62522	0.84522	0.61522	0.54713	2.0758	0.73522	0.49522	0.75522	0.095218
100	6.3889	0.50648	0.5013	0.6213	0.8413	1.4516	2.2512	0.9413	0.7313	0.4913	0.7513
Expected Value	10.0	N/A	0.5	0.5	0.5	1.24	2.21	0.5	0.5	0.5	0.5

real. #	SRC2X	SRC3Y	SRC1Y	SRC1X	HAVO	LISP	KDTCAL	Kc_Am_gw_Colloid
1	0.75425	0.094248	0.68425	0.26425	0.48425	1.4395	0.59699	0.0007464
2	0.49046	0.75046	0.090463	0.68046	0.26046	1.9673	0.34716	0.16403
3	0.73643	0.49643	0.75643	0.096429	0.68643	1.5392	0.44025	0.076408
4	0.9455	0.7355	0.4955	0.7555	0.095502	2.3647	0.36293	0.0078553
5	0.34395	0.94395	0.73395	0.49395	0.75395	1.0284	0.50938	0.00018104
6	0.54214	0.34214	0.94214	0.73214	0.49214	2.5131	0.30225	0.027341
7	0.33006	0.54006	0.34006	0.94006	0.73006	1.9852	0.53252	0.0035083
8	0.42565	0.33565	0.54565	0.34565	0.94565	2.4747	0.44348	0.0075039
9	0.31954	0.42954	0.33954	0.54954	0.34954	3.2321	0.52884	0.0021179
10	0.72976	0.31976	0.42976	0.33976	0.54976	1.7162	0.60242	0.00016014
11	0.86082	0.72082	0.31082	0.42082	0.33082	2.0802	0.38929	0.00050339
12	0.14597	0.86597	0.72597	0.31597	0.42597	1.6882	0.46109	0.02347
13	0.13441	0.14441	0.86441	0.72441	0.31441	1.8617	0.38704	0.0015228
14	0.61303	0.13303	0.14303	0.86303	0.72303	1.6407	0.41806	5.72E-05
15	0.84687	0.61687	0.13687	0.14687	0.86687	2.4547	0.3809	0.002605
16	0.62929	0.84929	0.61929	0.13929	0.14929	2.8442	0.52525	0.00037346
17	0.50532	0.62532	0.84532	0.61532	0.13532	1.2187	0.57286	0.0037136
18	0.91838	0.50838	0.62838	0.84838	0.61838	1.196	0.32193	0.025951
19	0.71406	0.91406	0.50406	0.62406	0.84406	2.2202	0.31692	0.00062273
20	0.44465	0.71465	0.91465	0.50465	0.62465	2.7623	0.48513	3.35E-05
21	0.27233	0.44233	0.71233	0.91233	0.50233	2.2364	0.56482	0.00030453
22	0.9502	0.2702	0.4402	0.7102	0.9102	2.0041	0.48707	0.0032617
23	0.92299	0.95299	0.27299	0.44299	0.71299	3.0214	0.44605	1.52E-05
24	0.66501	0.92501	0.95501	0.27501	0.44501	2.4283	0.59025	0.0071107
25	0.11203	0.66203	0.92203	0.95203	0.27203	1.8951	0.51921	8.69E-05
26	0.83326	0.11326	0.66326	0.92326	0.95326	1.5546	0.42514	0.0045639
27	0.52229	0.83229	0.11229	0.66229	0.92229	3.2523	0.3653	0.00043773
28	0.65304	0.52304	0.83304	0.11304	0.66304	3.0712	0.60356	0.19843
29	0.43903	0.65903	0.52903	0.83903	0.11903	2.3304	0.59516	0.0017148

Input and Results of the Base Case Saturated Zone Flow and Transport Model for TSPA

real. #	SRC2X	SRC3Y	SRC1Y	SRC1X	HAVO	LDISP	KDTCAL	Kc_Am_gw_Colloid
30	0.10534	0.43534	0.65534	0.52534	0.83534	1.1146	0.50287	0.00011791
31	0.21371	0.10371	0.43371	0.65371	0.52371	2.7287	0.3098	0.2666
32	0.81039	0.21039	0.10039	0.43039	0.65039	2.0419	0.56064	0.0009509
33	0.38061	0.81061	0.21061	0.10061	0.43061	2.2927	0.45221	0.00089547
34	0.045844	0.38584	0.81584	0.21584	0.10584	1.8834	0.49955	0.00012081
35	0.47585	0.045848	0.38585	0.81585	0.21585	1.0778	0.42255	0.00055718
36	0.18947	0.47947	0.049473	0.38947	0.81947	1.4276	0.30832	0.0052679
37	0.53294	0.18294	0.47294	0.042942	0.38294	2.6686	0.34453	0.0010347
38	0.82158	0.53158	0.18158	0.47158	0.041577	1.7792	0.55405	0.0050291
39	0.2404	0.8204	0.5304	0.1804	0.4704	0.72235	0.40314	0.0067559
40	0.02321	0.24321	0.82321	0.53321	0.18321	1.9537	0.28512	0.0054948
41	0.16725	0.027247	0.24725	0.82725	0.53725	1.3431	0.43704	0.0099798
42	0.51815	0.16815	0.028149	0.24815	0.82815	2.0752	0.33585	0.017142
43	0.014316	0.51432	0.16432	0.024316	0.24432	2.7009	0.45701	0.0040705
44	0.64396	0.013959	0.51396	0.16396	0.023959	1.4873	0.55839	4.35E-05
45	0.062405	0.64241	0.012405	0.51241	0.16241	0.54655	0.35484	0.054841
46	0.57816	0.068163	0.64816	0.018163	0.51816	1.2889	0.27986	0.045025
47	0.20846	0.57846	0.068456	0.64846	0.018456	2.0383	0.32896	0.00027703
48	0.96655	0.20655	0.57655	0.066549	0.64655	0.46717	0.45079	0.0014183
49	0.40266	0.96266	0.20266	0.57266	0.06266	2.2767	0.27443	0.0012702
50	0.070784	0.40078	0.96078	0.20078	0.57078	0.86162	0.49427	0.00078746
51	0.97826	0.078258	0.40826	0.96826	0.20826	2.1511	0.29389	0.0003446
52	0.30425	0.97425	0.074255	0.40425	0.96425	1.3887	0.47099	0.002443
53	0.29045	0.30045	0.97045	0.070451	0.40045	3.3187	0.34016	0.0044625
54	0.088579	0.29858	0.30858	0.97858	0.078579	1.8315	0.609	0.0017796
55	0.23514	0.085142	0.29514	0.30514	0.97514	0.94025	0.4118	0.022189
56	0.59341	0.23341	0.083411	0.29341	0.30341	3.4517	0.29569	0.034893
57	0.32354	0.59354	0.23354	0.083539	0.29354	1.6206	0.61074	0.0023656
58	0.58099	0.32099	0.59099	0.23099	0.080994	1.5937	0.37535	1.24E-05
59	0.63278	0.58278	0.32278	0.59278	0.23278	0.97774	0.37247	0.001579
60	0.60399	0.63399	0.58399	0.32399	0.59399	1.4634	0.2994	0.018968

real. #	SRC2X	SRC3Y	SRC1Y	SRC1X	HAVO	LDISP	KDTCAL	Kc_Am_gw_Colloid
61	0.6964	0.6064	0.6364	0.5864	0.3264	2.1859	0.35274	0.060738
62	0.77701	0.69701	0.60701	0.63701	0.58701	1.6698	0.47895	2.3425
63	0.55646	0.77646	0.69646	0.60646	0.63646	2.1667	0.38426	0.0013164
64	0.032132	0.55213	0.77213	0.69213	0.60213	2.2557	0.47375	0.44001
65	0.89568	0.035681	0.55568	0.77568	0.69568	2.2038	0.49249	0.0084801
66	0.88649	0.89649	0.036486	0.55649	0.77649	2.3881	0.48227	0.00039745
67	0.15675	0.88675	0.89675	0.036749	0.55675	2.573	0.51386	7.10E-05
68	0.37803	0.15803	0.88803	0.89803	0.038031	2.1126	0.54231	0.010251
69	0.35896	0.37896	0.15896	0.88896	0.89896	0.71061	0.46563	0.041701
70	0.28398	0.35398	0.37398	0.15398	0.88398	2.9379	0.28189	0.013322
71	0.17239	0.28239	0.35239	0.37239	0.15239	2.8922	0.58234	0.016242
72	0.4691	0.1791	0.2891	0.3591	0.3791	1.2618	0.58119	0.00022292
73	0.56881	0.46881	0.17881	0.28881	0.35881	1.7738	0.32558	0.019445
74	0.41634	0.56634	0.46634	0.17634	0.28634	1.7294	0.40172	0.00066242
75	0.80616	0.41616	0.56616	0.46616	0.17616	1.5831	0.39465	0.099809
76	0.8567	0.8067	0.4167	0.5667	0.4667	1.3136	0.37035	0.00054266
77	0.45503	0.85503	0.80503	0.41503	0.56503	1.9384	0.33126	0.0027697
78	0.0057527	0.45575	0.85575	0.80575	0.41575	2.1273	0.43301	0.00069321
79	0.3967	0.0067021	0.4567	0.8567	0.8067	1.847	0.46835	0.0092829
80	0.78264	0.39264	0.0026406	0.45264	0.85264	2.6404	0.41442	0.00014545
81	0.902	0.782	0.392	0.0020044	0.452	2.7857	0.5507	0.01437
82	0.99599	0.90599	0.78599	0.39599	0.0059894	1.9214	0.5696	0.0028945
83	0.36409	0.99409	0.90409	0.78409	0.39409	0.19643	0.42893	0.012373
84	0.98687	0.36687	0.99687	0.90687	0.78687	1.8089	0.2724	0.12973
85	0.67905	0.98905	0.36905	0.99905	0.90905	2.6044	0.40967	0.0012363
86	0.19071	0.67071	0.98071	0.36071	0.99071	2.9661	0.54325	0.0039774
87	0.058422	0.19842	0.67842	0.98842	0.36842	4.2152	0.58795	0.0011503
88	0.70449	0.05449	0.19449	0.67449	0.98449	1.7456	0.61807	0.0019342
89	0.87262	0.70262	0.052616	0.19262	0.67262	3.5848	0.39692	0.00097594
90	0.74216	0.87216	0.70216	0.052163	0.19216	2.3368	0.61376	0.011987
91	0.76481	0.74481	0.87481	0.70481	0.054813	1.3637	0.50618	0.036748

Input and Results of the Base Case Saturated Zone Flow and Transport Model for TSPA

real. #	SRC2X	SRC3Y	SRC1Y	SRC1X	HAVO	L DISP	KDTCAL	Kc_Am_gw_Colloid
92	0.12937	0.76937	0.74937	0.87937	0.70937	0.85318	0.33978	0.00025055
93	0.79509	0.12509	0.76509	0.74509	0.87509	2.4066	0.28928	0.00023246
94	0.25201	0.79201	0.12201	0.76201	0.74201	2.8539	0.5157	0.0057209
95	0.9308	0.2508	0.7908	0.1208	0.7608	2.4865	0.57478	0.030588
96	0.2284	0.9384	0.2584	0.7984	0.1284	2.5523	0.53194	0.0061657
97	0.48672	0.22672	0.93672	0.25672	0.79672	1.156	0.53835	0.0030419
98	0.26295	0.48295	0.22295	0.93295	0.25295	2.6146	0.31303	0.071407
99	0.68522	0.26522	0.48522	0.22522	0.93522	1.5136	0.54833	0.011256
100	0.091304	0.6813	0.2613	0.4813	0.2213	3.116	0.35796	0.0022025
Expected Value	0.5	0.5	0.5	0.5	0.5	2.0	0.45	0.01

ATTACHMENT II

Software Routine SZ_PRE v. 1.0

SZ_Pre is an automated method for preparing the FEHM input files for the SZ site-scale flow and transport model for use in TSPA analyses. This routine reads a file containing a table of the stochastic parameter values (Attachment I of this report) that are to be used in the realizations of the SZ site-scale flow and transport model. The routine also reads a file containing tabulated information used to control the FEHM simulation, such as the time step and total simulation time for each realization. Using an existing set of FEHM input files as templates, the SZ_Pre routine writes the appropriate parameter values into the input files for each stochastic realization.

Validation of the SZ_PRE software routine is accomplished by inspection of the stochastic parameter values contained in the file "RIP.dat", hand calculation of transformed values, and examination of the FEHM input files written by the routine. A systematic examination of all variable parameter values in the input files written for realization 1 shows that the correct values are being written to the FEHM input files in the correct locations within the files. The relevant parameter transformations are described in Section 6.2.1.3 of this report.

FORTRAN Source Code Listing for Software Routine SZ_PRE v. 1.0

```
c
c SZ_PREPROCESSOR
c This program writes out the FEHMN input files needed to
c produce the radionuclide breakthrough curves for the SZ part
c of a TSPA calculation.

c PARAMETERS
c   n_rn -- number of radionuclides
c   n_region -- number of source regions
c   n_realization -- number of realizations

c INPUT
c Input is 5 output-file templates:
c Input is a RIP file containing sampled parameter values.

c OUTPUT
c Output is a series of files with some sections replaced with
c sampled parameters read from a RIP file.

program SZ_preprocessor
implicit none
character*1 ch
integer*4 inum_rn
10      write(*,*) 'Enter number of radionuclide to generate files for '
write(*,*) '(0=ALL, 1=C, 2=I, 3=Pu, 4=Np, 5=Kact, 6=Tc, 7=U, 8=Kcfis)...'
read(*,*,err=10,end=20) inum_rn
if(inum_rn.eq.0) then
write(*,*) 'Confirm ALL radionuclides (enter y or n)...'
```

```

else if(inum_rn.eq.1) then
write(*,*) 'Confirm radionuclide "C" (enter y or n)...'
else if(inum_rn.eq.2) then
write(*,*) 'Confirm radionuclide "I" (enter y or n)...'
else if(inum_rn.eq.3) then
write(*,*) 'Confirm radionuclide "Pu" (enter y or n)...'
else if(inum_rn.eq.4) then
write(*,*) 'Confirm radionuclide "Np" (enter y or n)...'
else if(inum_rn.eq.5) then
write(*,*) 'Confirm radionuclide "K_c (actinides)" (enter y or n)...'
else if(inum_rn.eq.6) then
write(*,*) 'Confirm radionuclide "Tc" (enter y or n)...'
else if(inum_rn.eq.7) then
write(*,*) 'Confirm radionuclide "U" (enter y or n)...'
else if(inum_rn.eq.8) then
write(*,*) 'Confirm radionuclide "K_c (fiss. prod.)" (enter y or n)...'
else
goto 10
endif
read(*,*,err=10,end=20) ch
if((ch.eq.'y').or.(ch.eq.'Y')) goto 15
goto 10
15      continue
call initialize
call read_RIP
call read_CONTROL
call make_01_base_case(inum_rn)
call make_final_05_w_fence(inum_rn)
call make_sptr_1000(inum_rn)
call make_props_05_ism3(inum_rn)
c       call debug(1)
c       call debug(100)
20      stop
end

```

```

c READ_CONTROL reads the courant and time parameter values for a FEHM run
c saved in a file named control_runs.txt
subroutine read_CONTROL
implicit none
character*127 file_name
character*127 line
integer*4 find_eol
integer*4 i,idummy
character*127 main_directory
common /dir/ main_directory
integer*4 n_rn,n_region,n_realization
common /control/ n_rn,n_region,n_realization
real*4 cfc(128),cfi(128),cfkc(128),cfnp(128),
*           cfp(128),cftc(128),cfu(128),cfkf(128)
real*4 tottc(128),totti(128),tottkc(128),tottnp(128),
*           tottpu(128),totttc(128),tottu(128),tottkf(128)
real*4 deltc(128),delti(128),deltkc(128),deltnp(128),
*           deltpu(128),delttc(128),deltu(128),deltkf(128)
common /fehm_control/
*           cfc,cfi,cfkc,cfnp,cfpu,cftc,cfu,cfkf,
*           tottc,totti,tottkc,tottnp,tottpu,totttc,tottu,tottkf,
*           deltc,delti,deltkc,deltnp,deltpu,delttc,deltu,deltkf
c
c open file of FEHM control values
file_name=main_directory(1:find_eol(main_directory))
*           //'control_runs.txt'
open(1,file=file_name,status='OLD',err=90)
c skip first line of header
read(1,'(a)',end=91,err=91) line
c read in FEHM control values
c 1 CFC = "courant factor" for C
c 2 CFI = "courant factor" for I
c 3 CFKC = "courant factor" for K_c (actinides)

```

```

c 4 CFNP = "courant factor" for Np
c 5 CFPu = "courant factor" for Pu
c 6 CFTC = "courant factor" for Tc
c 7 CFU = "courant factor" for U
c 8 CFKF = "courant factor" for K_c (fiss. prod.)

c 1 TOTTC = total time for C
c 2 TOTTI = total time for I
c 3 TOTTKC = total time for K_c (actinides)
c 4 TOTTNP = total time for Np
c 5 TOTTPU = total time for Pu
c 6 TOTTTC = total time for Tc
c 7 TOTTU = total time for U
c 8 TOTTKF = total time for K_c (fiss. prod.)

c 1 DELTC = time step for C
c 2 DELTI = time step for I
c 3 DELTKC = time step for K_c (actinides)
c 4 DELTNP = time step for Np
c 5 DELTPU = time step for Pu
c 6 DELTTC = time step for Tc
c 7 DELTU = time step for U
c 8 DELTKF = time step for K_c (fiss. prod.)

do 10 i=1,n_realization
read(1,* ,end=91,err=91)
*           idummy,
*           cfc(i),deltc(i),tottc(i),
*           cfi(i),delti(i),totti(i),
*           cfkc(i),deltkc(i),tottkc(i),
*           cfnp(i),deltnp(i),tottnp(i),
*           cfpu(i),deltpu(i),tottpu(i),
*           cftc(i),delttc(i),totttc(i),
*           cfu(i),deltu(i),tottu(i),
*           cfkf(i),deltkf(i),tottkf(i)
10      continue
goto 100
c
90      write(*,*) 'ERROR opening ',file_name(1:find_eol(file_name)),
*                  ' in READ_CONTROL'
goto 100
91      write(*,*) 'ERROR reading file=',file_name(1:find_eol(file_name)),
*                  ' on realization=',i,
*                  ' in READ_CONTROL'
100     close(1)
return
end

subroutine initialize
implicit none
character*127 main_directory
common /dir/ main_directory
integer*4 n_rn,n_region,n_realization
common /control/ n_rn,n_region,n_realization
real*4 matrix_porosity
real*4 alluv_xmin(8),alluv_xmax(8),alluv_ymin(8),alluv_ymax(8)
real*4 type_num
real*4 r_frac,bulk_den_al,max_al_por
real*4 zone1_1_x,zone1_1_y,zone1_2_x,zone1_2_y
real*4 zone1_3_x,zone1_3_y,zone1_4_x,zone1_4_y
real*4 zone2_1_x,zone2_1_y,zone2_2_x,zone2_2_y
real*4 zone2_3_x,zone2_3_y,zone2_4_x,zone2_4_y
real*4 zone3_1_x,zone3_1_y,zone3_2_x,zone3_2_y
real*4 zone3_3_x,zone3_3_y,zone3_4_x,zone3_4_y
real*4 zone4_1_x,zone4_1_y,zone4_2_x,zone4_2_y
real*4 zone4_3_x,zone4_3_y,zone4_4_x,zone4_4_y
real*4 a1_1_x,a1_1_y,a1_2_x,a1_2_y,a1_3_x,a1_3_y,a1_4_x,a1_4_y
real*4 a2_1_x,a2_1_y,a2_2_x,a2_2_y,a2_3_x,a2_3_y,a2_4_x,a2_4_y
real*4 a3_1_x,a3_1_y,a3_2_x,a3_2_y,a3_3_x,a3_3_y,a3_4_x,a3_4_y
real*4 a4_1_x,a4_1_y,a4_2_x,a4_2_y,a4_3_x,a4_3_y,a4_4_x,a4_4_y

```

```

common /param_constants/ matrix_porosity,
*           alluv_xmin,alluv_xmax,alluv_ymin,alluv_ymax,
*           type_num,
*           r_frac,bulk_den_al,max_al_por,
*           zone1_1_x,zone1_1_y,zone1_2_x,zone1_2_y,
*           zone1_3_x,zone1_3_y,zone1_4_x,zone1_4_y,
*           zone2_1_x,zone2_1_y,zone2_2_x,zone2_2_y,
*           zone2_3_x,zone2_3_y,zone2_4_x,zone2_4_y,
*           zone3_1_x,zone3_1_y,zone3_2_x,zone3_2_y,
*           zone3_3_x,zone3_3_y,zone3_4_x,zone3_4_y,
*           zone4_1_x,zone4_1_y,zone4_2_x,zone4_2_y,
*           zone4_3_x,zone4_3_y,zone4_4_x,zone4_4_y,
*           a1_1_x,a1_1_y,a1_2_x,a1_2_y,a1_3_x,a1_3_y,a1_4_x,a1_4_y,
*           a2_1_x,a2_1_y,a2_2_x,a2_2_y,a2_3_x,a2_3_y,a2_4_x,a2_4_y,
*           a3_1_x,a3_1_y,a3_2_x,a3_2_y,a3_3_x,a3_3_y,a3_4_x,a3_4_y,
*           a4_1_x,a4_1_y,a4_2_x,a4_2_y,a4_3_x,a4_3_y,a4_4_x,a4_4_y
c
real*4 fplaw(128),fplan(128),nfv19(128),nfv7(128)
real*4 fisvo(128),fpvo(128),dcvo(128)
real*4 kdnpvo(128),kdnpal(128),kdial(128)
real*4 kduvo(128),kdual(128),kcpu(128)
real*4 gwspd(128)
real*4 kckdact(128),kckdfis(128)
real*4 coral(128),corvo(128)
real*4 zone1_ran1(128),zone1_ran2(128),zone2_ran1(128),zone2_ran2(128)
real*4 zone3_ran1(128),zone3_ran2(128),zone4_ran1(128),zone4_ran2(128)
real*4 ha(128),l_disp(128),kdtcal(128)
real*4 kcpunew(128),kcam(128)
real*4 ht_disp(128),vt_disp(128)
common /rip_data/
*           fplaw,fplan,nfv19,nfv7,
*           fisvo,fpvo,dcvo,
*           kdnpvo,kdnpal,kdial,
*           kduvo,kdual,kcpu,
*           gwspd,
*           kckdact,kckdfis,
*           coral,corvo,
*           zone1_ran1,zone1_ran2,zone2_ran1,zone2_ran2,
*           zone3_ran1,zone3_ran2,zone4_ran1,zone4_ran2,
*           ha,l_disp,kdtcal,
*           kcpunew,kcam,
*           ht_disp,vt_disp
c
c set the main directory name
c (directory structure is predetermined!!!)
main_directory='/home/bwarnol2/tspa00/nominal_case/inputs/'
c     main_directory='/home/jhgauth/sz99test/'
c     main_directory='/home/jhgauth/sz99new/nominal_case/inputs/'
c set number of radionuclides (N_RN),
c number of source regions (N_REGION),
c and number of realizations (N_REALIZATION),
n_rn=8
n_region=4
n_realization=100
c     n_rn=8
c     n_region=2
c     n_realization=2
c set points that determine rectangular-solid boundaries of the alluvium
alluv_xmin(1)=548588.
alluv_xmax(1)=546653.
alluv_ymin(1)=4.05709E+6
alluv_ymax(1)=4.05762E+6
alluv_xmin(2)=555550.
alluv_xmax(2)=555550.
alluv_ymin(2)=4.0554E+6
alluv_ymax(2)=4.0554E+6
alluv_xmin(3)=557577.
alluv_xmax(3)=557577.
alluv_ymin(3)=4.06632E+6
alluv_ymax(3)=4.06632E+6
alluv_xmin(4)=554152.

```

```

alluv_xmax(4)=552791.
alluv_ymin(4)=4.06632E+6
alluv_ymax(4)=4.06637E+6
alluv_xmin(5)=alluv_xmin(1)
alluv_xmax(5)=alluv_xmax(1)
alluv_ymin(5)=alluv_ymin(1)
alluv_ymax(5)=alluv_ymax(1)
alluv_xmin(6)=alluv_xmin(2)
alluv_xmax(6)=alluv_xmax(2)
alluv_ymin(6)=alluv_ymin(2)
alluv_ymax(6)=alluv_ymax(2)
alluv_xmin(7)=alluv_xmin(3)
alluv_xmax(7)=alluv_xmax(3)
alluv_ymin(7)=alluv_ymin(3)
alluv_ymax(7)=alluv_ymax(3)
alluv_xmin(8)=alluv_xmin(4)
alluv_xmax(8)=alluv_xmax(4)
alluv_ymin(8)=alluv_ymin(4)
alluv_ymax(8)=alluv_ymax(4)

c set points that determine boundaries of 4 rectangular (appox.)
c source regions. A2_1_X means the x coordinate for the first point
c in the second region. points are numbered beginning in the
c southwest corner and proceeding counter clockwise.
c regions are numbered beginning 1=northwest region,
c 2=northeast region, 3=southwest region, 4=southeast region.
c A1_1_X etc. mark the actual boundaries in UTM
c coordinates. ZONE1_1_X etc. mark the rectangular region around
c the actual boundaries (to have a uniform distribution of
c source points, sampling is on these rectangles:
c see GET_SOURCE_LOCATION).
a1_1_x=547586.
a1_1_y=4078757.
a1_2_x=548510.
a1_2_y=4078760.
a1_3_x=548503.
a1_3_y=4080949.
a1_4_x=547579.
a1_4_y=4080946.

c      a2_1_x=a1_2_x
c      a2_1_y=a1_2_y
c      a2_2_x=549942.
c      a2_2_y=4078765.
c      a2_3_x=548865.
c      a2_3_y=4080950.
c      a2_4_x=a1_3_x
c      a2_4_y=a1_3_y

a2_1_x=a1_2_x
a2_1_y=a1_2_y
a2_2_x=548873.
a2_2_y=4078762.
a2_3_x=548865.
a2_3_y=4080950.
a2_4_x=a1_3_x
a2_4_y=a1_3_y

a3_1_x=547458.
a3_1_y=4076168.
a3_2_x=548519.
a3_2_y=4076171.
a3_3_x=a1_2_x
a3_3_y=a1_2_y
a3_4_x=547449.
a3_4_y=4078757.

a4_1_x=a3_2_x
a4_1_y=a3_2_y
a4_2_x=548882.
a4_2_y=4076173.
a4_3_x=548873.

```

```

a4_3_y=4078762.
a4_4_x=a1_2_x
a4_4_y=a1_2_y

zone1_1_x=a1_4_x
zone1_1_y=a1_1_y
zone1_2_x=a1_2_x
zone1_2_y=a1_1_y
zone1_3_x=a1_2_x
zone1_3_y=a1_3_y
zone1_4_x=a1_4_x
zone1_4_y=a1_3_y

zone2_1_x=a2_4_x
zone2_1_y=a2_1_y
zone2_2_x=a2_2_x
zone2_2_y=a2_1_y
zone2_3_x=a2_2_x
zone2_3_y=a2_3_y
zone2_4_x=a2_4_x
zone2_4_y=a2_3_y

zone3_1_x=a3_4_x
zone3_1_y=a3_1_y
zone3_2_x=a3_2_x
zone3_2_y=a3_1_y
zone3_3_x=a3_2_x
zone3_3_y=a3_3_y
zone3_4_x=a3_4_x
zone3_4_y=a3_3_y

zone4_1_x=a4_4_x
zone4_1_y=a4_1_y
zone4_2_x=a4_2_x
zone4_2_y=a4_1_y
zone4_3_x=a4_2_x
zone4_3_y=a4_3_y
zone4_4_x=a4_4_x
zone4_4_y=a4_3_y
c miscellaneous constants
c bulk_den_al = bulk density of the alluvium
c max_al_por = maximum porosity of the alluvium
bulk_den_al=1.27
max_al_por=0.35

goto 100
90      write(*,*) 'ERROR in INITIALIZE'
100     return
end

c READ_RIP reads the (stochastic) parameter values sampled in RIP and
c saved in a file named RIP.dat
subroutine read_RIP
implicit none
character*127 file_name
character*127 line
integer*4 find_eol
integer*4 i
real*4 f1,f2,f3,f4,f5,f6,f7,f8
real*4 l_disp_mean,l_disp_sd,dht_mean,dht_sd,dvt_mean,dvt_sd,sd
character*127 main_directory
common /dir/ main_directory
integer*4 n_rn,n_region,n_realization
common /control/ n_rn,n_region,n_realization
real*4 matrix_porosity
real*4 alluv_xmin(8),alluv_xmax(8),alluv_ymin(8),alluv_ymax(8)
real*4 type_num
real*4 r_frac,bulk_den_al,max_al_por
real*4 zone1_1_x,zone1_1_y,zone1_2_x,zone1_2_y
real*4 zone1_3_x,zone1_3_y,zone1_4_x,zone1_4_y

```

```

real*4 zone2_1_x,zone2_1_y,zone2_2_x,zone2_2_y
real*4 zone2_3_x,zone2_3_y,zone2_4_x,zone2_4_y
real*4 zone3_1_x,zone3_1_y,zone3_2_x,zone3_2_y
real*4 zone3_3_x,zone3_3_y,zone3_4_x,zone3_4_y
real*4 zone4_1_x,zone4_1_y,zone4_2_x,zone4_2_y
real*4 zone4_3_x,zone4_3_y,zone4_4_x,zone4_4_y
real*4 a1_1_x,a1_1_y,a1_2_x,a1_2_y,a1_3_x,a1_3_y,a1_4_x,a1_4_y
real*4 a2_1_x,a2_1_y,a2_2_x,a2_2_y,a2_3_x,a2_3_y,a2_4_x,a2_4_y
real*4 a3_1_x,a3_1_y,a3_2_x,a3_2_y,a3_3_x,a3_3_y,a3_4_x,a3_4_y
real*4 a4_1_x,a4_1_y,a4_2_x,a4_2_y,a4_3_x,a4_3_y,a4_4_x,a4_4_y
common /param_constants/ matrix_porosity,
*           alluv_xmin,alluv_xmax,alluv_ymin,alluv_ymax,
*           type_num,
*           r_frac,bulk_den_al,max_al_por,
*           zone1_1_x,zone1_1_y,zone1_2_x,zone1_2_y,
*           zone1_3_x,zone1_3_y,zone1_4_x,zone1_4_y,
*           zone2_1_x,zone2_1_y,zone2_2_x,zone2_2_y,
*           zone2_3_x,zone2_3_y,zone2_4_x,zone2_4_y,
*           zone3_1_x,zone3_1_y,zone3_2_x,zone3_2_y,
*           zone3_3_x,zone3_3_y,zone3_4_x,zone3_4_y,
*           zone4_1_x,zone4_1_y,zone4_2_x,zone4_2_y,
*           zone4_3_x,zone4_3_y,zone4_4_x,zone4_4_y,
*           a1_1_x,a1_1_y,a1_2_x,a1_2_y,a1_3_x,a1_3_y,a1_4_x,a1_4_y,
*           a2_1_x,a2_1_y,a2_2_x,a2_2_y,a2_3_x,a2_3_y,a2_4_x,a2_4_y,
*           a3_1_x,a3_1_y,a3_2_x,a3_2_y,a3_3_x,a3_3_y,a3_4_x,a3_4_y,
*           a4_1_x,a4_1_y,a4_2_x,a4_2_y,a4_3_x,a4_3_y,a4_4_x,a4_4_y
c
real*4 fplaw(128),fplan(128),nvf19(128),nvf7(128)
real*4 fisvo(128),fpvo(128),dcvo(128)
real*4 kdnpvo(128),kdnpal(128),kdial(128)
real*4 kduvo(128),kdual(128),kcpsi(128)
real*4 gwspd(128)
real*4 kckdact(128),kckdfis(128)
real*4 coral(128),corvo(128)
real*4 zone1_ran1(128),zone1_ran2(128),zone2_ran1(128),zone2_ran2(128)
real*4 zone3_ran1(128),zone3_ran2(128),zone4_ran1(128),zone4_ran2(128)
real*4 ha(128),l_disp(128),kdtcal(128)
real*4 kcpunew(128),kcam(128)
real*4 ht_disp(128),vt_disp(128)
common /rip_data/
*           fplaw,fplan,nvf19,nvf7,
*           fisvo,fpvo,dcvo,
*           kdnpvo,kdnpal,kdial,
*           kduvo,kdual,kcpsi,
*           gwspd,
*           kckdact,kckdfis,
*           coral,corvo,
*           zone1_ran1,zone1_ran2,zone2_ran1,zone2_ran2,
*           zone3_ran1,zone3_ran2,zone4_ran1,zone4_ran2,
*           ha,l_disp,kdtcal,
*           kcpunew,kcam,
*           ht_disp,vt_disp
c
real*4 b_frac(128)
common /work/ b_frac
c
c open file of sampled parameter values generated by RIP
file_name=main_directory(1:find_eol(main_directory))//RIP.dat'
open(1,file=file_name,status='OLD',err=90)
c skip first lines of header
i=0
read(1,'(a)',end=91,err=91) line
c     read(1,'(a)',end=91,err=91) line
c     read(1,'(a)',end=91,err=91) line
c     read(1,'(a)',end=91,err=91) line
c     read(1,'(a)',end=91,err=91) line
c read in parameter values
c 1  RIP name=FPLAW  new name=fplaw
c 2  RIP name=FPLAN  new name=fplan
c 3  RIP name=NVF19  new name=nvf19
c 4  RIP name=NVF7  new name=nvf7

```

```

c 5 RIP name=FISVO new name=fisvo
c 6 RIP name=FPVO new name=fpvo
c 7 RIP name=DCVO new name=dcvo

c 8 RIP name=KDPV0 new name=kdpv0
c 9 RIP name=KDPAL new name=kdpal
c 10 RIP name=KDIAL new name=kdial
c 11 RIP name=KDUVO new name=kduvo
c 12 RIP name=KDUAL new name=kdual
c 13 RIP name=KCPU new name=kcpsi

c 14 RIP name=GWSPD new name=gwspd

c 15 RIP name=KDRN10 new name=kckdact (k_d for actinides in k_c model)
c 16 RIP name=KDRN9 new name=kckdfis (k_d for fission products in k_c model)
c 17 RIP name=KDRN8 new name=f8
c 18 RIP name=KDRN7 new name=f7
c 19 RIP name=KDRN6 new name=f6
c 20 RIP name=KDRN5 new name=f5
c 21 RIP name=KDRN4 new name=f4
c 22 RIP name=KDRN3 new name=f3
c 23 RIP name=KDRN2 new name=f2
c 24 RIP name=KDRN1 new name=f1

c 25 RIP name=CORAL new name=coral
c 26 RIP name=CORVO new name=corvo

c 27 RIP name=SRC4Y new name=zone4_ran2
c 28 RIP name=SRC4X new name=zone4_ran1
c 29 RIP name=SRC3X new name=zone3_ran1
c 30 RIP name=SRC2Y new name=zone2_ran2
c 31 RIP name=SRC2X new name=zone2_ran1
c 32 RIP name=SRC3Y new name=zone3_ran2
c 33 RIP name=SRC1Y new name=zone1_ran2
c 34 RIP name=SRC1X new name=zone1_ran1

c 35 RIP name=HAVO new name=ha
c 36 RIP name=L DISP new name=l_disp
c 37 RIP name=KDTCAL new name=kdtcal
c 38 RIP name=KC????????? new name=kcpunew
c 39 RIP name=KC????????? new name=kcam

do 10 i=1,n_realization
read(1,* ,end=91,err=91)
*          fplaw(i),fplan(i),nvf19(i),nvf7(i),
*          fisvo(i),fpvo(i),dcvo(i),
*          kdnpvo(i),kdpal(i),kdial(i),
*          kduvo(i),kdual(i),kcpsi(i),
*          gwspd(i),
*          kckdact(i),kckdfis(i),
*          f8,f7,f6,f5,f4,f3,f2,f1,
*          coral(i),corvo(i),
*          zone4_ran2(i),zone4_ran1(i),zone3_ran1(i),
*          zone2_ran2(i),zone2_ran1(i),zone3_ran2(i),
*          zone1_ran2(i),zone1_ran1(i),
*          ha(i),l_disp(i),kdtcal(i),
*          kcpunew(i),kcam(i)
10      continue
c
c convert variables sampled from log distributions into linear
do 20 i=1,n_realization
fisvo(i)=10.*fisvo(i)
fpvo(i)=10.*fpvo(i)
dcvo(i)=10.*dcvo(i)
kcpsi(i)=10.*kcpsi(i)
coral(i)=10.*coral(i)
corvo(i)=10.*corvo(i)
20      continue
c
c NOTE: we did not have Vinod resample the k_c model k_ds for matrix, so here
c we convert k_d for the k_c models into distributions

```

```

c      kckdact = U(0,100)
c      kckdfis = U(0,50)
c NOTE: we use the same values for the tuff matrix and the alluvium
c (i.e., we assume perfect correlation)
do 21 i=1,n_realization
kckdact(i)=100.*kckdact(i)
kckdfis(i)=50.*kckdfis(i)
21      continue
c
c determine lateral dispersivities for each realization, then
c convert dispersivities from log to linear values
c NOTE: the SD for all dispersivites is the same (SD=0.75), but
c this part is written to allow them to be easily changed
c   DHT_MEAN is the mean value of the horizontal transverse dispersivity in log space
c   DHT_SD is the std. dev. of the horizontal transverse dispersivity in log space
c   DVT_MEAN is the mean value of the vertical transverse dispersivity in log space
c   DVT_SD is the std. dev. of the vertical transverse dispersivity in log space
l_disp_mean=2.0
l_disp_sd=0.75
dht_mean=-0.3
dht_sd=0.75
dvt_mean=-2.3
dvt_sd=0.75
do 30 i=1,n_realization
sd=(l_disp(i)-l_disp_mean)/l_disp_sd
ht_disp(i)=sd*dht_sd+dht_mean
vt_disp(i)=sd*dvt_sd+dvt_mean
l_disp(i)=10.**l_disp(i)
ht_disp(i)=10.**ht_disp(i)
vt_disp(i)=10.**vt_disp(i)
30      continue
c
c calculate fracture aperture B_FRAC=10***FISVO*10***FPVO
do 40 i=1,n_realization
c      b_frac(i)=10.***(fisvo(i)+fpvo(i))
b_frac(i)=fisvo(i)*fpvo(i)
40      continue
goto 100
c
90      write(*,*) 'ERROR opening ',file_name(1:find_eol(file_name)),
*                  ' in READ_RIP'
goto 100
91      write(*,*) 'ERROR reading file=',file_name(1:find_eol(file_name)),
*                  ' on realization=',i,
*                  ' in READ_RIP'
100     close(1)
return
end

subroutine make_01_base_case(inum_rn)
implicit none
character*127 file2,file3,file_name
character*127 line,new_line
integer*4 i_realization,i_rn,i_region,inum_rn
integer*4 find_eol,find_comment
integer*4 i1,i2,i3
integer*4 i,i_start
real*4 f1,f2,f3
character*127 main_directory
common /dir/ main_directory
integer*4 n_rn,n_region,n_realization
common /control/ n_rn,n_region,n_realization
real*4 matrix_porosity
real*4 alluv_xmin(8),alluv_xmax(8),alluv_ymin(8),alluv_ymax(8)
real*4 type_num
real*4 r_frac,bulk_den_al,max_al_por
real*4 zone1_1_x,zone1_1_y,zone1_2_x,zone1_2_y
real*4 zone1_3_x,zone1_3_y,zone1_4_x,zone1_4_y
real*4 zone2_1_x,zone2_1_y,zone2_2_x,zone2_2_y
real*4 zone2_3_x,zone2_3_y,zone2_4_x,zone2_4_y

```

```

real*4 zone3_1_x,zone3_1_y,zone3_2_x,zone3_2_y
real*4 zone3_3_x,zone3_3_y,zone3_4_x,zone3_4_y
real*4 zone4_1_x,zone4_1_y,zone4_2_x,zone4_2_y
real*4 zone4_3_x,zone4_3_y,zone4_4_x,zone4_4_y
real*4 a1_1_x,a1_1_y,a1_2_x,a1_2_y,a1_3_x,a1_3_y,a1_4_x,a1_4_y
real*4 a2_1_x,a2_1_y,a2_2_x,a2_2_y,a2_3_x,a2_3_y,a2_4_x,a2_4_y
real*4 a3_1_x,a3_1_y,a3_2_x,a3_2_y,a3_3_x,a3_3_y,a3_4_x,a3_4_y
real*4 a4_1_x,a4_1_y,a4_2_x,a4_2_y,a4_3_x,a4_3_y,a4_4_x,a4_4_y
common /param_constants/ matrix_porosity,
*           alluv_xmin,alluv_xmax,alluv_ymin,alluv_ymax,
*           type_num,
*           r_frac,bulk_den_al,max_al_por,
*           zone1_1_x,zone1_1_y,zone1_2_x,zone1_2_y,
*           zone1_3_x,zone1_3_y,zone1_4_x,zone1_4_y,
*           zone2_1_x,zone2_1_y,zone2_2_x,zone2_2_y,
*           zone2_3_x,zone2_3_y,zone2_4_x,zone2_4_y,
*           zone3_1_x,zone3_1_y,zone3_2_x,zone3_2_y,
*           zone3_3_x,zone3_3_y,zone3_4_x,zone3_4_y,
*           zone4_1_x,zone4_1_y,zone4_2_x,zone4_2_y,
*           zone4_3_x,zone4_3_y,zone4_4_x,zone4_4_y,
*           a1_1_x,a1_1_y,a1_2_x,a1_2_y,a1_3_x,a1_3_y,a1_4_x,a1_4_y,
*           a2_1_x,a2_1_y,a2_2_x,a2_2_y,a2_3_x,a2_3_y,a2_4_x,a2_4_y,
*           a3_1_x,a3_1_y,a3_2_x,a3_2_y,a3_3_x,a3_3_y,a3_4_x,a3_4_y,
*           a4_1_x,a4_1_y,a4_2_x,a4_2_y,a4_3_x,a4_3_y,a4_4_x,a4_4_y
C
real*4 fplaw(128),fplan(128),nvf19(128),nvf7(128)
real*4 fisvo(128),fpvo(128),dcvo(128)
real*4 kdnpvo(128),kdnpal(128),kdial(128)
real*4 kduvo(128),kdual(128),kcpcu(128)
real*4 gwspd(128)
real*4 kckdact(128),kckdfis(128)
real*4 coral(128),corvo(128)
real*4 zone1_ran1(128),zone1_ran2(128),zone2_ran1(128),zone2_ran2(128)
real*4 zone3_ran1(128),zone3_ran2(128),zone4_ran1(128),zone4_ran2(128)
real*4 ha(128),l_disp(128),kdtcal(128)
real*4 kcpunew(128),kcam(128)
real*4 ht_disp(128),vt_disp(128)
common /rip_data/
*           fplaw,fplan,nvf19,nvf7,
*           fisvo,fpvo,dcvo,
*           kdnpvo,kdnpal,kdial,
*           kduvo,kdual,kcpcu,
*           gwspd,
*           kckdact,kckdfis,
*           coral,corvo,
*           zone1_ran1,zone1_ran2,zone2_ran1,zone2_ran2,
*           zone3_ran1,zone3_ran2,zone4_ran1,zone4_ran2,
*           ha,l_disp,kdtcal,
*           kcpunew,kcam,
*           ht_disp,vt_disp
C
real*4 cfc(128),cfi(128),cfkc(128),cfnp(128),
*           cfpu(128),cftc(128),cfu(128),cfkf(128)
real*4 tottc(128),totti(128),tottkc(128),tottnp(128),
*           tottpu(128),totttc(128),tottu(128),tottkf(128)
real*4 deltc(128),delti(128),deltkc(128),deltnp(128),
*           deltpu(128),delttc(128),deltu(128),deltkf(128)
common /fehm_control/
*           cfc,cfi,cfkc,cfnp,cfpu,cftc,cfu,cfkf,
*           tottc,totti,tottkc,tottnp,tottpu,totttc,tottu,tottkf,
*           deltc,delti,deltkc,deltnp,deltpu,delttc,deltu,deltkf
C
c loop through the number of realizations (one 01_base_case file per realization)
c (modification as of 12-8-1999: make files for each radionuclide too)
i_region=0
do 60 i_realization=1,n_realization
do 10 i_rn=1,n_rn
c skip some radionuclides for now
c (1=C, 2=I, 3=Pu, 4=Np, 5=Kc, 6=Tc, 7=U)
c      if(i_rn.eq.1) goto 10
c      if(i_rn.eq.2) goto 10

```

```

c      if(i_rn.eq.3) goto 10
c      if(i_rn.eq.4) goto 10
c      if(i_rn.eq.5) goto 10
c      if(i_rn.eq.6) goto 10
c      if(i_rn.eq.7) goto 10
if(inum_rn.eq.0) goto 9
if(i_rn.ne.inum_rn) goto 10
9      continue
c open template 01_base_case file2 and
c open new 01_base_case file3
i=i_realization
if((ha(i).lt.0.5).and.(gwspd(i).lt.0.24)) then
file2=main_directory(1:find_eol(main_directory))
*      //'01_base_case/low_iso/01_base_case.dat_low_iso'
file3=main_directory(1:find_eol(main_directory))
*      //'01_base_case/low_iso/01_base_case.dat'
else if((ha(i).lt.0.5).and.(gwspd(i).le.0.76)) then
file2=main_directory(1:find_eol(main_directory))
*      //'01_base_case/mean_iso/01_base_case.dat_mean_iso'
file3=main_directory(1:find_eol(main_directory))
*      //'01_base_case/mean_iso/01_base_case.dat'
else if((ha(i).lt.0.5).and.(gwspd(i).gt.0.76)) then
file2=main_directory(1:find_eol(main_directory))
*      //'01_base_case/high_iso/01_base_case.dat_high_iso'
file3=main_directory(1:find_eol(main_directory))
*      //'01_base_case/high_iso/01_base_case.dat'
else if((ha(i).ge.0.5).and.(gwspd(i).lt.0.24)) then
file2=main_directory(1:find_eol(main_directory))
*      //'01_base_case/low_aniso/01_base_case.dat_low_aniso'
file3=main_directory(1:find_eol(main_directory))
*      //'01_base_case/low_aniso/01_base_case.dat'
else if((ha(i).ge.0.5).and.(gwspd(i).le.0.76)) then
file2=main_directory(1:find_eol(main_directory))
*      //'01_base_case/mean_aniso/01_base_case.dat_mean_aniso'
file3=main_directory(1:find_eol(main_directory))
*      //'01_base_case/mean_aniso/01_base_case.dat'
else
file2=main_directory(1:find_eol(main_directory))
*      //'01_base_case/high_aniso/01_base_case.dat_high_aniso'
file3=main_directory(1:find_eol(main_directory))
*      //'01_base_case/high_aniso/01_base_case.dat'
endif
file_name=file2
open(2,file=file2,status='OLD',err=90)
call new_file_name(i_realization,i_rn,i_region,file3)
file_name=file3
open(3,file=file3,status='UNKNOWN',err=90)
write(*,*) 'open file='
write(*,*) file3(1:find_eol(file3))
c copy from template onto new file up to the block that needs to be changed
call copy_to(2,3,'rock')
c copy from template onto new file the next 7 lines
call copy_lines(2,3,7)
c modify next line
read(2,'(a)',end=100,err=91) line
read(line,*,err=92) i1,i2,i3,f1,f2,f3
write(new_line,*) i1,i2,i3,f1,f2,nvf7(i_realization)
new_line(find_eol(new_line)+2:)=line(find_comment(line):)
write(3,'(a)') new_line(1:find_eol(new_line))
c modify next 8 lines
do 20 i=1,8
read(2,'(a)',end=100,err=91) line
read(line,*,err=92) i1,i2,i3,f1,f2,f3
write(new_line,*) i1,i2,i3,f1,f2,fpvo(i_realization)
new_line(find_eol(new_line)+2:)=line(find_comment(line):)
write(3,'(a)') new_line(1:find_eol(new_line))
20      continue
c copy from template onto new file the next 2 lines
call copy_lines(2,3,2)
c modify next line
read(2,'(a)',end=100,err=91) line

```

```

read(line,*,err=92) i1,i2,i3,f1,f2,f3
write(new_line,*) i1,i2,i3,f1,f2,nvf19(i_realization)
new_line(find_eol(new_line)+2:)=line(find_comment(line):)
write(3,'(a)') new_line(1:find_eol(new_line))
c copy from template onto new file up to the block that needs to be changed
call copy_to(2,3,'time')
call copy_to(2,3,'time')
c modify next line to set total simulation time, which is dependent on
c the radionuclide (1=C, 2=I, 3=Pu, 4=Np, 5=Kc, 6=Tc, 7=U)
read(2,'(a)',end=100,err=91) line
if(i_rn.eq.1) then
write(new_line,*) tottc(i_realization),tottc(i_realization)
else if(i_rn.eq.2) then
write(new_line,*) totti(i_realization),totti(i_realization)
else if(i_rn.eq.3) then
write(new_line,*) tottpu(i_realization),tottpu(i_realization)
else if(i_rn.eq.4) then
write(new_line,*) tottnp(i_realization),tottnp(i_realization)
else if(i_rn.eq.5) then
write(new_line,*) tottkc(i_realization),tottkc(i_realization)
else if(i_rn.eq.6) then
write(new_line,*) totttc(i_realization),totttc(i_realization)
else if(i_rn.eq.7) then
write(new_line,*) tottu(i_realization),tottu(i_realization)
else if(i_rn.eq.8) then
write(new_line,*) tottkf(i_realization),tottkf(i_realization)
endif
istart=index(line,' 10 ')
write(3,'(a)') new_line(1:find_eol(new_line))
*           //line(istart:find_eol(line))
c copy from template onto new file up to the block that needs to be changed
call copy_to(2,3,'rock')
c modify next line
read(2,'(a)',end=100,err=91) line
read(line,*,err=92) i1,i2,i3,f1,f2,f3
write(new_line,*) i1,i2,i3,f1,f2,nvf19(i_realization)
new_line(find_eol(new_line)+2:)=line(find_comment(line):)
write(3,'(a)') new_line(1:find_eol(new_line))
c copy the rest of the template onto new file
call copy_to(2,3,'GOTO THE END')
close(2)
close(3)
10      continue
60      continue
goto 100
90      write(*,*) 'ERROR opening ',file_name(1:find_eol(file_name)),
*                  ' on realization=',i_realization,
*                  ' in MAKE_01_BASE_CASE'
goto 100
91      write(*,*) 'ERROR reading file=',file2(1:find_eol(file2)),
*                  ' on realization=',i_realization,
*                  ' in MAKE_01_BASE_CASE'
goto 100
92      write(*,*) 'ERROR reading line=',line(1:find_eol(line)),
*                  ' on realization=',i_realization,
*                  ' in MAKE_01_BASE_CASE'
100     close(2)
return
end

subroutine make_final_05_w_fence(inum_rn)
implicit none
character*127 file2,file3,file_name
integer*4 i_realization,i_rn,i_region,inum_rn
integer*4 find_eol
integer*4 j
real*4 x(8),y(8)
character*127 main_directory
common /dir/ main_directory
integer*4 n_rn,n_region,n_realization
common /control/ n_rn,n_region,n_realization

```

```

real*4 matrix_porosity
real*4 alluv_xmin(8),alluv_xmax(8),alluv_ymin(8),alluv_ymax(8)
real*4 type_num
real*4 r_frac,bulk_den_al,max_al_por
real*4 zone1_1_x,zone1_1_y,zone1_2_x,zone1_2_y
real*4 zone1_3_x,zone1_3_y,zone1_4_x,zone1_4_y
real*4 zone2_1_x,zone2_1_y,zone2_2_x,zone2_2_y
real*4 zone2_3_x,zone2_3_y,zone2_4_x,zone2_4_y
real*4 zone3_1_x,zone3_1_y,zone3_2_x,zone3_2_y
real*4 zone3_3_x,zone3_3_y,zone3_4_x,zone3_4_y
real*4 zone4_1_x,zone4_1_y,zone4_2_x,zone4_2_y
real*4 zone4_3_x,zone4_3_y,zone4_4_x,zone4_4_y
real*4 a1_1_x,a1_1_y,a1_2_x,a1_2_y,a1_3_x,a1_3_y,a1_4_x,a1_4_y
real*4 a2_1_x,a2_1_y,a2_2_x,a2_2_y,a2_3_x,a2_3_y,a2_4_x,a2_4_y
real*4 a3_1_x,a3_1_y,a3_2_x,a3_2_y,a3_3_x,a3_3_y,a3_4_x,a3_4_y
real*4 a4_1_x,a4_1_y,a4_2_x,a4_2_y,a4_3_x,a4_3_y,a4_4_x,a4_4_y
common /param_constants/ matrix_porosity,
*           alluv_xmin,alluv_xmax,alluv_ymin,alluv_ymax,
*           type_num,
*           r_frac,bulk_den_al,max_al_por,
*           zone1_1_x,zone1_1_y,zone1_2_x,zone1_2_y,
*           zone1_3_x,zone1_3_y,zone1_4_x,zone1_4_y,
*           zone2_1_x,zone2_1_y,zone2_2_x,zone2_2_y,
*           zone2_3_x,zone2_3_y,zone2_4_x,zone2_4_y,
*           zone3_1_x,zone3_1_y,zone3_2_x,zone3_2_y,
*           zone3_3_x,zone3_3_y,zone3_4_x,zone3_4_y,
*           zone4_1_x,zone4_1_y,zone4_2_x,zone4_2_y,
*           zone4_3_x,zone4_3_y,zone4_4_x,zone4_4_y,
*           a1_1_x,a1_1_y,a1_2_x,a1_2_y,a1_3_x,a1_3_y,a1_4_x,a1_4_y,
*           a2_1_x,a2_1_y,a2_2_x,a2_2_y,a2_3_x,a2_3_y,a2_4_x,a2_4_y,
*           a3_1_x,a3_1_y,a3_2_x,a3_2_y,a3_3_x,a3_3_y,a3_4_x,a3_4_y,
*           a4_1_x,a4_1_y,a4_2_x,a4_2_y,a4_3_x,a4_3_y,a4_4_x,a4_4_y
c
real*4 fplaw(128),fplan(128),nvf19(128),nvf7(128)
real*4 fisvo(128),fpvo(128),dcvo(128)
real*4 kdnpvo(128),kdnpal(128),kdial(128)
real*4 kduvo(128),kdual(128),kcpcu(128)
real*4 gwspd(128)
real*4 kckdact(128),kckdfis(128)
real*4 coral(128),corvo(128)
real*4 zone1_ran1(128),zone1_ran2(128),zone2_ran1(128),zone2_ran2(128)
real*4 zone3_ran1(128),zone3_ran2(128),zone4_ran1(128),zone4_ran2(128)
real*4 ha(128),l_disp(128),kdtcal(128)
real*4 kcpnew(128),kcam(128)
real*4 ht_disp(128),vt_disp(128)
common /rip_data/
*           fplaw,fplan,nvf19,nvf7,
*           fisvo,fpvo,dcvo,
*           kdnpvo,kdnpal,kdial,
*           kduvo,kdual,kcpcu,
*           gwspd,
*           kckdact,kckdfis,
*           coral,corvo,
*           zone1_ran1,zone1_ran2,zone2_ran1,zone2_ran2,
*           zone3_ran1,zone3_ran2,zone4_ran1,zone4_ran2,
*           ha,l_disp,kdtcal,
*           kcpnew,kcam,
*           ht_disp,vt_disp
c
if(inum_rn.ne.0) goto 200
c
c open template final_05_w_fence file
file2=main_directory(1:find_eol(main_directory))
*           //'final_05_w_fence/final_05_w_fence.macro.00_00.0000'
file_name=file2
open(2,file=file2,status='OLD',err=90)
c loop through the number of realizations (one final_05_w_fence file per realization)
i_rn=0
i_region=0
do 10 i_realization=1,n_realization
c open new final_05_w_fence file

```

```

file3=main_directory(1:find_eol(main_directory))
*          //'final_05_w_fence/final_05_w_fence.macro'
call new_file_name(i_realization,i_rn,i_region,file3)
file_name=file3
open(3,file=file3,status='UNKNOWN',err=90)
write(*,*) 'open file=',file3(1:find_eol(file3))
c copy from template onto new file up to the block that needs to be changed
call copy_to(2,3,'Alluvial uncertainty')
c calculate new X,Y values for the alluvial region with fplaw and fplan
call new_alluvial_region(x,y,i_realization)
c write new X,Y values onto new final_05_w_fence file
write(3,*) (x(j),j=1,4)
write(3,*) (x(j),j=5,8)
write(3,*) (y(j),j=1,4)
write(3,*) (y(j),j=5,8)
c ??????????????????????????????????????????????????????????
c skip the replaced lines on the template file
read(2,*,end=91,err=91)
read(2,*,end=91,err=91)
read(2,*,end=91,err=91)
read(2,*,end=91,err=91)
c copy the rest of the template onto new file
call copy_to(2,3,'GOTO THE END')
rewind(2)
close(3)
10      continue
goto 100
90      write(*,*) 'ERROR opening ',file_name(1:find_eol(file_name)),
*                  ' on realization=',i_realization,
*                  ' in MAKE_FINAL_05_W_FENCE'
goto 100
91      write(*,*) 'ERROR reading file=',file2(1:find_eol(file2)),
*                  ' on realization=',i_realization,
*                  ' in MAKE_FINAL_05_W_FENCE'
100     close(2)
200     return
end

subroutine new_alluvial_region(x,y,i)
implicit none
integer*4 i
real*4 x(8),y(8)
real*4 xtemp,ytemp
character*127 main_directory
common /dir/ main_directory
integer*4 n_rn,n_region,n_realization
common /control/ n_rn,n_region,n_realization
real*4 matrix_porosity
real*4 alluv_xmin(8),alluv_xmax(8),alluv_ymin(8),alluv_ymax(8)
real*4 type_num
real*4 r_frac,bulk_den_al,max_al_por
real*4 zone1_1_x,zone1_1_y,zone1_2_x,zone1_2_y
real*4 zone1_3_x,zone1_3_y,zone1_4_x,zone1_4_y
real*4 zone2_1_x,zone2_1_y,zone2_2_x,zone2_2_y
real*4 zone2_3_x,zone2_3_y,zone2_4_x,zone2_4_y
real*4 zone3_1_x,zone3_1_y,zone3_2_x,zone3_2_y
real*4 zone3_3_x,zone3_3_y,zone3_4_x,zone3_4_y
real*4 zone4_1_x,zone4_1_y,zone4_2_x,zone4_2_y
real*4 zone4_3_x,zone4_3_y,zone4_4_x,zone4_4_y
real*4 a1_1_x,a1_1_y,a1_2_x,a1_2_y,a1_3_x,a1_3_y,a1_4_x,a1_4_y
real*4 a2_1_x,a2_1_y,a2_2_x,a2_2_y,a2_3_x,a2_3_y,a2_4_x,a2_4_y
real*4 a3_1_x,a3_1_y,a3_2_x,a3_2_y,a3_3_x,a3_3_y,a3_4_x,a3_4_y
real*4 a4_1_x,a4_1_y,a4_2_x,a4_2_y,a4_3_x,a4_3_y,a4_4_x,a4_4_y
common /param_constants/ matrix_porosity,
*                  alluv_xmin,alluv_xmax,alluv_ymin,alluv_ymax,
*                  type_num,
*                  r_frac,bulk_den_al,max_al_por,
*                  zone1_1_x,zone1_1_y,zone1_2_x,zone1_2_y,
*                  zone1_3_x,zone1_3_y,zone1_4_x,zone1_4_y,
*                  zone2_1_x,zone2_1_y,zone2_2_x,zone2_2_y,
*                  zone2_3_x,zone2_3_y,zone2_4_x,zone2_4_y

```

```

*
*      zone3_1_x,zone3_1_y,zone3_2_x,zone3_2_y,
*      zone3_3_x,zone3_3_y,zone3_4_x,zone3_4_y,
*      zone4_1_x,zone4_1_y,zone4_2_x,zone4_2_y,
*      zone4_3_x,zone4_3_y,zone4_4_x,zone4_4_y,
*      a1_1_x,a1_1_y,a1_2_x,a1_2_y,a1_3_x,a1_3_y,a1_4_x,a1_4_y,
*      a2_1_x,a2_1_y,a2_2_x,a2_2_y,a2_3_x,a2_3_y,a2_4_x,a2_4_y,
*      a3_1_x,a3_1_y,a3_2_x,a3_2_y,a3_3_x,a3_3_y,a3_4_x,a3_4_y,
*      a4_1_x,a4_1_y,a4_2_x,a4_2_y,a4_3_x,a4_3_y,a4_4_x,a4_4_y
c
real*4 fplaw(128),fplan(128),nvvf19(128),nvvf7(128)
real*4 fisvo(128),fpvo(128),dcvo(128)
real*4 kdnpvo(128),kdnpal(128),kdial(128)
real*4 kduvo(128),kdual(128),kcpsi(128)
real*4 gwspd(128)
real*4 kckdact(128),kckdfis(128)
real*4 coral(128),corvo(128)
real*4 zone1_ran1(128),zone1_ran2(128),zone2_ran1(128),zone2_ran2(128)
real*4 zone3_ran1(128),zone3_ran2(128),zone4_ran1(128),zone4_ran2(128)
real*4 ha(128),l_disp(128),kdtcal(128)
real*4 kcpunew(128),kcam(128)
real*4 ht_disp(128),vt_disp(128)
common /rip_data/
*
*      fplaw,fplan,nvvf19,nvvf7,
*      fisvo,fpvo,dcvo,
*      kdnpvo,kdnpal,kdial,
*      kduvo,kdual,kcpsi,
*      gwspd,
*      kckdact,kckdfis,
*      coral,corvo,
*      zone1_ran1,zone1_ran2,zone2_ran1,zone2_ran2,
*      zone3_ran1,zone3_ran2,zone4_ran1,zone4_ran2,
*      ha,l_disp,kdtcal,
*      kcpunew,kcam,
*      ht_disp,vt_disp
c
c area of alluvium is a rectangle in plan view,
c indicies are numbered as follows:
c     1 is SW corner
c     2 is SE corner (a constant)
c     3 is NE corner
c     4 is NW corner.
c ALLUVIAL_RAN1 controls the location of western side
c ALLUVIAL_RAN2 controls the location of northern side
x(1)=fplaw(i)*(alluv_xmax(1)-alluv_xmin(1))+alluv_xmin(1)
y(1)=fplaw(i)*(alluv_ymax(1)-alluv_ymin(1))+alluv_ymin(1)
x(2)=alluv_xmin(2)
y(2)=alluv_ymin(2)
x(3)=fplan(i)*(alluv_xmax(3)-alluv_xmin(2))+alluv_xmin(2)
y(3)=fplan(i)*(alluv_ymax(3)-alluv_ymin(2))+alluv_ymin(2)
xtemp=fplaw(i)*(alluv_xmax(4)-alluv_xmin(4))+alluv_xmin(4)
ytemp=fplaw(i)*(alluv_ymax(4)-alluv_ymin(4))+alluv_ymin(4)
x(4)=fplan(i)*(xtemp-x(1))+x(1)
y(4)=fplan(i)*(ytemp-y(1))+y(1)
x(5)=x(1)
y(5)=y(1)
x(6)=x(2)
y(6)=y(2)
x(7)=x(3)
y(7)=y(3)
x(8)=x(4)
y(8)=y(4)
return
end

subroutine make_sptr_1000(inum_rn)
implicit none
character*127 line,new_line
character*127 file2,file3,file_name
integer*4 i_realization,i_rn,i_region,inum_rn
integer*4 find_eol
integer*4 i,idummy

```

```

integer*4 i1,i2,i3
character*127 main_directory
common /dir/ main_directory
integer*4 n_rn,n_region,n_realization
common /control/ n_rn,n_region,n_realization
real*4 matrix_porosity
real*4 alluv_xmin(8),alluv_xmax(8),alluv_ymin(8),alluv_ymax(8)
real*4 type_num
real*4 r_frac,bulk_den_al,max_al_por
real*4 zone1_1_x,zone1_1_y,zone1_2_x,zone1_2_y
real*4 zone1_3_x,zone1_3_y,zone1_4_x,zone1_4_y
real*4 zone2_1_x,zone2_1_y,zone2_2_x,zone2_2_y
real*4 zone2_3_x,zone2_3_y,zone2_4_x,zone2_4_y
real*4 zone3_1_x,zone3_1_y,zone3_2_x,zone3_2_y
real*4 zone3_3_x,zone3_3_y,zone3_4_x,zone3_4_y
real*4 zone4_1_x,zone4_1_y,zone4_2_x,zone4_2_y
real*4 zone4_3_x,zone4_3_y,zone4_4_x,zone4_4_y
real*4 a1_1_x,a1_1_y,a1_2_x,a1_2_y,a1_3_x,a1_3_y,a1_4_x,a1_4_y
real*4 a2_1_x,a2_1_y,a2_2_x,a2_2_y,a2_3_x,a2_3_y,a2_4_x,a2_4_y
real*4 a3_1_x,a3_1_y,a3_2_x,a3_2_y,a3_3_x,a3_3_y,a3_4_x,a3_4_y
real*4 a4_1_x,a4_1_y,a4_2_x,a4_2_y,a4_3_x,a4_3_y,a4_4_x,a4_4_y
common /param_constants/ matrix_porosity,
*           alluv_xmin,alluv_xmax,alluv_ymin,alluv_ymax,
*           type_num,
*           r_frac,bulk_den_al,max_al_por,
*           zone1_1_x,zone1_1_y,zone1_2_x,zone1_2_y,
*           zone1_3_x,zone1_3_y,zone1_4_x,zone1_4_y,
*           zone2_1_x,zone2_1_y,zone2_2_x,zone2_2_y,
*           zone2_3_x,zone2_3_y,zone2_4_x,zone2_4_y,
*           zone3_1_x,zone3_1_y,zone3_2_x,zone3_2_y,
*           zone3_3_x,zone3_3_y,zone3_4_x,zone3_4_y,
*           zone4_1_x,zone4_1_y,zone4_2_x,zone4_2_y,
*           zone4_3_x,zone4_3_y,zone4_4_x,zone4_4_y,
*           a1_1_x,a1_1_y,a1_2_x,a1_2_y,a1_3_x,a1_3_y,a1_4_x,a1_4_y,
*           a2_1_x,a2_1_y,a2_2_x,a2_2_y,a2_3_x,a2_3_y,a2_4_x,a2_4_y,
*           a3_1_x,a3_1_y,a3_2_x,a3_2_y,a3_3_x,a3_3_y,a3_4_x,a3_4_y,
*           a4_1_x,a4_1_y,a4_2_x,a4_2_y,a4_3_x,a4_3_y,a4_4_x,a4_4_y
c
real*4 fplaw(128),fplan(128),nvf19(128),nvf7(128)
real*4 fisvo(128),fpvo(128),dcvo(128)
real*4 kdnpvo(128),kdnpal(128),kdial(128)
real*4 kduvo(128),kdual(128),kcpsi(128)
real*4 gwspd(128)
real*4 kckdact(128),kckdfis(128)
real*4 coral(128),corvo(128)
real*4 zone1_ran1(128),zone1_ran2(128),zone2_ran1(128),zone2_ran2(128)
real*4 zone3_ran1(128),zone3_ran2(128),zone4_ran1(128),zone4_ran2(128)
real*4 ha(128),l_disp(128),kdtcal(128)
real*4 kcpunew(128),kcam(128)
real*4 ht_disp(128),vt_disp(128)
common /rip_data/
*           fplaw,fplan,nvf19,nvf7,
*           fisvo,fpvo,dcvo,
*           kdnpvo,kdnpal,kdial,
*           kduvo,kdual,kcpsi,
*           gwspd,
*           kckdact,kckdfis,
*           coral,corvo,
*           zone1_ran1,zone1_ran2,zone2_ran1,zone2_ran2,
*           zone3_ran1,zone3_ran2,zone4_ran1,zone4_ran2,
*           ha,l_disp,kdtcal,
*           kcpunew,kcam,
*           ht_disp,vt_disp
c
real*4 b_frac(128)
common /work/ b_frac
c
real*4 cfc(128),cfi(128),cfkc(128),cfnp(128),
*           cfpu(128),cftc(128),cfu(128),cfkf(128)
real*4 tottc(128),totti(128),tottkc(128),tottnp(128),
*           totppu(128),totttc(128),tottu(128),tottkf(128)

```

```

real*4 deltc(128),delti(128),deltkc(128),deltnp(128),
*           deltpu(128),delttc(128),deltu(128),deltkf(128)
common /fehm_control/
*           cfc,cfi,cfkc,cfnp,cfpu,cftc,cfu,cfkf,
*           tottc,totti,tottkc,tottnp,tottpu,totttc,tottu,tottkf,
*           deltc,delti,deltkc,deltnp,deltpu,delttc,deltu,deltkf
c
character*127 line
integer*4 kount
c           real*4 f3,f4
real*4 f1,f2,f3,f5,f6,f7,f8,f9,f10
real*4 source_x,source_y,source_z
real*4 kdvo,kdal17,kdal19,r_adjust7,r_adjust19,dctmp
c
c loop through the number of radionuclides, regions, and realizations
c (one sptr_1000.macro file per n_rn*n_region*n_realization)
do 30 i_realization=1,n_realization
do 20 i_region=1,n_region
source_z=725.0
call get_source_location
*           (i_realization,i_region,source_x,source_y)
do 10 i_rn=1,n_rn
c skip some radionuclides for now
c (1=C, 2=I, 3=Pu, 4=Np, 5=Kc, 6=Tc, 7=U)
c           if(i_rn.eq.1) goto 10
c           if(i_rn.eq.2) goto 10
c           if(i_rn.eq.3) goto 10
c           if(i_rn.eq.4) goto 10
c           if(i_rn.eq.5) goto 10
c           if(i_rn.eq.6) goto 10
c           if(i_rn.eq.7) goto 10
if(inum_rn.eq.0) goto 9
if(i_rn.ne.inum_rn) goto 10
9      continue
c open template sptr_1000.macro file
if(i_rn.eq.1) then
file2=main_directory(1:find_eol(main_directory))
*           //'sptr_1000/sptr_1000.macro.Cx_01.0000'
else if(i_rn.eq.2) then
file2=main_directory(1:find_eol(main_directory))
*           //'sptr_1000/sptr_1000.macro.Ix_01.0000'
else if(i_rn.eq.3) then
file2=main_directory(1:find_eol(main_directory))
*           //'sptr_1000/sptr_1000.macro.Pu_01.0000'
else if(i_rn.eq.4) then
file2=main_directory(1:find_eol(main_directory))
*           //'sptr_1000/sptr_1000.macro.Np_01.0000'
else if(i_rn.eq.5) then
file2=main_directory(1:find_eol(main_directory))
*           //'sptr_1000/sptr_1000.macro.Kc_01.0000'
else if(i_rn.eq.6) then
file2=main_directory(1:find_eol(main_directory))
*           //'sptr_1000/sptr_1000.macro.Tc_01.0000'
else if(i_rn.eq.7) then
file2=main_directory(1:find_eol(main_directory))
*           //'sptr_1000/sptr_1000.macro.Ux_01.0000'
else if(i_rn.eq.8) then
file2=main_directory(1:find_eol(main_directory))
*           //'sptr_1000/sptr_1000.macro.Kf_01.0000'
endif
c           file2=main_directory(1:find_eol(main_directory))
c           *           //'sptr_1000/sptr_1000.macro.xx_01.0000'
file_name=file2
open(2,file=file2,status='OLD',err=90)
c open new sptr_1000.macro file
file3=main_directory(1:find_eol(main_directory))
c           *           //'sptr_1000.macro'
*           //'sptr_1000/sptr_1000.macro'
call new_file_name(i_realization,i_rn,i_region,file3)
file_name=file3
open(3,file=file3,status='UNKNOWN',err=90)

```

```

write(*,*) 'open file=',file3(1:find_eol(file3))
c modify next line to set total simulation time, which is dependent on
c the radionuclide (1=C, 2=I, 3=Pu, 4=Np, 5=Kc, 6=Tc, 7=U, 8=Kf)
read(2,'(a)',end=100,err=91) line
write(3,'(a)') line(1:find_eol(new_line))
read(2,*,end=100,err=91) f1,i1,i2
read(2,*,end=100,err=91) f2,i3
if(i_rn.eq.1) then
write(3,*) deltc(i_realization),i1,i2
write(3,*) cfc(i_realization),i3
else if(i_rn.eq.2) then
write(3,*) delti(i_realization),i1,i2
write(3,*) cfi(i_realization),i3
else if(i_rn.eq.3) then
write(3,*) deltpu(i_realization),i1,i2
write(3,*) cfpu(i_realization),i3
else if(i_rn.eq.4) then
write(3,*) deltnp(i_realization),i1,i2
write(3,*) cfnp(i_realization),i3
else if(i_rn.eq.5) then
write(3,*) deltkc(i_realization),i1,i2
write(3,*) cfkc(i_realization),i3
else if(i_rn.eq.6) then
write(3,*) delttc(i_realization),i1,i2
write(3,*) cftc(i_realization),i3
else if(i_rn.eq.7) then
write(3,*) deltu(i_realization),i1,i2
write(3,*) cfu(i_realization),i3
else if(i_rn.eq.8) then
write(3,*) deltkf(i_realization),i1,i2
write(3,*) cfkf(i_realization),i3
endif
c copy from template onto new file up to the block that needs to be changed
call copy_to(2,3,'tprp')
c fix K_d's
c (1=C, 2=I, 3=Pu, 4=Np, 5=Kc, 6=Tc, 7=U, 8=Kf)
r_adjust7=min(1.0,nvf7(i_realization)/max_al_por)
r_adjust19=min(1.0,nvf19(i_realization)/max_al_por)
if(i_rn.eq.1) then
kdvo=0.
kdal7=r_adjust7*0.
kdal19=r_adjust19*0.
r_frac=1.
dctmp=dcv0(i_realization)
else if(i_rn.eq.2) then
kdvo=0.
kdal7=r_adjust7*kdial(i_realization)
kdal19=r_adjust19*kdial(i_realization)
r_frac=1.
dctmp=dcv0(i_realization)
else if(i_rn.eq.3) then
kdvo=0.
kdal7=
*      nvf7(i_realization)*(coral(i_realization)-1.)/bulk_den_al
kdal19=
*      nvf19(i_realization)*(coral(i_realization)-1.)/bulk_den_al
c      kdal7=r_adjust7*0.
c      kdal19=r_adjust19*0.
r_frac=corvo(i_realization)
dctmp=dcv0(i_realization)*1.e-10
else if(i_rn.eq.4) then
kdvo=kdnpvo(i_realization)
kdal7=r_adjust7*kdpal(i_realization)
kdal19=r_adjust19*kdpal(i_realization)
r_frac=1.
dctmp=dcv0(i_realization)
else if(i_rn.eq.5) then
kdvo=kckdact(i_realization)
kdal7=kckdact(i_realization)
*      *r_adjust7/(1.+kcam(i_realization))
kdal19=kckdact(i_realization)

```

```
*          *r_adjust19/(1.+kcam(i_realization))
r_frac=1.
dctmp=dcvo(i_realization)
*          /((1.+kcam(i_realization))*(1.+kcam(i_realization)))
else if(i_rn.eq.6) then
kdvo=0.
kdal7=r_adjust7*kdtcal(i_realization)
kdal19=r_adjust19*kdtcal(i_realization)
r_frac=1.
dctmp=dcvo(i_realization)
else if(i_rn.eq.7) then
kdvo=kduvo(i_realization)
kdal7=r_adjust7*kdual(i_realization)
kdal19=r_adjust19*kdual(i_realization)
r_frac=1.
dctmp=dcvo(i_realization)
else if(i_rn.eq.8) then
kdvo=kckdfis(i_realization)
kdal7=kckdfis(i_realization)
*          *r_adjust7/(1.+kcam(i_realization))
kdal19=kckdfis(i_realization)
*          *r_adjust19/(1.+kcam(i_realization))
r_frac=1.
dctmp=dcvo(i_realization)
*          /((1.+kcam(i_realization))*(1.+kcam(i_realization)))
endif
c write material values onto new sptr_1000.macro file
kount=0
do 7 i=1,28
c      read(2,* ,end=91,err=91) type_num
read(2,'(a)',end=91,err=91) line
read(line,* ,end=6,err=6)
*          type_num,f1,f2,f3,matrix_porosity,f5,f6,f7,f8,f9,f10
6      continue
if((type_num.eq.2).and.(kount.eq.0)) then
kount=kount+1
write(3,*) int(type_num),
*          f1,
*          l_disp(i_realization),
*          ht_disp(i_realization),
*          vt_disp(i_realization),
*          dcvo(i_realization),
*          f6
else if((type_num.eq.2).and.(kount.eq.1)) then
kount=kount+1
write(3,*) int(type_num),
*          kdal7,
*          l_disp(i_realization),
*          ht_disp(i_realization),
*          vt_disp(i_realization),
*          dcvo(i_realization),
*          f6
else if((type_num.eq.2).and.(kount.ge.2)) then
write(3,*) int(type_num),
*          kdal19,
*          l_disp(i_realization),
*          ht_disp(i_realization),
*          vt_disp(i_realization),
*          dcvo(i_realization),
*          f6
else
write(3,*) int(type_num),
*          kdvo,
*          dctmp,r_frac,
*          matrix_porosity,b_frac(i_realization),
*          l_disp(i_realization),
*          ht_disp(i_realization),
*          vt_disp(i_realization),
*          dcvo(i_realization),
*          f10
endif
```

```

7      continue
c copy from template onto new file up to the block that needs to be changed
call copy_to(2,3,'zbtc')
c copy from template onto new file the next 8 lines
call copy_lines(2,3,6)
c write starting coordinates for each of 1000 particles onto new sptr_1000.macro file
do 8 i=1,1000
read(2,* ,end=91,err=91) idummy
write(3,*) idummy,source_x,source_y,source_z
8      continue
c copy the rest of the template onto new file
call copy_to(2,3,'GOTO THE END')
close(2)
close(3)
10     continue
20     continue
30     continue
goto 100
90     write(*,*) 'ERROR opening ',file_name(1:find_eol(file_name)),
*           ' on realization=',i_realization,
*           ' in MAKE_SPTR_1000'
goto 100
91     write(*,*) 'ERROR reading file=',file2(1:find_eol(file2)),
*           ' on realization=',i_realization,
*           ' in MAKE_SPTR_1000'
100    return
end

subroutine get_source_location
*           (i_realization,i_region,source_x,source_y)
implicit none
integer*4 i_realization,i_region
c       integer*4 kount
c       logical*4 inside
real*4 source_x,source_y
c       real*4 scale
real*4 alx,aly,a2x,a2y,a3x,a3y,a4x,a4y
real*4 xran,yran,xmin,ymin,xmax,ymax,xdiff,ydiff
c
real*4 matrix_porosity
real*4 alluv_xmin(8),alluv_xmax(8),alluv_ymin(8),alluv_ymax(8)
real*4 type_num
real*4 r_frac,bulk_den_al,max_al_por
real*4 zone1_1_x,zone1_1_y,zone1_2_x,zone1_2_y
real*4 zone1_3_x,zone1_3_y,zone1_4_x,zone1_4_y
real*4 zone2_1_x,zone2_1_y,zone2_2_x,zone2_2_y
real*4 zone2_3_x,zone2_3_y,zone2_4_x,zone2_4_y
real*4 zone3_1_x,zone3_1_y,zone3_2_x,zone3_2_y
real*4 zone3_3_x,zone3_3_y,zone3_4_x,zone3_4_y
real*4 zone4_1_x,zone4_1_y,zone4_2_x,zone4_2_y
real*4 zone4_3_x,zone4_3_y,zone4_4_x,zone4_4_y
real*4 a1_1_x,a1_1_y,a1_2_x,a1_2_y,a1_3_x,a1_3_y,a1_4_x,a1_4_y
real*4 a2_1_x,a2_1_y,a2_2_x,a2_2_y,a2_3_x,a2_3_y,a2_4_x,a2_4_y
real*4 a3_1_x,a3_1_y,a3_2_x,a3_2_y,a3_3_x,a3_3_y,a3_4_x,a3_4_y
real*4 a4_1_x,a4_1_y,a4_2_x,a4_2_y,a4_3_x,a4_3_y,a4_4_x,a4_4_y
common /param_constants/ matrix_porosity,
*           alluv_xmin,alluv_xmax,alluv_ymin,alluv_ymax,
*           type_num,
*           r_frac,bulk_den_al,max_al_por,
*           zone1_1_x,zone1_1_y,zone1_2_x,zone1_2_y,
*           zone1_3_x,zone1_3_y,zone1_4_x,zone1_4_y,
*           zone2_1_x,zone2_1_y,zone2_2_x,zone2_2_y,
*           zone2_3_x,zone2_3_y,zone2_4_x,zone2_4_y,
*           zone3_1_x,zone3_1_y,zone3_2_x,zone3_2_y,
*           zone3_3_x,zone3_3_y,zone3_4_x,zone3_4_y,
*           zone4_1_x,zone4_1_y,zone4_2_x,zone4_2_y,
*           zone4_3_x,zone4_3_y,zone4_4_x,zone4_4_y,
*           a1_1_x,a1_1_y,a1_2_x,a1_2_y,a1_3_x,a1_3_y,a1_4_x,a1_4_y,
*           a2_1_x,a2_1_y,a2_2_x,a2_2_y,a2_3_x,a2_3_y,a2_4_x,a2_4_y,
```

```

*           a3_1_x,a3_1_y,a3_2_x,a3_2_y,a3_3_x,a3_3_y,a3_4_x,a3_4_y,
*           a4_1_x,a4_1_y,a4_2_x,a4_2_y,a4_3_x,a4_3_y,a4_4_x,a4_4_y
c
real*4 fplaw(128),fplan(128),nvf19(128),nvf7(128)
real*4 fisvo(128),fpvo(128),dcvo(128)
real*4 kdnpvo(128),kdnpal(128),kdial(128)
real*4 kduvo(128),kdual(128),kcpsi(128)
real*4 gwspd(128)
real*4 kckdact(128),kckdfis(128)
real*4 coral(128),corvo(128)
real*4 zone1_ran1(128),zone1_ran2(128),zone2_ran1(128),zone2_ran2(128)
real*4 zone3_ran1(128),zone3_ran2(128),zone4_ran1(128),zone4_ran2(128)
real*4 ha(128),l_disp(128),kdtcal(128)
real*4 kcpunew(128),kcam(128)
real*4 ht_disp(128),vt_disp(128)
common /rip_data/
*           fplaw,fplan,nvf19,nvf7,
*           fisvo,fpvo,dcvo,
*           kdnpvo,kdnpal,kdial,
*           kduvo,kdual,kcpsi,
*           gwspd,
*           kckdact,kckdfis,
*           coral,corvo,
*           zone1_ran1,zone1_ran2,zone2_ran1,zone2_ran2,
*           zone3_ran1,zone3_ran2,zone4_ran1,zone4_ran2,
*           ha,l_disp,kdtcal,
*           kcpunew,kcam,
*           ht_disp,vt_disp
c
c      scale=1.0
if(i_region.eq.1) then
xran=zone1_ran1(i_realization)
yran=zone1_ran2(i_realization)
alx=a1_1_x
aly=a1_1_y
a2x=a1_2_x
a2y=a1_2_y
a3x=a1_3_x
a3y=a1_3_y
a4x=a1_4_x
a4y=a1_4_y
xmin=zone1_1_x
xmax=zone1_2_x
ymin=zone1_1_y
ymax=zone1_4_y
else if(i_region.eq.2) then
xran=zone2_ran1(i_realization)
yran=zone2_ran2(i_realization)
alx=a2_1_x
aly=a2_1_y
a2x=a2_2_x
a2y=a2_2_y
a3x=a2_3_x
a3y=a2_3_y
a4x=a2_4_x
a4y=a2_4_y
xmin=zone2_1_x
xmax=zone2_2_x
ymin=zone2_1_y
ymax=zone2_4_y
else if(i_region.eq.3) then
xran=zone3_ran1(i_realization)
yran=zone3_ran2(i_realization)
alx=a3_1_x
aly=a3_1_y
a2x=a3_2_x
a2y=a3_2_y
a3x=a3_3_x
a3y=a3_3_y
a4x=a3_4_x
a4y=a3_4_y

```

```

xmin=zone3_1_x
xmax=zone3_2_x
ymin=zone3_1_y
ymax=zone3_4_y
else
xran=zone4_ran1(i_realization)
yran=zone4_ran2(i_realization)
alx=a4_1_x
aly=a4_1_y
a2x=a4_2_x
a2y=a4_2_y
a3x=a4_3_x
a3y=a4_3_y
a4x=a4_4_x
a4y=a4_4_y
xmin=zone4_1_x
xmax=zone4_2_x
ymin=zone4_1_y
ymax=zone4_4_y
endif
xdiff=xmax-xmin
ydiff=ymax-ymin
c      kount=0
c10    kount=kount+1
c      if(kount.gt.10) goto 20
c      source_x=xran*scale*xdiff+xmin+0.5*(1.-scale)*xdiff
c      source_y=yran*scale*ydiff+ymin+0.5*(1.-scale)*ydiff
source_x=xran*xdiff+xmin
source_y=yran*ydiff+ymin
call inside(source_x,source_y,alx,aly,a2x,a2y,a3x,a3y,a4x,a4y)

c      write(*,*) 'i_realization=',i_realization,' i_region=',i_region
c      write(*,*) 
c      * 'xmin=',xmin,' xmax=',xmax,' ymin=',ymin,' ymax=',ymax
c      write(*,*) 'xran=',xran,' yran=',yran
c      write(*,*) 'xdiff=',xdiff,' ydiff=',ydiff
c      write(*,*) 'source_x=',source_x,' source_y=',source_y
c      write(*,*) 'alx=',alx,' aly=',aly
c      write(*,*) 'a2x=',a2x,' a2y=',a2y
c      write(*,*) 'a3x=',a3x,' a3y=',a3y
c      write(*,*) 'a4x=',a4x,' a4y=',a4y

c      if(inside(source_x,source_y,alx,aly,a2x,a2y,a3x,a3y,a4x,a4y))
c      *           goto 20
c      scale=scale*0.9
c      goto 10
20    return
end

c INSIDE returns the point (XRAN,YRAN) that is either inside or on
c the boundary of the c convex 4-sided polygon defined by
c (x1,y1), (x2,y2), (x3,y3), (x4,y4).
c The idea is to draw a vertical line thru (XRAN,YRAN), determine the
c 2 points it intersects in the polygon, and see if (XRAN,YRAN) is
c between them. If not, INSIDE returns the point on the boundary
c intersected by the vertical line
subroutine inside(xran,yran,x1,y1,x2,y2,x3,y3,x4,y4)
implicit none
real*4 xran,yran,x1,y1,x2,y2,x3,y3,x4,y4
real*4 ytemp1,ytemp2,ytemp3,ytemp4,yup,ydn
real*4 ycross
ytemp1=ycross(xran,x1,y1,x2,y2)
ytemp2=ycross(xran,x2,y2,x3,y3)
ytemp3=ycross(xran,x3,y3,x4,y4)
ytemp4=ycross(xran,x4,y4,x1,y1)

c      write(*,*) 'ytemp1,ytemp2,ytemp3,ytemp4=',
c      * ytemp1,ytemp2,ytemp3,ytemp4

c      if((ytemp1.eq.ytemp2)

```

```

c      *      .and.(ytemp2.eq.ytemp3)
c      *      .and.(ytemp3.eq.ytemp4) goto 60
yup=max(ytemp1,ytemp2,ytemp3,ytemp4)
if(yup.eq.ytemp1) ytemp1=-1.e-38
if(yup.eq.ytemp2) ytemp2=-1.e-38
if(yup.eq.ytemp3) ytemp3=-1.e-38
if(yup.eq.ytemp4) ytemp4=-1.e-38
ydn=max(ytemp1,ytemp2,ytemp3,ytemp4)

c      write(*,*) 'yup,ydn=',yup,ydn

c      if((yran.lt.ydn).or.(yran.gt.yup)) goto 60
if(yran.lt.ydn) then
yran=ydn
else if(yran.gt.yup) then
yran=yup
endif
return
end

c YCROSS returns the Y-coordinate of the intersection point of
c a vertical line that extends from XTRAN and the segment defined
c by (x1,y1), (x2,y2). If the vertical line does not intersect
c the segment, YCROSS returns -1.e-38.
real*4 function ycross(xran,x1,y1,x2,y2)
implicit none
real*4 xran,x1,y1,x2,y2
real*4 intercept,slope
if(((xran.lt.x1).and.(xran.lt.x2))
*      .or.((xran.gt.x1).and.(xran.gt.x2))) then
ycross=-1.e-38
else
if(x2.eq.x1) slope=1.e+38
if(x2.ne.x1) slope=(y2-y1)/(x2-x1)
intercept=y1-slope*x1
ycross=slope*xran+intercept
endif
return
end

subroutine make_props_05_ism3(inum_rn)
implicit none
character*127 file2,file3,file_name,line
integer*4 i_realization,i_rn,i_region,inum_rn
integer*4 find_eol
integer*4 i1,i2,i3
real*4 f1,f2,f3
character*127 main_directory
common /dir/ main_directory
integer*4 n_rn,n_region,n_realization
common /control/ n_rn,n_region,n_realization
real*4 matrix_porosity
real*4 alluv_xmin(8),alluv_xmax(8),alluv_ymin(8),alluv_ymax(8)
real*4 type_num
real*4 r_frac,bulk_den_al,max_al_por
real*4 zone1_1_x,zone1_1_y,zone1_2_x,zone1_2_y
real*4 zone1_3_x,zone1_3_y,zone1_4_x,zone1_4_y
real*4 zone2_1_x,zone2_1_y,zone2_2_x,zone2_2_y
real*4 zone2_3_x,zone2_3_y,zone2_4_x,zone2_4_y
real*4 zone3_1_x,zone3_1_y,zone3_2_x,zone3_2_y
real*4 zone3_3_x,zone3_3_y,zone3_4_x,zone3_4_y
real*4 zone4_1_x,zone4_1_y,zone4_2_x,zone4_2_y
real*4 zone4_3_x,zone4_3_y,zone4_4_x,zone4_4_y
real*4 a1_1_x,a1_1_y,a1_2_x,a1_2_y,a1_3_x,a1_3_y,a1_4_x,a1_4_y
real*4 a2_1_x,a2_1_y,a2_2_x,a2_2_y,a2_3_x,a2_3_y,a2_4_x,a2_4_y
real*4 a3_1_x,a3_1_y,a3_2_x,a3_2_y,a3_3_x,a3_3_y,a3_4_x,a3_4_y
real*4 a4_1_x,a4_1_y,a4_2_x,a4_2_y,a4_3_x,a4_3_y,a4_4_x,a4_4_y
common /param_constants/ matrix_porosity,

```



```

goto 7
c copy the rest of the template onto new file
8      call copy_to(2,3,'GOTO THE END')
rewind(2)
close(3)
10     continue
goto 100
90      write(*,*) 'ERROR opening ',file_name(1:find_eol(file_name)),
*           ' on realization=',i_realization,
*           ' in MAKE_PROPS_05_ISM'
goto 100
91      write(*,*) 'ERROR reading file=',file2(1:find_eol(file2)),
*           ' on realization=',i_realization,
*           ' in MAKE_PROPS_05_ISM'
100    close(2)
200    return
end

subroutine copy_to(file1,file2,string)
implicit none
character(*) string
character*127 line
integer*4 file1,file2
integer*4 find_eol
10      read(file1,'(a)',err=90,end=100) line
write(file2,'(a)') line(1:find_eol(line))
if(index(line,string).eq.0) goto 10
goto 100
90      write(*,*) 'ERROR reading file=',file1,' in COPY_TO'
100    return
end

integer*4 function find_eol(line)
character(*) line
integer*4 i
do 10 i=len(line),2,-1
if(line(i:i).ne.' ') goto 100
10     continue
100    find_eol=i
return
end

integer*4 function find_comment(line)
character(*) line
integer*4 i
do 10 i=1,len(line)
if(line(i:i).eq.'#') goto 100
10     continue
100    find_comment=i
return
end

subroutine copy_lines(file1,file2,n_lines)
implicit none
character*127 line
integer*4 file1,file2,n_lines
integer*4 find_eol
integer*4 i
do 10 i=1,n_lines
read(file1,'(a)',err=90,end=100) line
write(file2,'(a)') line(1:find_eol(line))
10     continue
goto 100
90      write(*,*) 'ERROR reading file=',file1,' in COPY_LINES'
100    return
end

subroutine new_file_name(i_realization,i_rn,i_region,file_name)
implicit none
character(*) file_name
integer*4 i_realization,i_rn,i_region

```

```

integer*4 find_eol
character*2 c_rn,c_region
character*4 c_realization
write(c_realization,'(i4)') i_realization
call zero_pad(4,c_realization)
if(i_rn.eq.0) then
write(c_rn,'(i2)') i_rn
call zero_pad(2,c_rn)
else if(i_rn.eq.1) then
c_rn='Cx'
else if(i_rn.eq.2) then
c_rn='Ix'
else if(i_rn.eq.3) then
c_rn='Pu'
else if(i_rn.eq.4) then
c_rn='Np'
else if(i_rn.eq.5) then
c_rn='Kc'
else if(i_rn.eq.6) then
c_rn='Tc'
else if(i_rn.eq.7) then
c_rn='Ux'
else if(i_rn.eq.8) then
c_rn='Kf'
endif
write(c_region,'(i2)') i_region
call zero_pad(2,c_region)
file_name=file_name(1:find_eol(file_name))
*           //'.//c_rn//'_//c_region//'.//c_realization

c           write(*,'(a)') file_name(1:find_eol(file_name))//!!!!!
100      return
end

subroutine zero_pad(i_end,string)
implicit none
character(*) string
integer*4 i_end
integer*4 i
do 10 i=1,i_end
if(string(i:i).eq.' ') string(i:i)='0'
10      continue
return
end

subroutine debug(i)
implicit none
integer*4 i
character*127 main_directory
common /dir/ main_directory
integer*4 n_rn,n_region,n_realization
common /control/ n_rn,n_region,n_realization
real*4 matrix_porosity
real*4 alluv_xmin(8),alluv_xmax(8),alluv_ymin(8),alluv_ymax(8)
real*4 type_num
real*4 r_frac,bulk_den_al,max_al_por
real*4 zone1_1_x,zone1_1_y,zone1_2_x,zone1_2_y
real*4 zone1_3_x,zone1_3_y,zone1_4_x,zone1_4_y
real*4 zone2_1_x,zone2_1_y,zone2_2_x,zone2_2_y
real*4 zone2_3_x,zone2_3_y,zone2_4_x,zone2_4_y
real*4 zone3_1_x,zone3_1_y,zone3_2_x,zone3_2_y
real*4 zone3_3_x,zone3_3_y,zone3_4_x,zone3_4_y
real*4 zone4_1_x,zone4_1_y,zone4_2_x,zone4_2_y
real*4 zone4_3_x,zone4_3_y,zone4_4_x,zone4_4_y
real*4 a1_1_x,a1_1_y,a1_2_x,a1_2_y,a1_3_x,a1_3_y,a1_4_x,a1_4_y
real*4 a2_1_x,a2_1_y,a2_2_x,a2_2_y,a2_3_x,a2_3_y,a2_4_x,a2_4_y
real*4 a3_1_x,a3_1_y,a3_2_x,a3_2_y,a3_3_x,a3_3_y,a3_4_x,a3_4_y
real*4 a4_1_x,a4_1_y,a4_2_x,a4_2_y,a4_3_x,a4_3_y,a4_4_x,a4_4_y
common /param_constants/ matrix_porosity,

```

```

*
*      alluv_xmin,alluv_xmax,alluv_ymin,alluv_ymax,
*      type_num,
*      r_frac,bulk_den_al,max_al_por,
*      zone1_1_x,zone1_1_y,zone1_2_x,zone1_2_y,
*      zone1_3_x,zone1_3_y,zone1_4_x,zone1_4_y,
*      zone2_1_x,zone2_1_y,zone2_2_x,zone2_2_y,
*      zone2_3_x,zone2_3_y,zone2_4_x,zone2_4_y,
*      zone3_1_x,zone3_1_y,zone3_2_x,zone3_2_y,
*      zone3_3_x,zone3_3_y,zone3_4_x,zone3_4_y,
*      zone4_1_x,zone4_1_y,zone4_2_x,zone4_2_y,
*      zone4_3_x,zone4_3_y,zone4_4_x,zone4_4_y,
*      a1_1_x,a1_1_y,a1_2_x,a1_2_y,a1_3_x,a1_3_y,a1_4_x,a1_4_y,
*      a2_1_x,a2_1_y,a2_2_x,a2_2_y,a2_3_x,a2_3_y,a2_4_x,a2_4_y,
*      a3_1_x,a3_1_y,a3_2_x,a3_2_y,a3_3_x,a3_3_y,a3_4_x,a3_4_y,
*      a4_1_x,a4_1_y,a4_2_x,a4_2_y,a4_3_x,a4_3_y,a4_4_x,a4_4_y
c
real*4 fplaw(128),fplan(128),nvf19(128),nvf7(128)
real*4 fisvo(128),fpvo(128),dcvo(128)
real*4 kdnpvo(128),kdnpal(128),kdial(128)
real*4 kduvo(128),kdual(128),kcpsi(128)
real*4 gwspd(128)
real*4 kckdact(128),kckdfis(128)
real*4 coral(128),corvo(128)
real*4 zone1_ran1(128),zone1_ran2(128),zone2_ran1(128),zone2_ran2(128)
real*4 zone3_ran1(128),zone3_ran2(128),zone4_ran1(128),zone4_ran2(128)
real*4 ha(128),l_disp(128),kdtcal(128)
real*4 kcpunew(128),kcam(128)
real*4 ht_disp(128),vt_disp(128)
common /rip_data/
*
*      fplaw,fplan,nvf19,nvf7,
*      fisvo,fpvo,dcvo,
*      kdnpvo,kdnpal,kdial,
*      kduvo,kdual,kcpsi,
*      gwspd,
*      kckdact,kckdfis,
*      coral,corvo,
*      zone1_ran1,zone1_ran2,zone2_ran1,zone2_ran2,
*      zone3_ran1,zone3_ran2,zone4_ran1,zone4_ran2,
*      ha,l_disp,kdtcal,
*      kcpunew,kcam,
*      ht_disp,vt_disp
c
write(*,*) 'gwspd(''i,'')='gwspd(i)
write(*,*) 'fisvo(''i,'')='fisvo(i),' fpvo(''i,'')='fpvo(i)
write(*,*) 'fplaw(''i,'')='fplaw(i),' fplan(''i,'')='fplan(i)
write(*,*) 'kdnpal(''i,'')='kdnpal(i),
*      ' kdnpvo(''i,'')='kdnpvo(i)
write(*,*) 'l_disp(''i,'')='l_disp(i),
*      ' ht_disp(''i,'')='ht_disp(i),' vt_disp(''i,'')='vt_disp(i)
write(*,*) 'dcvo(''i,'')='dcvo(i),
*      ' nvf7(''i,'')='nvf7(i),' nvf19(''i,'')='nvf19(i)
write(*,*) 'ha(''i,'')='ha(i),
*      ' kdtcal(''i,'')='kdtcal(i)
return
end

```

ATTACHMENT III

Software Routine SZ_POST v. 1.0

The software routine SZ_Post v. 1.0 combines the particle tracking results from the 100 realizations of the SZ site-scale flow and transport model for a given radionuclide and source region. The combined results are written to a file that can be read by the SZ_Convolute software code for incorporation into the TSPA-SR analyses with the GoldSim software code.

Validation of the SZ_Post software routine is accomplished by spot checking the output file from the routine in comparison to one of the FEHM output files that serve as input to the routine. As an example, the file named “01_calib.sptr3.Ux_01.0001” is the SZ site-scale model output for uranium transport from source region 1 in realization number 1. This file is copied to a file named “SZ_07_01.0001” by the macro entitled “xcopy_files” in preparation for post-processing by the SZ_Post software routine. The corresponding output file from the SZ_Post software routine is named “SZ_07_01”, which contains the results for realizations 1 through 100. In this example, the seventh line in the file “SZ_07_01” gives the time as 1.0000E+02 years, which is a correct conversion of the time in the second line of file “01_calib.sptr3.Ux_01.0001” that is 0.3652500E+05 days. The relative mass flux at this time for 5 km distance given in the second column of file “SZ_07_01” is 1.3179E-01, which is the correct calculation based on the number of particles having arrived as indicated in the second column of file “01_calib.sptr3.Ux_01.0001” (131) and the total number of particles at the end of the simulation in the second column (994).

FORTRAN Source Code Listing for Software Routine SZ_POST v. 1.0

```
C      Last change: H   15 Dec 1999   2:46 pm
C This file takes the FEHM output files, extracts the needed
c information, and smooths the breakthrough curves for each radionuclide
c and each source sub-region. The program prompts for the desired
c radionuclide number, name, and source region to post-process, so some or
c all of the output can be post-processed during one run.
C
c Input to this program includes all of the realizations for a
c radionuclide in a source region at three distances(5,20,30km),
C Input files are sz##_0$.* where ## is the radionuclide number,
c $ is the source sub-region, and *** is the realization number.
C The program is currently configured to read all required input files
c from within the sub-directory where the program is run.
c
C Output from this program is breakthrough curves for each
c radionuclide in a source region: output file names are
C sz##_0$ where ## is the radionuclide number, $ is the source sub-region
c
      program ppcon
      implicit REAL*8(a-h,o-z)
```

```
character*80 radname
character*4 dum
character*1 dum1
character*7 file2(50)
character*9 file3(50)
character*13 file1(50)
dimension timeadd(5)
file2(1)='SZ_01_0'
file2(2)='SZ_02_0'
file2(3)='SZ_03_0'
file2(4)='SZ_04_0'
file2(5)='SZ_05_0'
file2(6)='SZ_06_0'
file2(7)='SZ_07_0'
file2(8)='SZ_08_0'
file2(9)='SZ_09_0'
file2(10)='SZ_10_0'
file2(11)='SZ_11_0'
file2(12)='SZ_12_0'
file2(13)='SZ_13_0'
file2(14)='SZ_14_0'
file2(15)='SZ_15_0'
file2(16)='SZ_16_0'
file2(17)='SZ_17_0'
file2(18)='SZ_18_0'
file2(19)='SZ_19_0'
file2(20)='SZ_20_0'
file2(21)='SZ_21_0'
file2(22)='SZ_22_0'
file2(23)='SZ_23_0'
file2(24)='SZ_24_0'
file2(25)='SZ_25_0'
file2(26)='SZ_26_0'
file2(27)='SZ_27_0'
file2(28)='SZ_28_0'
file2(29)='SZ_29_0'
file2(30)='SZ_30_0'
file2(31)='SZ_31_0'
file2(32)='SZ_32_0'
file2(33)='SZ_33_0'
file2(34)='SZ_34_0'
file2(35)='SZ_35_0'
file2(36)='SZ_36_0'
file2(37)='SZ_37_0'
file2(38)='SZ_38_0'
file2(39)='SZ_39_0'
file2(40)='SZ_40_0'
file2(41)='SZ_41_0'
file2(42)='SZ_42_0'
file2(43)='SZ_43_0'
file2(44)='SZ_44_0'
file2(45)='SZ_45_0'
file2(46)='SZ_46_0'
file2(47)='SZ_47_0'
file2(48)='SZ_48_0'
file2(49)='SZ_49_0'
file2(50)='SZ_50_0'
write(6,*)'Radionuclide no. >'
read(5,*)irad
write(6,*)'Radionuclide name. >'
read(5,80)radname
write(6,*)'No. of realizations >'
read(5,*)nrealiz
write(6,*)'Source region No.>'
read(5,*)iregion
write(6,*)'Number of times to be added>'
read(5,*)naddt
write(6,*)'Adding times in years>'
read(5,*)(timeadd(i),i=1,naddt)
call retoch2(iregion,dum1)
open (9,file=file2(irad)//dum1,status='unknown')
```

```

file3(irad)=file2(irad)//dum1//'.'
WRITE(9,80)radname
WRITE(9,*)iregion
WRITE(9,*)nrealiz
c pts : number of data points used for smoothing,if pts>1,smoothing
c npart: number of particles
    pts =15
    npart = 1000
do 100 l=1,nrealiz
    WRITE(9,*)l
    call retoch1(l,dum)
    file1(irad)=file3(irad)//dum
    call smooth(file1(irad),pts,npart,timeadd,naddt)
100 continue
close(9)
format(a80)
stop
end
subroutine retoch1(irun,dummy)
character*4 dummy
open(19,file='dum.dat',status='unknown')
if (irun.ge.10) then
    if (irun.ge.100) then
        write(19,310)irun
    else
        write(19,320)irun
    end if
else
    write(19,330)irun
end if
close(19)
open(21,file='dum.dat',status='old')
read(21,231)dummy
close(21)
231 format(a4)
310 format('0',i3)
320 format('00',i2)
330 format('000',i1)
return
end
subroutine retoch2(irun,dummy)
character*1 dummy
open(19,file='dum1.dat',status='unknown')
write(19,330)irun
close(19)
open(21,file='dum1.dat',status='old')
read(21,231)dummy
close(21)
231 format(a1)
330 format(i1)
return
end
subroutine smooth(filenamel,pts,npart,timeadd,naddt)
implicit REAL*8(a-h,o-z)
parameter (mxn=100000)
CHARACTER*13 filenamel
dimension yold(3*mxn),ynew(mxn,3),timeadd(*)
dimension x(mxn),y(mxn),df(mxn),c(mxn,3),
& wk((mxn+2)*7),se(mxn)
INTEGER mn5(3),icon(3),icheck(3),mxpath(3)
dimension fmxpath(3)
open (8, file=filenamel,STATUS='old')
mn=0
do i=1,3
mn5(i)=0
icheck(i)=0
    mxpath(i)=0
    fmxpath(i)=0
end do
c determine the number of records in the file
1      read (8,*,end=999) xx2,icon(1),icon(2),icon(3)

```

```

c
c check for nonzero concentration at first distance
c
if(mxpart(1).lt.icon(1)) mxpart(1)=icon(1)
if(mxpart(2).lt.icon(2)) mxpart(2)=icon(2)
if(mxpart(3).lt.icon(3)) mxpart(3)=icon(3)
IF(icon(1).lt.1.and.icheck(1).eq.0)then
mn5(1)=mn5(1)+1
else
icheck(1)=1
END if
c
c check for nonzero concentration at second distance
c
IF(icon(2).lt.1.and.icheck(2).eq.0)then
mn5(2)=mn5(2)+1
else
icheck(2)=1
END if
c
c check for nonzero concentration at third distance
c
IF(icon(3).lt.1.and.icheck(3).eq.0)then
mn5(3)=mn5(3)+1
else
icheck(3)=1
END if
mn=mn+1
GO TO 1
999 continue
WRITE(9,*)mn+naddt
n7=mn+2*pts
n6=Dlog(dble(n7))/DLOG(2.0d0)+2.0
n7=2**n6
c read in time
REWIND(8)
do i=1,mn
read(8,*)x(i)
end do
do iii=1,3
REWIND(8)
idex=0
mn5(iii)=mn5(iii)
n=mn-mn5(iii)
DO 5 I=1,mn5(iii)
idex=idex+1
read(8,*)xx2,icon(1),icon(2),icon(3)
c
ynew(idex,iii)=icon(iii)/dble(mxpart(iii))
ynew(idex,iii)=icon(iii)/dble(npart)
5 CONTINUE
DO 10 I=1,N
read(8,*)xx2,icon(1),icon(2),icon(3)
yold(i)=icon(iii)/dble(npart)
c
yold(i)=icon(iii)/dble(mxpart(iii))
10 CONTINUE
ismooth=0
IF(ismooth.eq.1) then
IF(pts.gt.1)call smoof (yold, n, pts,n7)
do i=1,n
idex=idex+1
ynew(idex,iii)=yold(i)
end do
else
IC=n-1
JOB=1
VAR=-1.0D0
DN=N
n7=7*(n+2)
DO 101 I=1,N
DF(I)=1.0D0
101 CONTINUE

```

```

      IF(ismooth.eq.2) then
C       CALL CUBGCV(X,yold,DF,N,Y,C,IC,VAR,JOB,SE,WK,IER)
      else
C       if(ismooth.eq.3) then
C         fsmoth=0.50
C         nste=2
C         delt=0.0
C         call lowess(x,yold,n,fsoth,nste,delt,y,df,se)
      else
        do i1=1,n
          y(i1)=yold(i1)
        end do
        end if
        END if
        do i=1,n
          idex=idex+1
          ynew(idex,iii)=y(i)
        end do
        END if
        do i=1,mn
          if(fmxpath(iii).lt.ynew(i,iii))fmxpath(iii)=ynew(i,iii)
        end do
        do i=1,mn
          ynew(i,iii)=ynew(i,iii)/fmxpath(iii)
        end do
        end do
      c
      do 40 i = 1, mn
        do j=1,3
          IF(ynew(i,j).lt.0) ynew(i,j)=0.0
        end do
        write (9,35)x(i)/365.25,ynew(i,1),ynew(i,2),ynew(i,3)
      40 continue
        do i=1,naddt
          write(9,35)timeadd(i),1.0,1.0,1.0
        end do
      35 format(4(1pe12.4))
CLOSE(8)
return
end
c
c-----
c-----  

SUBROUTINE SMOOFT(Y,N,PTS,n7)
implicit REAL*8(a-h,o-z)
dimension Y(n7)
M=2
NMIN=N+2.*PTS
1  IF(M.LT.NMIN)THEN
    M=2*M
    GO TO 1
  ENDIF
  CONST=(PTS/M)**2
  Y1=Y(1)
  YN=Y(N)
  RN1=1./(N-1.)
  DO 11 J=1,N
    c           write (*, *) Y(j)
    Y(J)=Y(J)-RN1*(Y1*(N-J)+YN*(J-1))
  11 CONTINUE
  IF(N+1.LE.M)THEN
    DO 12 J=N+1,M
      Y(J)=0.
  12 CONTINUE
  ENDIF
  MO2=M/2
  CALL REALFT(Y,MO2,1,n7)
  Y(1)=Y(1)/MO2
  FAC=1.
  DO 13 J=1,MO2-1
    K=2*j+1

```

```

        IF(FAC.NE.0.)THEN
          FAC=dMAX1(0.d0,(1.d0-CONST*J**2.0d0)/MO2)
          Y(K)=FAC*Y(K)
          Y(K+1)=FAC*Y(K+1)
        ELSE
          Y(K)=0.
          Y(K+1)=0.
        ENDIF
13    CONTINUE
      FAC=dMAX1(0.d0,(1.d0-0.25d0*PTS**2.0d0)/MO2)
      Y(2)=FAC*Y(2)
      CALL REALFT(Y,MO2,-1,n7)
      DO 14 J=1,N
        Y(J)=RN1*(Y1*(N-J)+YN*(J-1))+Y(J)
      c      write (*, *) Y(j)
14    CONTINUE
      c      write (*, *) n, m
      RETURN
      END
c
c-----
c
      SUBROUTINE REALFT(DATA,N,ISIGN,n7)
      implicit REAL*8(a-h,o-z)
      REAL*8 WR,WI,WPR,WPI,WTEMP,THETA
      DIMENSION DATA(n7)
      THETA=6.28318530717959D0/2.0D0/DBLE(N)
      WR=1.0D0
      WI=0.0D0
      C1=0.5
      IF (ISIGN.EQ.1) THEN
        C2=-0.5
        CALL FOUR1(DATA,N,+1,n7)
        DATA(2*N+1)=DATA(1)
        DATA(2*N+2)=DATA(2)
      ELSE
        C2=0.5
        THETA=-THETA
        DATA(2*N+1)=DATA(2)
        DATA(2*N+2)=0.0
        DATA(2)=0.0
      ENDIF
      WPR=-2.0D0*DSIN(0.5D0*THETA)**2
      WPI=DSIN(THETA)
      N2P3=2*N+3
      DO 11 I=1,N/2+1
        I1=2*I-1
        I2=I1+1
        I3=N2P3-I2
        I4=I3+1
        WRS=SNGL(WR)
        WIS=SNGL(WI)
        H1R=C1*(DATA(I1)+DATA(I3))
        H1I=C1*(DATA(I2)-DATA(I4))
        H2R=-C2*(DATA(I2)+DATA(I4))
        H2I=C2*(DATA(I1)-DATA(I3))
        DATA(I1)=H1R+WRS*H2R-WIS*H2I
        DATA(I2)=H1I+WRS*H2I+WIS*H2R
        DATA(I3)=H1R-WRS*H2R+WIS*H2I
        DATA(I4)=-H1I+WRS*H2I+WIS*H2R
        WTEMP=WR
        WR=WR*WPR-WI*WPI+WR
        WI=WI*WPR+WTEMP*WPI+WI
11    CONTINUE
      IF (ISIGN.EQ.1) THEN
        DATA(2)=DATA(2*N+1)
      ELSE
        CALL FOUR1(DATA,N,-1,n7)
      ENDIF
      RETURN
      END

```

```

C
C-----
C
      SUBROUTINE FOUR1(DATA,NN,ISIGN,n7)
      implicit REAL*8(a-h,o-z)
      REAL*8 WR,WI,WPR,WPI,WTEMP,THETA
      DIMENSION DATA(n7)
      N=2*NN
      J=1
      DO 11 I=1,N,2
         IF(J.GT.I)THEN
            TEMPR=DATA(J)
            TEMPI=DATA(J+1)
            DATA(J)=DATA(I)
            DATA(J+1)=DATA(I+1)
            DATA(I)=TEMPR
            DATA(I+1)=TEMPI
         ENDIF
         M=N/2
1      IF ((M.GE.2).AND.(J.GT.M)) THEN
            J=J-M
            M=M/2
            GO TO 1
         ENDIF
         J=J+M
11     CONTINUE
      MMAX=2
2      IF (N.GT.MMAX) THEN
         ISTEP=2*MMAX
         THETA=6.28318530717959D0/(ISIGN*MMAX)
         WPR=-2.D0*DSIN(0.5D0*THETA)**2
         WPI=DSIN(THETA)
         WR=1.D0
         WI=0.D0
         DO 13 M=1,MMAX,2
            DO 12 I=M,N,ISTEP
               J=I+MMAX
               TEMPR=SNGL(WR)*DATA(J)-SNGL(WI)*DATA(J+1)
               TEMPI=SNGL(WR)*DATA(J+1)+SNGL(WI)*DATA(J)
               DATA(J)=DATA(I)-TEMPR
               DATA(J+1)=DATA(I+1)-TEMPI
               DATA(I)=DATA(I)+TEMPR
               DATA(I+1)=DATA(I+1)+TEMPI
12         CONTINUE
               WTEMP=WR
               WR=WR*WPR-WI*WPI+WR
               WI=WI*WPR+WTEMP*WPI+WI
13         CONTINUE
         MMAX=ISTEP
         GO TO 2
      ENDIF
      RETURN
      END

```

ATTACHMENT IV

The UNIX script file “*xrun_C_mean_iso_all*” is an example from a series of script files used to execute the numerous stochastic realizations of the SZ site-scale flow and transport model for the TSPA analyses described in this AMR. This example script file executes all of the simulations for carbon transport, for the mean flux and isotropic horizontal permeability flow field, and for transport from the four source regions. The script file is simply a list of UNIX commands that are executed in the sequence presented in the file. Validation of the script files is accomplished by visual inspection of the files and by checking to see that the appropriate output files have been generated following execution of the script file.

UNIX Script file *xrun_C_mean_iso_all*

```
cp ../../inputs/01_base_case/mean_iso/01_base_case.dat.Cx_00.0002 02_calib.dat
cp ../../inputs/final_05_w_fence/final_05_w_fence.macro.00_00.0002 final_05_w_fence.macro
cp ../../inputs/props_05_ism3/props_05_ism3.macro.00_00.0002 props_05_ism3.macro
cp ../../inputs/sptr_1000/sptr_1000.macro.Cx_01.0002 sptr_1000.macro
xfehm_oct-26-99
cp 02_calib.sptr3 ./results/02_calib.sptr3.Cx_01.0002
cp ../../inputs/sptr_1000/sptr_1000.macro.Cx_02.0002 sptr_1000.macro
xfehm_oct-26-99
cp 02_calib.sptr3 ./results/02_calib.sptr3.Cx_02.0002
cp ../../inputs/sptr_1000/sptr_1000.macro.Cx_03.0002 sptr_1000.macro
xfehm_oct-26-99
cp 02_calib.sptr3 ./results/02_calib.sptr3.Cx_03.0002
cp ../../inputs/sptr_1000/sptr_1000.macro.Cx_04.0002 sptr_1000.macro
xfehm_oct-26-99
cp 02_calib.sptr3 ./results/02_calib.sptr3.Cx_04.0002

cp ../../inputs/01_base_case/mean_iso/01_base_case.dat.Cx_00.0004 02_calib.dat
cp ../../inputs/final_05_w_fence/final_05_w_fence.macro.00_00.0004 final_05_w_fence.macro
cp ../../inputs/props_05_ism3/props_05_ism3.macro.00_00.0004 props_05_ism3.macro
cp ../../inputs/sptr_1000/sptr_1000.macro.Cx_01.0004 sptr_1000.macro
xfehm_oct-26-99
cp 02_calib.sptr3 ./results/02_calib.sptr3.Cx_01.0004
cp ../../inputs/sptr_1000/sptr_1000.macro.Cx_02.0004 sptr_1000.macro
xfehm_oct-26-99
cp 02_calib.sptr3 ./results/02_calib.sptr3.Cx_02.0004
cp ../../inputs/sptr_1000/sptr_1000.macro.Cx_03.0004 sptr_1000.macro
xfehm_oct-26-99
cp 02_calib.sptr3 ./results/02_calib.sptr3.Cx_03.0004
cp ../../inputs/sptr_1000/sptr_1000.macro.Cx_04.0004 sptr_1000.macro
xfehm_oct-26-99
cp 02_calib.sptr3 ./results/02_calib.sptr3.Cx_04.0004

cp ../../inputs/01_base_case/mean_iso/01_base_case.dat.Cx_00.0011 02_calib.dat
cp ../../inputs/final_05_w_fence/final_05_w_fence.macro.00_00.0011 final_05_w_fence.macro
cp ../../inputs/props_05_ism3/props_05_ism3.macro.00_00.0011 props_05_ism3.macro
cp ../../inputs/sptr_1000/sptr_1000.macro.Cx_01.0011 sptr_1000.macro
xfehm_oct-26-99
cp 02_calib.sptr3 ./results/02_calib.sptr3.Cx_01.0011
cp ../../inputs/sptr_1000/sptr_1000.macro.Cx_02.0011 sptr_1000.macro
xfehm_oct-26-99
cp 02_calib.sptr3 ./results/02_calib.sptr3.Cx_02.0011
cp ../../inputs/sptr_1000/sptr_1000.macro.Cx_03.0011 sptr_1000.macro
```

```

xfehm_oct-26-99
cp 02_calib.sptr3 ./results/02_calib.sptr3.Cx_03.0011
cp ../../inputs/sptr_1000/sptr_1000.macro.Cx_04.0011 sptr_1000.macro
xfehm_oct-26-99
cp 02_calib.sptr3 ./results/02_calib.sptr3.Cx_04.0011

cp ../../inputs/01_base_case/mean_iso/01_base_case.dat.Cx_00.0012 02_calib.dat
cp ../../inputs/final_05_w_fence/final_05_w_fence.macro.00_00.0012 final_05_w_fence.macro
cp ../../inputs/props_05_ism3/props_05_ism3.macro.00_00.0012 props_05_ism3.macro
cp ../../inputs/sptr_1000/sptr_1000.macro.Cx_01.0012 sptr_1000.macro
xfehm_oct-26-99
cp 02_calib.sptr3 ./results/02_calib.sptr3.Cx_01.0012
cp ../../inputs/sptr_1000/sptr_1000.macro.Cx_02.0012 sptr_1000.macro
xfehm_oct-26-99
cp 02_calib.sptr3 ./results/02_calib.sptr3.Cx_02.0012
cp ../../inputs/sptr_1000/sptr_1000.macro.Cx_03.0012 sptr_1000.macro
xfehm_oct-26-99
cp 02_calib.sptr3 ./results/02_calib.sptr3.Cx_03.0012
cp ../../inputs/sptr_1000/sptr_1000.macro.Cx_04.0012 sptr_1000.macro
xfehm_oct-26-99
cp 02_calib.sptr3 ./results/02_calib.sptr3.Cx_04.0012

cp ../../inputs/01_base_case/mean_iso/01_base_case.dat.Cx_00.0016 02_calib.dat
cp ../../inputs/final_05_w_fence/final_05_w_fence.macro.00_00.0016 final_05_w_fence.macro
cp ../../inputs/props_05_ism3/props_05_ism3.macro.00_00.0016 props_05_ism3.macro
cp ../../inputs/sptr_1000/sptr_1000.macro.Cx_01.0016 sptr_1000.macro
xfehm_oct-26-99
cp 02_calib.sptr3 ./results/02_calib.sptr3.Cx_01.0016
cp ../../inputs/sptr_1000/sptr_1000.macro.Cx_02.0016 sptr_1000.macro
xfehm_oct-26-99
cp 02_calib.sptr3 ./results/02_calib.sptr3.Cx_02.0016
cp ../../inputs/sptr_1000/sptr_1000.macro.Cx_03.0016 sptr_1000.macro
xfehm_oct-26-99
cp 02_calib.sptr3 ./results/02_calib.sptr3.Cx_03.0016
cp ../../inputs/sptr_1000/sptr_1000.macro.Cx_04.0016 sptr_1000.macro
xfehm_oct-26-99
cp 02_calib.sptr3 ./results/02_calib.sptr3.Cx_04.0016

cp ../../inputs/01_base_case/mean_iso/01_base_case.dat.Cx_00.0025 02_calib.dat
cp ../../inputs/final_05_w_fence/final_05_w_fence.macro.00_00.0025 final_05_w_fence.macro
cp ../../inputs/props_05_ism3/props_05_ism3.macro.00_00.0025 props_05_ism3.macro
cp ../../inputs/sptr_1000/sptr_1000.macro.Cx_01.0025 sptr_1000.macro
xfehm_oct-26-99
cp 02_calib.sptr3 ./results/02_calib.sptr3.Cx_01.0025
cp ../../inputs/sptr_1000/sptr_1000.macro.Cx_02.0025 sptr_1000.macro
xfehm_oct-26-99
cp 02_calib.sptr3 ./results/02_calib.sptr3.Cx_02.0025
cp ../../inputs/sptr_1000/sptr_1000.macro.Cx_03.0025 sptr_1000.macro
xfehm_oct-26-99
cp 02_calib.sptr3 ./results/02_calib.sptr3.Cx_03.0025
cp ../../inputs/sptr_1000/sptr_1000.macro.Cx_04.0025 sptr_1000.macro
xfehm_oct-26-99
cp 02_calib.sptr3 ./results/02_calib.sptr3.Cx_04.0025

cp ../../inputs/01_base_case/mean_iso/01_base_case.dat.Cx_00.0029 02_calib.dat
cp ../../inputs/final_05_w_fence/final_05_w_fence.macro.00_00.0029 final_05_w_fence.macro
cp ../../inputs/props_05_ism3/props_05_ism3.macro.00_00.0029 props_05_ism3.macro
cp ../../inputs/sptr_1000/sptr_1000.macro.Cx_01.0029 sptr_1000.macro
xfehm_oct-26-99
cp 02_calib.sptr3 ./results/02_calib.sptr3.Cx_01.0029
cp ../../inputs/sptr_1000/sptr_1000.macro.Cx_02.0029 sptr_1000.macro
xfehm_oct-26-99
cp 02_calib.sptr3 ./results/02_calib.sptr3.Cx_02.0029
cp ../../inputs/sptr_1000/sptr_1000.macro.Cx_03.0029 sptr_1000.macro
xfehm_oct-26-99
cp 02_calib.sptr3 ./results/02_calib.sptr3.Cx_03.0029
cp ../../inputs/sptr_1000/sptr_1000.macro.Cx_04.0029 sptr_1000.macro
xfehm_oct-26-99
cp 02_calib.sptr3 ./results/02_calib.sptr3.Cx_04.0029

cp ../../inputs/01_base_case/mean_iso/01_base_case.dat.Cx_00.0035 02_calib.dat

```

```

cp ../../inputs/final_05_w_fence/final_05_w_fence.macro.00_00.0035 final_05_w_fence.macro
cp ../../inputs/props_05_ism3/props_05_ism3.macro.00_00.0035 props_05_ism3.macro
cp ../../inputs/sptr_1000/sptr_1000.macro.Cx_01.0035 sptr_1000.macro
xfehm_oct-26-99
cp 02_calib.spqr3 ./results/02_calib.spqr3.Cx_01.0035
cp ../../inputs/sptr_1000/sptr_1000.macro.Cx_02.0035 sptr_1000.macro
xfehm_oct-26-99
cp 02_calib.spqr3 ./results/02_calib.spqr3.Cx_02.0035
cp ../../inputs/sptr_1000/sptr_1000.macro.Cx_03.0035 sptr_1000.macro
xfehm_oct-26-99
cp 02_calib.spqr3 ./results/02_calib.spqr3.Cx_03.0035
cp ../../inputs/sptr_1000/sptr_1000.macro.Cx_04.0035 sptr_1000.macro
xfehm_oct-26-99
cp 02_calib.spqr3 ./results/02_calib.spqr3.Cx_04.0035

cp ../../inputs/01_base_case/mean_iso/01_base_case.dat.Cx_00.0039 02_calib.dat
cp ../../inputs/final_05_w_fence/final_05_w_fence.macro.00_00.0039 final_05_w_fence.macro
cp ../../inputs/props_05_ism3/props_05_ism3.macro.00_00.0039 props_05_ism3.macro
cp ../../inputs/sptr_1000/sptr_1000.macro.Cx_01.0039 sptr_1000.macro
xfehm_oct-26-99
cp 02_calib.spqr3 ./results/02_calib.spqr3.Cx_01.0039
cp ../../inputs/sptr_1000/sptr_1000.macro.Cx_02.0039 sptr_1000.macro
xfehm_oct-26-99
cp 02_calib.spqr3 ./results/02_calib.spqr3.Cx_02.0039
cp ../../inputs/sptr_1000/sptr_1000.macro.Cx_03.0039 sptr_1000.macro
xfehm_oct-26-99
cp 02_calib.spqr3 ./results/02_calib.spqr3.Cx_03.0039
cp ../../inputs/sptr_1000/sptr_1000.macro.Cx_04.0039 sptr_1000.macro
xfehm_oct-26-99
cp 02_calib.spqr3 ./results/02_calib.spqr3.Cx_04.0039

cp ../../inputs/01_base_case/mean_iso/01_base_case.dat.Cx_00.0040 02_calib.dat
cp ../../inputs/final_05_w_fence/final_05_w_fence.macro.00_00.0040 final_05_w_fence.macro
cp ../../inputs/props_05_ism3/props_05_ism3.macro.00_00.0040 props_05_ism3.macro
cp ../../inputs/sptr_1000/sptr_1000.macro.Cx_01.0040 sptr_1000.macro
xfehm_oct-26-99
cp 02_calib.spqr3 ./results/02_calib.spqr3.Cx_01.0040
cp ../../inputs/sptr_1000/sptr_1000.macro.Cx_02.0040 sptr_1000.macro
xfehm_oct-26-99
cp 02_calib.spqr3 ./results/02_calib.spqr3.Cx_02.0040
cp ../../inputs/sptr_1000/sptr_1000.macro.Cx_03.0040 sptr_1000.macro
xfehm_oct-26-99
cp 02_calib.spqr3 ./results/02_calib.spqr3.Cx_03.0040
cp ../../inputs/sptr_1000/sptr_1000.macro.Cx_04.0040 sptr_1000.macro
xfehm_oct-26-99
cp 02_calib.spqr3 ./results/02_calib.spqr3.Cx_04.0040

cp ../../inputs/01_base_case/mean_iso/01_base_case.dat.Cx_00.0043 02_calib.dat
cp ../../inputs/final_05_w_fence/final_05_w_fence.macro.00_00.0043 final_05_w_fence.macro
cp ../../inputs/props_05_ism3/props_05_ism3.macro.00_00.0043 props_05_ism3.macro
cp ../../inputs/sptr_1000/sptr_1000.macro.Cx_01.0043 sptr_1000.macro
xfehm_oct-26-99
cp 02_calib.spqr3 ./results/02_calib.spqr3.Cx_01.0043
cp ../../inputs/sptr_1000/sptr_1000.macro.Cx_02.0043 sptr_1000.macro
xfehm_oct-26-99
cp 02_calib.spqr3 ./results/02_calib.spqr3.Cx_02.0043
cp ../../inputs/sptr_1000/sptr_1000.macro.Cx_03.0043 sptr_1000.macro
xfehm_oct-26-99
cp 02_calib.spqr3 ./results/02_calib.spqr3.Cx_03.0043
cp ../../inputs/sptr_1000/sptr_1000.macro.Cx_04.0043 sptr_1000.macro
xfehm_oct-26-99
cp 02_calib.spqr3 ./results/02_calib.spqr3.Cx_04.0043

cp ../../inputs/01_base_case/mean_iso/01_base_case.dat.Cx_00.0044 02_calib.dat
cp ../../inputs/final_05_w_fence/final_05_w_fence.macro.00_00.0044 final_05_w_fence.macro
cp ../../inputs/props_05_ism3/props_05_ism3.macro.00_00.0044 props_05_ism3.macro
cp ../../inputs/sptr_1000/sptr_1000.macro.Cx_01.0044 sptr_1000.macro
xfehm_oct-26-99
cp 02_calib.spqr3 ./results/02_calib.spqr3.Cx_01.0044
cp ../../inputs/sptr_1000/sptr_1000.macro.Cx_02.0044 sptr_1000.macro
xfehm_oct-26-99

```

```
cp 02_calib.sptr3 ./results/02_calib.sptr3.Cx_02.0044
cp ../../inputs/sptr_1000/sptr_1000.macro.Cx_03.0044 sptr_1000.macro
xfehm_oct-26-99
cp 02_calib.sptr3 ./results/02_calib.sptr3.Cx_03.0044
cp ../../inputs/sptr_1000/sptr_1000.macro.Cx_04.0044 sptr_1000.macro
xfehm_oct-26-99
cp 02_calib.sptr3 ./results/02_calib.sptr3.Cx_04.0044

cp ../../inputs/01_base_case/mean_iso/01_base_case.dat.Cx_00.0051 02_calib.dat
cp ../../inputs/final_05_w_fence/final_05_w_fence.macro.00_00.0051 final_05_w_fence.macro
cp ../../inputs/props_05_ism3/props_05_ism3.macro.00_00.0051 props_05_ism3.macro
cp ../../inputs/sptr_1000/sptr_1000.macro.Cx_01.0051 sptr_1000.macro
xfehm_oct-26-99
cp 02_calib.sptr3 ./results/02_calib.sptr3.Cx_01.0051
cp ../../inputs/sptr_1000/sptr_1000.macro.Cx_02.0051 sptr_1000.macro
xfehm_oct-26-99
cp 02_calib.sptr3 ./results/02_calib.sptr3.Cx_02.0051
cp ../../inputs/sptr_1000/sptr_1000.macro.Cx_03.0051 sptr_1000.macro
xfehm_oct-26-99
cp 02_calib.sptr3 ./results/02_calib.sptr3.Cx_03.0051
cp ../../inputs/sptr_1000/sptr_1000.macro.Cx_04.0051 sptr_1000.macro
xfehm_oct-26-99
cp 02_calib.sptr3 ./results/02_calib.sptr3.Cx_04.0051

cp ../../inputs/01_base_case/mean_iso/01_base_case.dat.Cx_00.0053 02_calib.dat
cp ../../inputs/final_05_w_fence/final_05_w_fence.macro.00_00.0053 final_05_w_fence.macro
cp ../../inputs/props_05_ism3/props_05_ism3.macro.00_00.0053 props_05_ism3.macro
cp ../../inputs/sptr_1000/sptr_1000.macro.Cx_01.0053 sptr_1000.macro
xfehm_oct-26-99
cp 02_calib.sptr3 ./results/02_calib.sptr3.Cx_01.0053
cp ../../inputs/sptr_1000/sptr_1000.macro.Cx_02.0053 sptr_1000.macro
xfehm_oct-26-99
cp 02_calib.sptr3 ./results/02_calib.sptr3.Cx_02.0053
cp ../../inputs/sptr_1000/sptr_1000.macro.Cx_03.0053 sptr_1000.macro
xfehm_oct-26-99
cp 02_calib.sptr3 ./results/02_calib.sptr3.Cx_03.0053
cp ../../inputs/sptr_1000/sptr_1000.macro.Cx_04.0053 sptr_1000.macro
xfehm_oct-26-99
cp 02_calib.sptr3 ./results/02_calib.sptr3.Cx_04.0053

cp ../../inputs/01_base_case/mean_iso/01_base_case.dat.Cx_00.0056 02_calib.dat
cp ../../inputs/final_05_w_fence/final_05_w_fence.macro.00_00.0056 final_05_w_fence.macro
cp ../../inputs/props_05_ism3/props_05_ism3.macro.00_00.0056 props_05_ism3.macro
cp ../../inputs/sptr_1000/sptr_1000.macro.Cx_01.0056 sptr_1000.macro
xfehm_oct-26-99
cp 02_calib.sptr3 ./results/02_calib.sptr3.Cx_01.0056
cp ../../inputs/sptr_1000/sptr_1000.macro.Cx_02.0056 sptr_1000.macro
xfehm_oct-26-99
cp 02_calib.sptr3 ./results/02_calib.sptr3.Cx_02.0056
cp ../../inputs/sptr_1000/sptr_1000.macro.Cx_03.0056 sptr_1000.macro
xfehm_oct-26-99
cp 02_calib.sptr3 ./results/02_calib.sptr3.Cx_03.0056
cp ../../inputs/sptr_1000/sptr_1000.macro.Cx_04.0056 sptr_1000.macro
xfehm_oct-26-99
cp 02_calib.sptr3 ./results/02_calib.sptr3.Cx_04.0056

cp ../../inputs/01_base_case/mean_iso/01_base_case.dat.Cx_00.0057 02_calib.dat
cp ../../inputs/final_05_w_fence/final_05_w_fence.macro.00_00.0057 final_05_w_fence.macro
cp ../../inputs/props_05_ism3/props_05_ism3.macro.00_00.0057 props_05_ism3.macro
cp ../../inputs/sptr_1000/sptr_1000.macro.Cx_01.0057 sptr_1000.macro
xfehm_oct-26-99
cp 02_calib.sptr3 ./results/02_calib.sptr3.Cx_01.0057
cp ../../inputs/sptr_1000/sptr_1000.macro.Cx_02.0057 sptr_1000.macro
xfehm_oct-26-99
cp 02_calib.sptr3 ./results/02_calib.sptr3.Cx_02.0057
cp ../../inputs/sptr_1000/sptr_1000.macro.Cx_03.0057 sptr_1000.macro
xfehm_oct-26-99
cp 02_calib.sptr3 ./results/02_calib.sptr3.Cx_03.0057
cp ../../inputs/sptr_1000/sptr_1000.macro.Cx_04.0057 sptr_1000.macro
xfehm_oct-26-99
cp 02_calib.sptr3 ./results/02_calib.sptr3.Cx_04.0057
```

```
cp ../../inputs/01_base_case/mean_iso/01_base_case.dat.Cx_00.0068 02_calib.dat
cp ../../inputs/final_05_w_fence/final_05_w_fence.macro.00_00.0068 final_05_w_fence.macro
cp ../../inputs/props_05_ism3/props_05_ism3.macro.00_00.0068 props_05_ism3.macro
cp ../../inputs/sptr_1000/sptr_1000.macro.Cx_01.0068 sptr_1000.macro
xfehm_oct-26-99
cp 02_calib.sptr3 ./results/02_calib.sptr3.Cx_01.0068
cp ../../inputs/sptr_1000/sptr_1000.macro.Cx_02.0068 sptr_1000.macro
xfehm_oct-26-99
cp 02_calib.sptr3 ./results/02_calib.sptr3.Cx_02.0068
cp ../../inputs/sptr_1000/sptr_1000.macro.Cx_03.0068 sptr_1000.macro
xfehm_oct-26-99
cp 02_calib.sptr3 ./results/02_calib.sptr3.Cx_03.0068
cp ../../inputs/sptr_1000/sptr_1000.macro.Cx_04.0068 sptr_1000.macro
xfehm_oct-26-99
cp 02_calib.sptr3 ./results/02_calib.sptr3.Cx_04.0068

cp ../../inputs/01_base_case/mean_iso/01_base_case.dat.Cx_00.0071 02_calib.dat
cp ../../inputs/final_05_w_fence/final_05_w_fence.macro.00_00.0071 final_05_w_fence.macro
cp ../../inputs/props_05_ism3/props_05_ism3.macro.00_00.0071 props_05_ism3.macro
cp ../../inputs/sptr_1000/sptr_1000.macro.Cx_01.0071 sptr_1000.macro
xfehm_oct-26-99
cp 02_calib.sptr3 ./results/02_calib.sptr3.Cx_01.0071
cp ../../inputs/sptr_1000/sptr_1000.macro.Cx_02.0071 sptr_1000.macro
xfehm_oct-26-99
cp 02_calib.sptr3 ./results/02_calib.sptr3.Cx_02.0071
cp ../../inputs/sptr_1000/sptr_1000.macro.Cx_03.0071 sptr_1000.macro
xfehm_oct-26-99
cp 02_calib.sptr3 ./results/02_calib.sptr3.Cx_03.0071
cp ../../inputs/sptr_1000/sptr_1000.macro.Cx_04.0071 sptr_1000.macro
xfehm_oct-26-99
cp 02_calib.sptr3 ./results/02_calib.sptr3.Cx_04.0071

cp ../../inputs/01_base_case/mean_iso/01_base_case.dat.Cx_00.0073 02_calib.dat
cp ../../inputs/final_05_w_fence/final_05_w_fence.macro.00_00.0073 final_05_w_fence.macro
cp ../../inputs/props_05_ism3/props_05_ism3.macro.00_00.0073 props_05_ism3.macro
cp ../../inputs/sptr_1000/sptr_1000.macro.Cx_01.0073 sptr_1000.macro
xfehm_oct-26-99
cp 02_calib.sptr3 ./results/02_calib.sptr3.Cx_01.0073
cp ../../inputs/sptr_1000/sptr_1000.macro.Cx_02.0073 sptr_1000.macro
xfehm_oct-26-99
cp 02_calib.sptr3 ./results/02_calib.sptr3.Cx_02.0073
cp ../../inputs/sptr_1000/sptr_1000.macro.Cx_03.0073 sptr_1000.macro
xfehm_oct-26-99
cp 02_calib.sptr3 ./results/02_calib.sptr3.Cx_03.0073
cp ../../inputs/sptr_1000/sptr_1000.macro.Cx_04.0073 sptr_1000.macro
xfehm_oct-26-99
cp 02_calib.sptr3 ./results/02_calib.sptr3.Cx_04.0073

cp ../../inputs/01_base_case/mean_iso/01_base_case.dat.Cx_00.0081 02_calib.dat
cp ../../inputs/final_05_w_fence/final_05_w_fence.macro.00_00.0081 final_05_w_fence.macro
cp ../../inputs/props_05_ism3/props_05_ism3.macro.00_00.0081 props_05_ism3.macro
cp ../../inputs/sptr_1000/sptr_1000.macro.Cx_01.0081 sptr_1000.macro
xfehm_oct-26-99
cp 02_calib.sptr3 ./results/02_calib.sptr3.Cx_01.0081
cp ../../inputs/sptr_1000/sptr_1000.macro.Cx_02.0081 sptr_1000.macro
xfehm_oct-26-99
cp 02_calib.sptr3 ./results/02_calib.sptr3.Cx_02.0081
cp ../../inputs/sptr_1000/sptr_1000.macro.Cx_03.0081 sptr_1000.macro
xfehm_oct-26-99
cp 02_calib.sptr3 ./results/02_calib.sptr3.Cx_03.0081
cp ../../inputs/sptr_1000/sptr_1000.macro.Cx_04.0081 sptr_1000.macro
xfehm_oct-26-99
cp 02_calib.sptr3 ./results/02_calib.sptr3.Cx_04.0081

cp ../../inputs/01_base_case/mean_iso/01_base_case.dat.Cx_00.0082 02_calib.dat
cp ../../inputs/final_05_w_fence/final_05_w_fence.macro.00_00.0082 final_05_w_fence.macro
cp ../../inputs/props_05_ism3/props_05_ism3.macro.00_00.0082 props_05_ism3.macro
cp ../../inputs/sptr_1000/sptr_1000.macro.Cx_01.0082 sptr_1000.macro
xfehm_oct-26-99
cp 02_calib.sptr3 ./results/02_calib.sptr3.Cx_01.0082
```

```

cp ../../inputs/sptr_1000/sptr_1000.macro.Cx_02.0082 sptr_1000.macro
xfehm_oct-26-99
cp 02_calib.spqr3 ./results/02_calib.spqr3.Cx_02.0082
cp ../../inputs/sptr_1000/sptr_1000.macro.Cx_03.0082 sptr_1000.macro
xfehm_oct-26-99
cp 02_calib.spqr3 ./results/02_calib.spqr3.Cx_03.0082
cp ../../inputs/sptr_1000/sptr_1000.macro.Cx_04.0082 sptr_1000.macro
xfehm_oct-26-99
cp 02_calib.spqr3 ./results/02_calib.spqr3.Cx_04.0082

cp ../../inputs/01_base_case/mean_iso/01_base_case.dat.Cx_00.0090 02_calib.dat
cp ../../inputs/final_05_w_fence/final_05_w_fence.macro.00_00.0090 final_05_w_fence.macro
cp ../../inputs/props_05_ism3/props_05_ism3.macro.00_00.0090 props_05_ism3.macro
cp ../../inputs/sptr_1000/sptr_1000.macro.Cx_01.0090 sptr_1000.macro
xfehm_oct-26-99
cp 02_calib.spqr3 ./results/02_calib.spqr3.Cx_01.0090
cp ../../inputs/sptr_1000/sptr_1000.macro.Cx_02.0090 sptr_1000.macro
xfehm_oct-26-99
cp 02_calib.spqr3 ./results/02_calib.spqr3.Cx_02.0090
cp ../../inputs/sptr_1000/sptr_1000.macro.Cx_03.0090 sptr_1000.macro
xfehm_oct-26-99
cp 02_calib.spqr3 ./results/02_calib.spqr3.Cx_03.0090
cp ../../inputs/sptr_1000/sptr_1000.macro.Cx_04.0090 sptr_1000.macro
xfehm_oct-26-99
cp 02_calib.spqr3 ./results/02_calib.spqr3.Cx_04.0090

cp ../../inputs/01_base_case/mean_iso/01_base_case.dat.Cx_00.0091 02_calib.dat
cp ../../inputs/final_05_w_fence/final_05_w_fence.macro.00_00.0091 final_05_w_fence.macro
cp ../../inputs/props_05_ism3/props_05_ism3.macro.00_00.0091 props_05_ism3.macro
cp ../../inputs/sptr_1000/sptr_1000.macro.Cx_01.0091 sptr_1000.macro
xfehm_oct-26-99
cp 02_calib.spqr3 ./results/02_calib.spqr3.Cx_01.0091
cp ../../inputs/sptr_1000/sptr_1000.macro.Cx_02.0091 sptr_1000.macro
xfehm_oct-26-99
cp 02_calib.spqr3 ./results/02_calib.spqr3.Cx_02.0091
cp ../../inputs/sptr_1000/sptr_1000.macro.Cx_03.0091 sptr_1000.macro
xfehm_oct-26-99
cp 02_calib.spqr3 ./results/02_calib.spqr3.Cx_03.0091
cp ../../inputs/sptr_1000/sptr_1000.macro.Cx_04.0091 sptr_1000.macro
xfehm_oct-26-99
cp 02_calib.spqr3 ./results/02_calib.spqr3.Cx_04.0091

cp ../../inputs/01_base_case/mean_iso/01_base_case.dat.Cx_00.0100 02_calib.dat
cp ../../inputs/final_05_w_fence/final_05_w_fence.macro.00_00.0100 final_05_w_fence.macro
cp ../../inputs/props_05_ism3/props_05_ism3.macro.00_00.0100 props_05_ism3.macro
cp ../../inputs/sptr_1000/sptr_1000.macro.Cx_01.0100 sptr_1000.macro
xfehm_oct-26-99
cp 02_calib.spqr3 ./results/02_calib.spqr3.Cx_01.0100
cp ../../inputs/sptr_1000/sptr_1000.macro.Cx_02.0100 sptr_1000.macro
xfehm_oct-26-99
cp 02_calib.spqr3 ./results/02_calib.spqr3.Cx_02.0100
cp ../../inputs/sptr_1000/sptr_1000.macro.Cx_03.0100 sptr_1000.macro
xfehm_oct-26-99
cp 02_calib.spqr3 ./results/02_calib.spqr3.Cx_03.0100
cp ../../inputs/sptr_1000/sptr_1000.macro.Cx_04.0100 sptr_1000.macro
xfehm_oct-26-99
cp 02_calib.spqr3 ./results/02_calib.spqr3.Cx_04.0100

```